UT GSBS Dissertations and Theses (Open Access)   Graduate School of Biomedical Sciences

5-2017

PHOPSPHORYLATION AND UBIQUITIN MODIFICATION AT DNA DAMAGE SITES IN RESPONSE TO DOUBLE-STRAND BREAKS

Atanu Paul

Follow this and additional works at: http://digitalcommons.library.tmc.edu/utgsbs_dissertations

Part of the Biochemistry Commons, Cell Biology Commons, and the Molecular Biology Commons

The TMC LIBRARY
Health Sciences Resource Center

PHOPSPHORYLATION AND UBIQUITIN MODIFICATION

AT DNA DAMAGE SITES IN RESPONSE TO DOUBLE-STRAND BREAKS

by

Atanu Paul, M.S.

APPROVED:

_____

Bin Wang, Ph.D. Advisory Professor

_____

Pierre McCrea , Ph.D.

_____

Xiaobing Shi, Ph.D.

_____

Zahid Hussain Siddik, Ph.D.

_____

Grzegorz Ira, Ph.D.

APPROVED:

_____

Dean, The University of Texas
MD Anderson Cancer Center UTHealth Graduate School of Biomedical Sciences

PHOPSPHORYLATION AND UBIQUITIN MODIFICATION

AT DNA DAMAGE SITES IN RESPONSE TO DOUBLE-STRAND BREAKS

A

DISSERTATION

Presented to the Faculty of

The University of Texas MD Anderson Cancer Center

UT Health Graduate School of Biomedical Sciences

in Partial Fulfillment

of the Requirements for the Degree of

DOCTOR OF PHILOSOPHY

by

Atanu Paul, M.S.

Houston, Texas

May 2017

Dedication

To my parents Bimal Kanti Paul and Banani Paul and my late grandmother Nivanani Paul for their unconditional love and support throughout all these years.

ACKNOWLEDGEMENTS

This work would not have been possible without the continuous support and help of many people. Firstly, I would like to express my deepest gratitude and appreciation to Dr. Bin Wang for her guidance, encouragement and mentoring she has provided throughout my entire graduate career in her lab. She not only motivated me to pursue my PhD thesis project but also provided me the opportunity to learn from other projects as well. At many stages during my PhD training I benefited from her invaluable scientific advice. She has always been very supportive and motivated me to explore new things.

Secondly, of course the former and current members of the Wang lab. Without the help and co-operation from each and everybody around me in the lab, I would not be able to finish this work. I am thankful to all past members of the lab – Dr. Xin Hu, Dr. Andrew Castillo, Dr. Baohua Sun, Dr. Dan Su and Dr. JinAh Kim, who helped me tremendously both intellectually and technically. I am also grateful to the current members of the lab. Special thanks to Ella (Dr. Shengfeng Xu) for listening to my problems and continuous encouragement during my ups and downs. Also, Erin, Dr. Xiao Wu for their cooperation and help whenever I needed. Our everyday discussion about experiments, seminars, frustration, happiness and so on made our lab a happening places.

I am extremely fortunate to have the support and guidance from my former and current members of PhD thesis committee. I would like to thank all of my committee members, Dr. Pierre D. McCrea, Dr. Grzegorz Ira, Dr. Xiaobing Shi, Dr. Zahid Hussain Siddik, Jessica Tyler, Dr. Michelle Barton, Dr. Jeffrey Frost, Dr. Jianpin Jing for their guidance, scientific support and time commitment to attend my

committee meetings. I would also like to acknowledge Dr. Tyler and Dr. Elsa Flores for giving me the opportunity for lab rotation in their labs.

My success in graduate school is also greatly attributed to the help and support from my seniors and friends I came to know during my training. I am sincerely thankful to Dr. Abhinav Jain and Dr. Srikanth Appikonda from Barton lab, Dr. William Munoz from McCrea lab for their support. Also, I would like to thank my friends in the graduate school Kaushik Thakkar, Aundrietta Duncan, Niza Nemkul, Amanda Haltom, Avinash Venkatanarayan, Alejandro Villar-Prados, Vinay Nath, Andrew Davis, Pingping Wang, Richard Huang, Kenneth Trimmer for their encouragement and support.

My sincere gratitude is also extended to my graduate school UT-GSBS for having the most helpful and considerate people for students. I am thankful to Dr. Mattox, Lily, Joy, Bunny, Brenda, Tracey, Elisabet and everybody else at the GSBS for their unconditional support and help whenever I needed. I am also thankful to Genes & Development PhD program for providing education, training, and support I needed for my training as a researcher. I especially thank the Center for Cancer Epigenetics and Schissler Foundation for their generous fellowships, graduate school for awarding me the Andrew Sowell-Wade Huggins and Presidents' Research Scholarships. Also, I would like to thank Elisabeth Lindheim for be there always for any support I needed during my stay in the program.

I would like to thank my parents, who have unconditionally supported me to pursue my career in the US. Without their help and support, I would not be able to come this far. Their inspiration and encouragement even when far away from home helped me a lot to finish my graduate study. I also thank my brother, my sister-in-law

and parents-in-law for being a constant source of support and helping me stay focused.

And last but not least, most importantly, I would like to thank my dear wife Sangita, who stood by me through all my ups and downs, my absences and impatience during my PhD. Her unwavering love, quiet patience, continuous support, and encouragement helped me get through this tough time of my career in the most positive way. But most of all, I thank her for being my best friend. I owe her everything. Without her presence in my life, this journey would have been much more difficult and harder for me.

PHOPSPHORYLATION AND UBIQUITIN MODIFICATION

AT DNA DAMAGE SITES IN RESPONSE TO DOUBLE-STRAND BREAKS

Atanu Paul, M.S

Advisory Professor: Bin Wang, Ph.D.

Genomes of all organisms are continuously damaged by numerous exogenous and endogenous sources leading to different kinds of DNA lesions, which if not repaired efficiently may trigger wide-scale genomic instability, a hallmark of cancer development. To overcome this, cells have evolved a sophisticated sensory network called the DNA damage response (DDR) comprised of a large number of distinct protein complexes categorized as sensor, mediator, transducer and effector proteins that amplify the DNA damage signal and activate cell cycle checkpoint to initiate DNA repair or trigger apoptosis where the defect is beyond repair. This intricate signaling pathway is tightly regulated by modulating DDR factors recruitment, retention and dissociation from the sites of DNA damage in a spatiotemporal manner mediated by numerous reversible post-translational modification (PTMs) including phosphorylation, ubiquitination, SUMOylation, methylation, acetylation, poly(ADP-ribosyl)ation, and Neddylation. In this study, I examined the role of phosphorylation and ubiquitination in regulating the DDR signaling at the DNA damage sites.

DNA double-strand breaks triggers a phosphorylation-mediated signaling at the damage sites leading to histone ubiquitination in Lys63-linked manner that recruits BRCA1-A complex to the damage sites. The A complex is comprised of BRCA1, Rap80, NBA1, BRE, BRCC36 and the adaptor protein Abraxas, which has

been shown previously to constitutively interact with BRCA1-BRCT (BRCA1 C-terminal) domain through its C-terminal phosphorylated S406 residue. In this study, we found that DNA damage-induced Abraxas phosphorylation at neighboring S404 residue induces stable BRCA1 dimerization through its BRCT domain. Both crystal structure and *in vivo* analysis confirmed that phosphorylation at Abraxas S404 residue is essential for stable BRCA1-BRCT dimer formation and mutation in the S404 residue leads to impaired accumulation of BRCA1 to damaged chromatin. In addition, we found two germline mutations in the BRCA1-BRCT dimerization interface disrupt stable dimer formation both *in vitro* and *in vivo.*

Although phosphorylation has been shown to be the major PTM at the DSB sites, over the last decade, ubiquitination has also emerged as a key regulatory player in the DDR. Irradiation (IR)-induced DNA damage catalyzes Lys63-linked polyubiquitination of histones, H2A and H2A.X that leads to accumulation of BRCA1-A complex to DSBs. In my second study, we sought to determine whether non-lys63-linked ubiquitination also exists at the DSBs regulating the DDR pathway. My findings indicate that along with Lys63-linked ubiquitination, chromatin-bound proteins are also modified with Lys11-linked polyubiquitination at DNA damage sites in an ATM-dependent manner by Ube2S/Ube2C E2 conjugating and RNF8 E3 ligase enzymes and deubiquitinated by OTUD7B (Cezanne) enzyme. I further showed that histones H2A and H2A.X is modified with Lys11-linked polyubiquitination in a DNA damage-dependent manner that is essential for inhibiting transcriptional silencing at proximity to DSB sites to maintain genomic stability. Overall, my findings provide insights into how post-translational modifications regulate DDR factors dynamics at DSB sites and play a crucial role in maintaining genomic integrity.

Table of Contents

x

xi

List of Figures

List of Tables

CHAPTER 1
OVERVIEW OF THE DNA DAMAGE RESPONSE

1.1 Introduction:

The genomic integrity of all organisms is continually threatened by DNA damage. The human genome regularly encounters and repairs a large number of DNA damage lesions, estimated at 10^4 to 10^5 lesions per cell per day (1, 2). Exogenous exposure to carcinogens, ionizing radiation (IR), or the ultraviolet light from the sun can all damage DNA. Additionally, many cellular processes generate endogenous sources of DNA damage. Reactive oxygen and nitrogen species generated during cellular metabolism, misincorporation of dNTPs during DNA replication, cytosine deamination, DNA alkylation, and abortive topoisomerase activities all generate DNA lesions that must be repaired faithfully (2-5). Unrepaired DNA can physically interfere with fundamental cellular processes such as replication and transcription. Moreover, improper repair of these lesions can lead to gene mutations, deletions, or translocations that, in turn, either inactivate tumor suppressor genes or activate oncogenes. Together, these events trigger wide-scale genomic instability, a characteristic hallmark of cancer development (6-8)

To combat the DNA lesions and maintain genome integrity, cells have evolved highly orchestrated sensory signaling cascades collectively called the DNA damage response (DDR) (Figure 1). The DDR senses DNA damage and initiates DNA repair. Distinct protein complexes categorized as sensors, mediators, transducers and effectors amplify the DNA damage signal, activate cell cycle checkpoints, and initiate repair or trigger apoptosis should the defect be irreparable
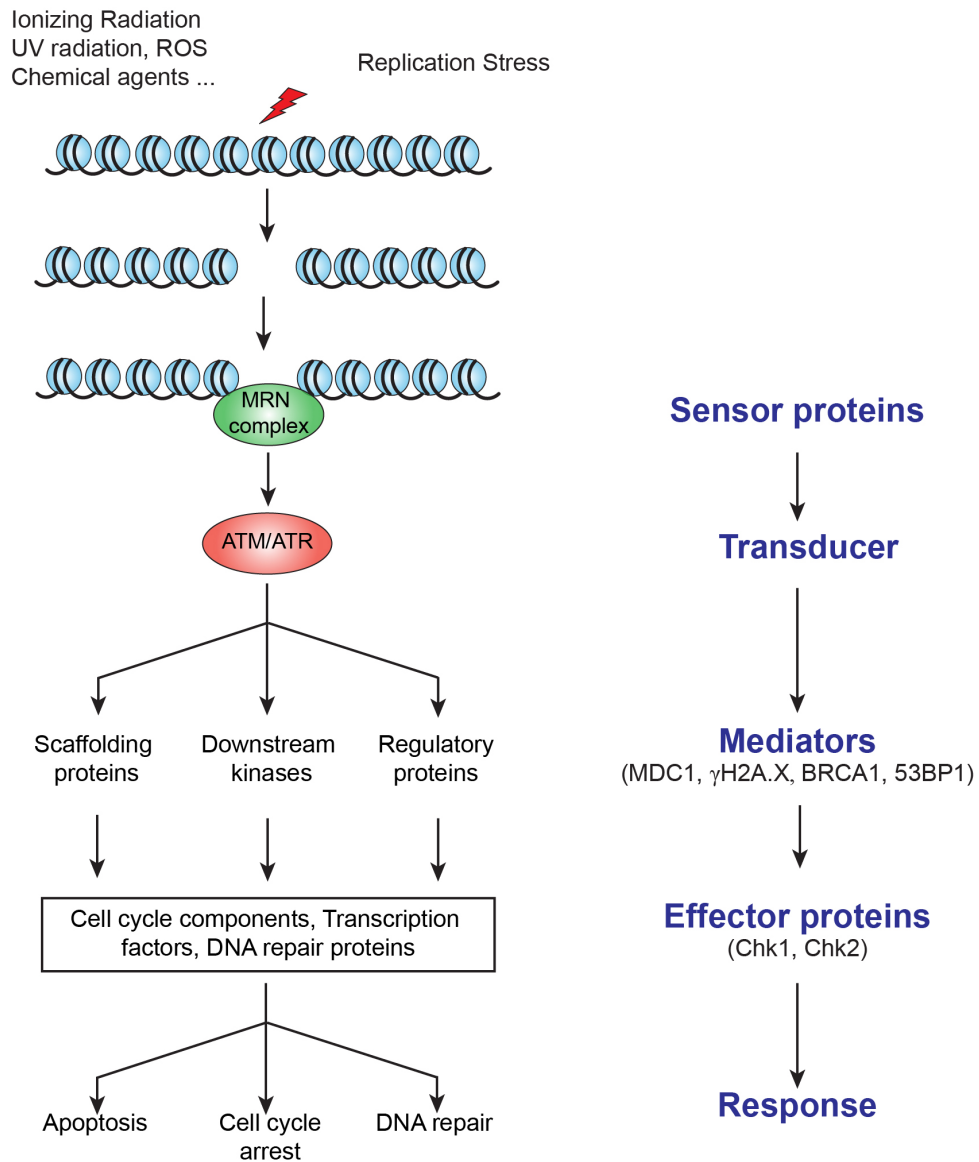
Figure 1: Organization of cellular DNA damage response pathway. Cellular response to DNA damage from different sources involves sensing the damage signal, amplifying and transducing the signal to mediator proteins that regulate spatio-temporal organization of effector proteins to exert appropriate response that involves activation of a cell cycle checkpoint, transcriptional regulation, execution of DNA repair or induction of apoptosis in case of severe DNA damage.

(2, 4, 9). Recruitment, retention and dissociation of DDR factors to and from the sites of DNA damage are tightly regulated in a time-dependent manner to maintain cellular homeostasis. This is mainly mediated by numerous reversible post-translational modifications (PTMs) (10-13).

1.2 DNA repair pathways in mammalian cells

To counteract DNA damage, cells have developed lesion-specific repair mechanisms. In mammalian cells, these constitute 4 major repair pathways: base excision repair (BER), nucleotide excision repair (NER), mismatch repair (MMR) and double-strand break repair pathways (Figure 2) (1). In this thesis, I examine the complexity of DNA damage response signaling involved in irradiation (IR)-induced DNA double-strand breaks (DSBs) and how post-translational modifications play an essential role in regulating the DDR signaling.

DNA double-strand breaks are one of the most cytotoxic lesions experienced by cells. If not properly repaired in a timely manner, DSBs may lead to a chromosomal deletion or translocation, triggering genomic instability and predisposing a cell to tumorigenesis (4, 5). Mammalian cells utilize two major repair pathways for DSB repair – non-homologous end joining (NHEJ) and homologous recombination (HR). In higher order vertebrates, NHEJ is the prevalent repair pathway choice. NHEJ operates throughout the cell cycle and is known to be inherently "error-prone". Conversely, HR predominantly occurs during S and G2 phases of the cell cycle as it requires the presence of the sister chromatid that is used as a homologous template for repair of the damaged DNA and is considered as an "error- free" repair pathway (14).
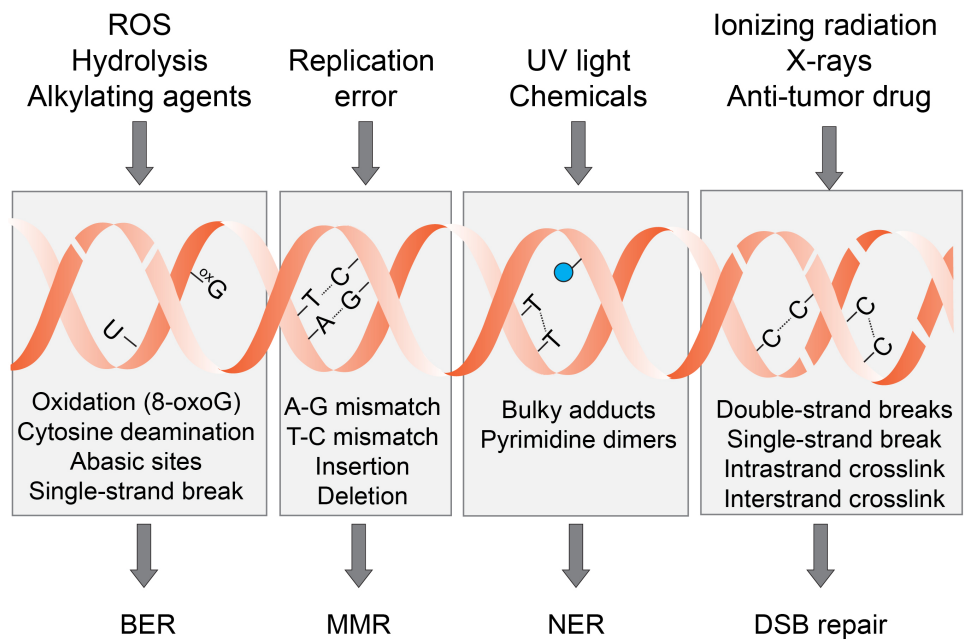
Figure 2: **Types of DNA damage and DNA repair mechanisms.** The figure illustrates sources of endogenous and exogenous DNA damages and relevant repair pathways repair the damaged DNA.

Figure is adapted and modified with permission from (1) Cedric Blanpain, Mary Mohrin, Panagiota A Sotiropoulou, and Emmanuelle Passegue, DNA-Damage Response in Tissue-Specific and Cancer Stem Cells. Cell Stem Cell 2011 8, 16-29 2011. License number 4092160106928.

1.3 Spatiotemporal dynamics of DDR factors at DNA damage sites:

One of the most notable features of the DNA damage response is the assembly and disassembly of chromatin regulators and DDR factors at damaged chromatin. This dynamic activity can be visualized by immunofluorescence as distinct nuclear 'foci' using antibodies. Although the focal accumulation of DDR proteins at damaged sites amplifies the damage signal, the functional significance of these foci in the DDR pathway still remains unknown (10). It is important to note that not all DDR factors assemble and dissociate from the damaged chromatin at the same time. Rather, the assembly and disassembly of DDR factors occur in a hierarchical fashion in a time-dependent manner. For example, while accumulation of NHEJ repair proteins at DSB sites is rapid but transient, HR proteins show delayed but persistent retention at damage sites, illustrating the different repair kinetics of these two major repair pathways (15). This careful spatiotemporal regulation of DDR factors at damaged chromatin is in large mediated by numerous reversible post-translational modifications (PTMs). PTMs not only promote the recruitment and dissociation of DDR factors, but also regulate their residence time at damage sites. In DSB repair, the role of phosphorylation in initiating the DDR signaling cascade has been described in much detail. However, recent years have witnessed the characterization of an unprecedented number of post-translational modifications at the sites of DNA damage including ubiquitination, SUMOylation, Neddylation, methylation, acetylation, and poly(ADP-ribosyl)ation (10). These findings depict more complex picture of the DNA damage response pathway at DSB

sites. In addition, findings of cross talk between these different modifications illustrate the intricacy of PTM signaling in the DDR (12, 16, 17)

1.4 Activation of DNA damage response following DNA double-strand breaks

Activation of DDR signaling and the efficiency of DNA repair is largely dependent on chromosomal contexts, such as whether chromatin has an open or compacted structure at the sites of DNA damage. At densely packed chromatin regions, repair of damaged DNA is more difficult and takes a longer time to complete. Several DDR kinases play an essential role in altering chromatin structure to render damaged chromatin accessible to repair factors. In mammalian cells, members of the phosphatidylinositol-3-kinase-like kinase family (PIKKs) – ATM, ATR, and DNA-pk$_{cs}$ – act as the furthermost upstream kinases that transduce and amplify the DNA damage signal. ATM and ATR appear to be the major kinases that phosphorylate hundreds of substrates preferentially at S/TQ (serine/threonine-glutamine) sites to activate cell cycle checkpoints, chromatin remodeling, and initiate DNA repair (18). Although both ATM and ATR kinases share significant structural and functional similarity and have overlapping substrate proteins involved in the DNA damage response pathway, the activation of these two kinases requires different stimuli (19). While ATM is primarily activated in response to DNA double-strand breaks, ATR is activated to a broad spectrum of DNA damaging signals including lesions generated by UV, cross-linking agents, and replication stress, in addition to DSBs. Recent genome wide analysis reveals that ATM and ATR function as master signal transducers in the DDR pathway, coordinating a large cellular signaling network to maintain genomic integrity.

ATM is activated immediately after DSBs by the sensor protein complex, Mre11-Rad50-Nbs1 (MRN) (20-27). Following activation by MRN, ATM triggers DDR signaling by phosphorylating hundreds of downstream proteins (18, 28). One of the early events following ATM activation is the phosphorylation of histone variant H2A.X by ATM at Ser139 residue. The DSB-induced phosphorylation of H2A.X occurs immediately after DNA damage and spreads over megabases of chromatin flanking the damage site in both directions. H2A.X phosphorylation can be detected in cells as discrete "foci" following DSB induction by irradiation (IR) (29-31). Phosphorylated H2A.X (γH2A.X) directly recruits the mediator protein, MDC1 (mediator of DNA damage checkpoint 1), which recognizes and binds phosphorylated H2A.X through its BRCT domain. MDC1 also forms IR-induced foci (IRIF) that extensively co-localizes with γH2A.X (32-34). Interestingly, MDC1 also interacts with ATM through its FHA domain. ATM-MDC1 interaction targets activated ATM to DSB flanking chromatin regions, thereby propagating ATM-mediated H2A.X and MDC1 phosphorylation at damaged chromatin to amplify the damage signal. In addition, MDC1 has been shown to regulate damage-induced cell cycle arrest checkpoint (35, 36).

γH2A.X-MDC1 acts a molecular platform that orchestrates the recruitment of additional DDR factors to the sites of DNA damage in a hierarchical manner (Figure 3). Phosphorylated MDC1 binds and targets E3 ubiquitin ligase RNF8 to damage sites. RNF8 contains an FHA domain at its N-terminus and RING domain at its C-terminus. RNF8 interacts with ATM-phosphorylated MDC1 via its FHA domain. Interestingly, RNF8 localization to damage sites is independent of its RING domain

8
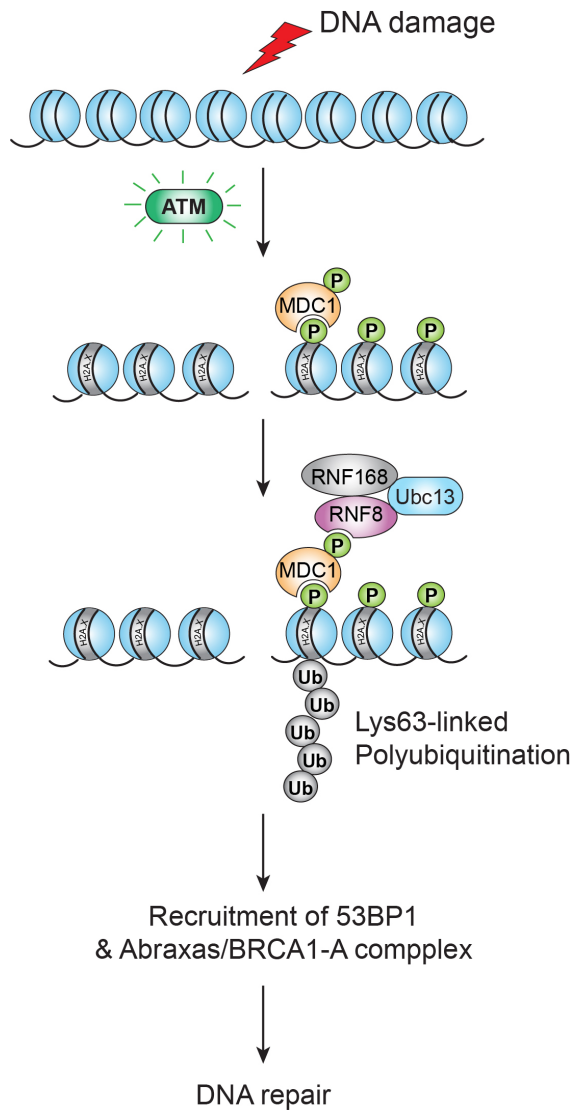
Figure 3: Phosphorylation-dependent ubiquitin signaling at DSB sites. DNA double-strand breaks induces a ATM-mediated phosphorylation-dependent ubiquitin signaling at DSB sites. Ubc13-RNF8-RNF168 enzymatic machinery catalyzes Lys63-linked ubiquitin chain that targets 53BP1 and BRCA1-A complex at damage sites to initiate repair.

but requires the FHA domain, indicating that a phosphorylation-dependent interaction with MDC1 is crucial for RNF8 accumulation to DSBs (37-39). RNF8 recruitment to damaged chromatin is consistent with earlier observations of ubiquitin conjugation at IRIF. In addition to MDC1 binding, the RNF8 FHA domain also interacts with another E3 ligase, HERC2, forming an MDC1-RNF8-HERC2 complex. This complex facilitates RNF8 interaction with the E2 ubiquitin conjugating enzyme, Ubc13, to catalyze Lys63-linked ubiquitination at damaged chromatin (40). The RNF8-Ubc13 enzymatic machinery ubiquitinates chromatin-bound proteins, including histone H2A and H2A.X, with non-proteolytic Lys63-linked ubiquitin chains in a DNA damage-dependent manner. This ubiquitination triggers the recruitment of downstream DDR factors recruitment including 53BP1 and components of BRCA1-A complex to damaged chromatin. In addition, RNF8 depletion has been shown to result in G2/M checkpoint arrest and hypersensitivity to IR-induced DNA damage, indicating that RNF8-dependent ubiquitination at DNA damage sites is essential for cells to cope with DNA double-strand breaks (37-39, 41). Later studies demonstrated that RNF8-mediated Lys63-linked ubiquitin conjugates are recognized by MIU (42) domains of another E3 ligase, RNF168, triggering its accumulation at DSB sites. RNF168, in association with the Ubc13 E2 conjugating enzyme, then amplifies the Lys63-linked ubiquitin chain on histone H2A and H2A.X, along with other unidentified substrates. Lys63-linked ubiquitin chains on histone and other chromatin-bound proteins are also recognized by the Ubiquitin Interacting Motif (UIM) of Rap80, which subsequently mediates accumulation of 53BP1 and components of BRCA1-A complex to sites of DNA damage (43-45). Recruitment of

BRCA1 and 53BP1 at DNA damage sites regulates the balance and repair pathway choice between HR and NHEJ at the damage sites. More recently, the Mailand group has shown that H1-type linker histones, but not core histones, serve as the major substrate for Ubc13-RNF8-mediated Lys63-linked ubiquitination and that RNF168 recognizes Lys63 ubiquitinated histone H1 at damaged chromatin, emphasizing the essential role of Ubc13 and RNF8 in recruiting RNF168 to DSBs (46).

1.5 Role of BRCA1-A complex in DSB repair

BRCA1-A complex, named after the adaptor protein Abraxas, consists of five different proteins: Rap80, Abraxas, NBA1, BRE, and BRCC36 (47-54). Abraxas mediates the interaction between BRCA1 and the other components of the A complex. The Abraxas-BRCA1 interaction is essential for Abraxas's role in DNA repair and maintenance of genome stability (55). Our lab and others have previously shown that Abraxas interacts with BRCA1 through its C-terminal pSPTF motif, in which phosphorylated Ser406 (S406) binds to BRCA1 C-terminal (BRCT) domain. Deletion of the pSPTF motif or mutation of the S406 residue disrupts both Abraxas-BRCA1 interaction and BRCA1 localization to DNA damage sites, thereby impairing efficient DNA repair (47, 49, 51). *Abraxas* knockout mice generated by our lab exhibit chromosomal instability and increased incidence of tumor development. Interestingly, a mutation in the phenylalanine residue of the Abraxas pSPTF motif (F409C) has been identified in human tumors (55), suggesting the importance of Abraxas-BRCA1 interaction in tumor suppression. Yet, it still remains unknown how Abraxas mediates BRCA1's tumor suppression function. Of note, Abraxas S406 is

constitutively phosphorylated in presence and absence of DNA damage (47). Therefore, it is tempting to speculate that there may be an additional regulatory mechanism that modulates Abraxas-BRCA1 interaction upon DNA damage.

1.6 Non Lys63-linked ubiquitination at DSB sites

Although Lys63-linked ubiquitination at damaged chromatin have been extensively studied, emerging evidence from different groups indicate that the ubiquitin landscape at DSB sites is much more complicated than previously anticipated and that additional linkage-specific ubiquitin chains (such as Lys6, Lys48, or Lys27-linked chains) exist at damaged chromatin. For instance, RNF168 has recently been shown to catalyze Lys27-linked ubiquitination at DSB sites that is essential for the proper activation of DDR signaling and regulates the recruitment of 53BP1, Rap80 and other DDR factors (56). In addition, RNF8 has been shown to interact with different E2 conjugating enzymes to catalyze different linkage-specific ubiquitin chain types. For example, recent findings have demonstrated that RNF8 can catalyze both Lys63 and Lys48-linked ubiquitin chains by interacting with Ubc13 and UbcH8 E2 enzymes, respectively (37-39, 57, 58). These findings depict that additional linkage-specific ubiquitin chain types exist at DSB sites to regulate efficient DDR signaling. Further study of different lysine residue-linked ubiquitination will therefore provide deeper understanding of the DDR signaling.

1.7 Transcription silencing in response to DSBs

Given DNA damage occurs in the context of chromatin structure, it potentially interferes with transcription and therefore coordination between DNA repair and transcription machinery is crucial for genomic stability. This coordination involves

chromatin organization by chromatin modulators, histone chaperones, and DDR factors that induce transcriptional silencing in response to DNA damage (59). DNA damage-induced transcriptional silencing was initially identified in human fibroblast cells where RNA synthesis is significantly depressed in a rapid and transient manner following UV-induced DNA damage (60). Following studies have shown that UV-irradiation induces local transcriptional silencing in damaged nuclei and recovery of transcription is dependent on nucleotide excision repair (NER) (60, 61). Interestingly, RNA synthesis is also inhibited at IR-induced DSB sites marked with γH2A.X foci (62). These findings were further confirmed by the Friedl group, who demonstrated that the repressive H3K27me3 mark is enriched at γH2A.X-marked DSB sites with concomitant exclusion of H3K4me3, which is associated with active transcription (63). Moreover, along with these repressive chromatin marks, several heterochromatin components (such as kap-1, HP1, suv39h1, and Polycomb group (PcG) that are known to be associated with transcription repression are enriched at DSBs (64, 65). Findings from the Elledge group suggest that PARP-dependent chromatin remodeling also plays an integral role in transcriptional silencing at DSB sites (66). However, the mechanistic detail of how the transcriptional silencing is achieved in the vicinity of DSBs is still poorly understood. Using a reporter-based assay system, a recent study has shown that transcription at the damaged sites is inhibited in an ATM-dependent manner. ATM kinase plays an essential role in inhibiting transcription elongation-dependent chromatin decompaction. In addition, their findings indicate that ATM-dependent transcriptional silencing at damaged chromatin is associated with RNF8 and RNF168 activity in a manner independent of

13

Lys63-linked ubiquitination (67). However, whether additional linkage-specific ubiquitin conjugation exists at DSB sites that play an essential role in inducing transcriptional silencing still remains unknown. Further research is needed to provide meaningful insights into ubiquitin-dependent transcriptional silencing at DNA damage sites.

1.8 Objective:

PTMs have emerged as key regulatory players in DDR signaling, In this thesis, I sought to explore two different PTMs, phosphorylation and ubiquitination, in the DDR pathway. In my first study, I examined how DNA damage-induced phosphorylation of Abraxas protein induces stable dimerization of the tumor suppressor protein, BRCA1, essential for efficient recruitment of BRCA1 to damaged chromatin. This study gleans structural and functional insights into how Abraxas-BRCA1 interaction is modulated in response to DNA damage in order to promote BRCA1 accumulation at damage sites for effective repair and maintenance of genomic stability. In my second study, I investigated the function of non-Lys63-linked ubiquitination in the DNA damage response pathway. I found that, in addition to Lys63-linked ubiquitination, chromatin-bound proteins are also modified by Lys11-linked ubiquitination and that these Lys11-linked chains are essential for transcriptional silencing at the DNA damage sites. Findings from these studies provide mechanistic insights into the complexity of the DNA damage response signaling, deepening our understanding of how PTMs regulate the DDR pathway to prevent genomic instability.

CHAPTER 2

INTRODUCTION: ABRAXAS PHOSPHORYLATION-DEPENDENT BRCA1-BRCT

DIMERIZATION AT DNA DAMAGE SITES

This chapter is based upon Wu Q*, **Paul A***, Su D, Mehmood S, Foo TK, Ochi T, Bunting EM, Robinson CV, Wang B, Blundell TL (2016). Structure of BRCA1-Abraxas complex reveals phosphorylation- dependent BRCT dimerization at DNA damage sites, **Molecular Cell**, 4;61(3):434-48

- These authors contributed equally to this work.
  Note: Only results generated from my study are included in the result section of this chapter

2.1 Introduction

The tumor suppressor BRCA1 has emerged as the master regulator of the genome integrity. Recent proteomic and genetic studies have revealed that BRCA1 associates with large number of proteins in cells forming distinct BRCA1 complexes *in vivo* to exert its function in DNA damage repair, transcription, cell cycle regulation, replication as well as other signaling pathways to maintain genomic stability and function as a tumor suppressor (68, 69). The majority of the hereditary breast and ovarian cancer syndrome (HBOC) patients carry mutations in the BRCA1 gene and to a lesser extent in the BRCA2 gene (70). HBOC patients have a lifetime risk of developing breast and ovarian cancer of up to 60-80% and 20-40%, respectively (71). In addition to early onset of breast and ovarian cancer, HBOC patients also have a higher risk of developing pancreatic, fallopian tube, prostate and stomach cancer. More than 800 clinically relevant mutations have been identified to date in the BRCA1 gene indicating BRCA1 plays crucial role as a tumor suppressor to maintain genome integrity (72-74). BRCA1 associates with multiple repair proteins forming distinct subcellular complexes to exert its role as in various cellular signaling pathways including DNA damage repair, DNA replication, DNA end resection, transcription, and cell cycle regulation (75, 76). BRCA1 deficiency leads to defective S phase, G2-M and spindle assembly checkpoints as well as defective DNA repair that trigger genome instability in cells. In addition, BRCA1-associated tumors have shown further genetic alteration that includes loss of heterozygosity of tumor suppressor genes as well as activation of oncogenes (such as cyclin D1, c-Myc and ErbB2) (77-79). These findings collectively indicate that BRCA1 functions as a

master regulator in maintaining genome stability and tumor suppression.

2.1.1 BRCA1 domain organization

BRCA1 is a large protein of 1863 amino acids containing an N-terminal RING E3 ubiquitin ligase domain and two C-terminal BRCT domains (80) (Figure 4). The RING domain is a motif found in many E3 ubiquitin ligase enzymes and involved in mediating protein ubiquitination. The BRCA1 RING domain mediates stable association with BRCA1-associated RING domain protein 1 (BARD1) and BRCA1-BARD1 heterodimer has been implicated in catalyzing Lys6-linked polyubiquitin chain that is recognized but not degraded by 26S proteasome (81-84). Although earlier studies indicated that BRCA1-BARD1 E3 ligase activity plays an essential role for BRCA1's tumor suppressor function, a recent study using genetically engineered mouse model has shown that BRCA1 E3 ligase activity is not required for its function in homologous recombination-mediated repair and tumor suppression (85).

The BRCT domains, each containing about 100 amino acid residues and arranged in a head-to-tail fashion, consist of three α-helices packed around four strands of β-sheet (86). BRCA1 BRCT domain has been characterized in regulating diverse biological processes by associating with multiple proteins forming distinct subcellular complexes. The BRCT domain directly interacts with phosphorylated proteins containing pSPxF (87) motif (68, 69). Using a knock-in mouse model, *Shakya et al* has recently shown that mutations in the BRCA1 BRCT domain that disrupt phosphoprotein recognition leads to tumorigenesis in mouse (85) emphasizing that BRCT interaction with pSPxF motif-containing proteins is
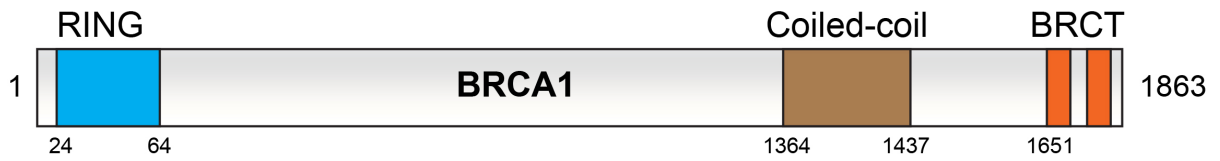
Figure 4: **Domain organization of BRCA1.** BRCA1 contains a RING domain at its N-terminus, a centrally located coiled-coil domain and two BRCT domains at its C-terminus.

essential for BRCA1's tumor suppressor function. Many tumor-derived clinically relevant mutations have been identified in the BRCA1 BRCT domain. While some of these mutations have been shown to destabilize the BRCT structure or interfere with its binding to the pSPxF motif-containing proteins leading to cancer predisposition, the function of a large number of BRCT domain mutations still remains to be determined. To date, three pSPxF motif containing proteins, Abraxas, BACH1, and CtIP, have been shown to directly interact with BRCA1 BRCT domain forming three mutually exclusive protein complexes with specific functions, designated as A, B, and C, respectively named after the main adaptor protein in these complexes (68). Although how these three complexes transmit BRCA1 signal has been largely unknown, it appears that BRCA1 involvement in these complexes plays a major role in its tumor suppressor function.

2.1.2 BRCA1-A complex

BRCA1-A complex consists of five different proteins: Rap80, Abraxas also known as CCDC98), NBA1 (also known as MERIT40), BRE (also known as BRCC45) and BRCC36 (47-54). Abraxas interacts with BRCA1 BRCT domain through its C-terminal pSPTF motif (p-S406) and thereby mediating BRCA1 interaction with the A complex. It is important to note that Abraxas does not only interact with BRCA1 but also bridges interaction with other members in the A complex. Therefore, Abraxas appears to serve as a central adaptor protein in the A complex.

As described in chapter 1, DNA damage induces ATM-dependent signaling cascade at the damaged chromatin. One of the earliest events in the DDR activation

is phosphorylation of histone H2A.X (γH2A.X) by ATM kinase. This leads to phosphorylation-dependent downstream signaling cascade that culminates with ubiquitination of histone H2A and H2A.X in Lys63-linked manner by Ubc13 conjugating enzyme and RNF8/RNF168 E3 ubiquitin ligases (37-39, 41, 43, 45). The Lys63-linked polyubiquitin chain is recognized by the Ubiquitin Interacting Motif (UIM) of Rap80 that interacts with Abraxas and subsequently, the BRCA1-A complex is localized to the damaged sites. It is important to note that NBA1 and BRE interaction is essential for the integrity of the A complex (88). In addition, BRCC36 in the BRCA1-A complex contains catalytically active MPN$^+$/JAMM domain, a domain found in zinc metalloprotease deubiquitinating enzymes (DUBs) (89) and cleaves Lys63-linked polyubiquitin chain at DSB sites (90, 91). Importantly, the BRCA1-A complex shares significant similarity with the lid of the 19S proteasome regulatory complex, which cleaves the polyubiquitin chain of substrates and facilitates entry into the proteasome core for proteolytic degradation (53). Since BRCC36 has deubiquitinating activity only towards Lys63-linked polyubiquitin chain, it appears that the BRCA1-A complex assembly at the DNA damage sites serves as a DUB complex to facilitate DUB activity of BRCC36 (53).

2.1.3 Abraxas-BRCA1 interaction is essential for tumor suppression and maintaining genome stability

Mass-spec-based analysis from our lab and others identified Abraxas as a BRCA1- BRCT interacting protein. Abraxas co-localizes with BRCA1 and is essential for BRCA1 recruitment to IR-induced DSB sites. Both *in vitro* and *in vivo* biochemical analysis confirmed that Abraxas interacts with BRCA1 BRCT domain through its C-

terminal pS[406]PTF motif in which Ser406 phosphorylation is essential for BRCT-Abraxas interaction. Deletion or S406A mutation in the motif impairs BRCA1 interaction with Abraxas resulting defective BRCA1 localization to IR-induced DSB sites. Abraxas deficient cells showed hypersensitivity to IR and UV-induced DNA damages. Moreover, in consistent with BRCA1's function in homologous recombination (HR)-mediated DNA repair and cell cycle regulation, Abraxas deficient cells also showed defects in HR repair and G2-M checkpoint (47, 49). Because Abraxas interacts with BRCA1 and this interaction is essential for BRCA1's function in maintaining genome stability, our lab has generated Abraxas knockout mouse to examine whether Abraxas functions as a tumor suppressor *in vivo*. We found that *Abraxas* knockout mice exhibit chromosomal instability and increased tumor incidence developing lymphomas and tumors of other origins. Furthermore, bioinformatics analysis of human tumors from TCGA and COSMIC databases revealed *Abraxas* gene expression is lost/reduced in multiple types of cancers including breast and ovarian cancer. Along with copy number loss or reduced expression, this analysis identified somatic mutations of Abraxas in endometrial, lung, colon, liver, kidney and leukemia (Figure 5). Of note, among 26 mutations found in *Abraxas* gene, six mutations were found to generate C-terminal pSPTF motif truncated products that cannot bind to BRCA1 protein highlighting the importance of this motif in interacting with BRCA1. Collectively, these findings suggest that Abraxas is a bona fide tumor suppressor and highlight the importance of Abraxas-BRCA1 interaction in DNA repair and maintaining genome stability (55).
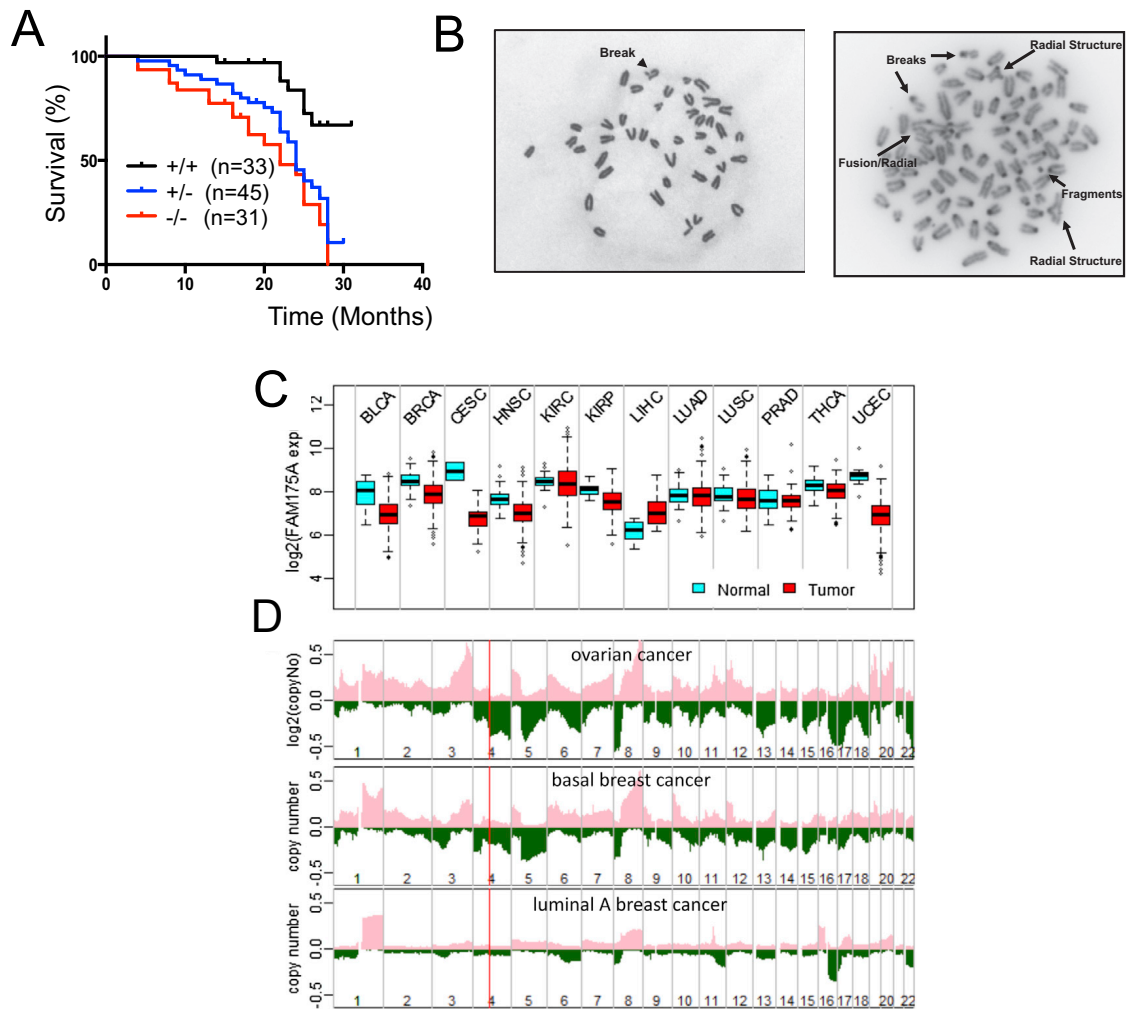
Figure 5: **Abraxas is required for tumor suppression and genome stability.**

A. *Abraxas -/+* and *Abraxas -/-* mice exhibit increased incidence of tumor susceptibility. **B.** *Abraxas -/-* MEFs (right) exhibit increased spontaneous breaks compared to *Abraxas +/+* MEFS (left). **C.** Reduced Abraxas mRNA expression in multiple tumors. **D.** Copy number loss of Abraxas in ovarian and basal breast cancer but not in luminal breast cancer.

Figure is taken from Castillo A, Paul A, Sun B, Huang TH, Wang Y, Yazinski SA, Tyler J, Li L, You MJ, Zou L, Yao J, Wang B. The BRCA1-interacting protein Abraxas is required for genomic stability and tumor suppression. Cell Rep. 2014 Aug 7;8(3):807-17.

2.1.4 Role of Abraxas phosphorylation in regulating Abraxas-BRCA1 interaction

Abraxas pSPxF motif at the C-terminus contains phosphorylated S406 residue that mediates interaction with BRCA1 and mutation in this residue (S406A) abrogates this interaction. Interestingly Abraxas S406 is constitutively phosphorylated even in absence of DNA damage. This raises the question of "how BRCA1 BRCT-Abraxas interaction is regulated in presence of DNA damage?" To address this, we analyzed the C-terminal sequence of Abraxas adjacent to the $pS^{406}PTF$ motif. Sequence analysis of the Abraxas C-terminal revealed that an additional Ser residue (S404) located adjacent to S406 in the pSPxF motif. Given the close proximity of this Ser404 residue to Ser406 in the pSPxF motif, we reason that this residue may regulate BRCA1 BRCT-Abraxas interaction. Mass-spec analysis of BRCA1-BRCT domain showed that double-phosphorylated Abraxas peptide containing phosphorylated S404 and S406 (pS404pS406) bound to BRCT and was enriched significantly upon IR-induced DNA damage, while the singly phosphorylated pS406 containing peptide bound to BRCT domain but was not enriched after IR (47). These findings indicate that while constitutive S406 phosphorylation is required for interaction with BRCA1, S404 phosphorylation may have some additional functional significance in regulating interaction with Abraxas. To gain further insights into Abraxas-BRCA1 interaction our lab generated an antibody that can specifically recognize doubly phosphorylated S404S406. The pS404pS406 specific antibody can detect Abraxas in control cells but not in Abraxas KO HEK293T cells. The double phosphorylation of Abraxas is abrogated in cells
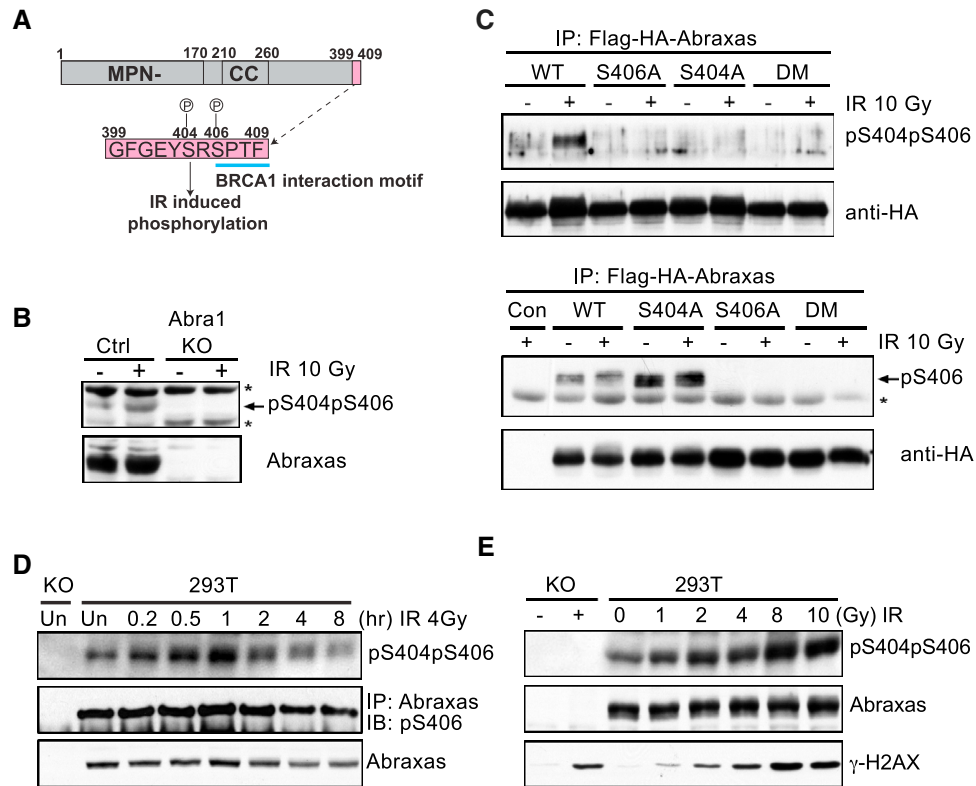
Figure 6: **IR-induced Abraxas phosphorylation at S404 and S406 is ATM dependent A.** Abraxas domain organization and C-terminal sequence containing phosphorylated S404 and S406 residues indicated as P. **B.** Double phosphorylation at S404 and S406 residues in response to IR in parental and Abraxas KO 293T cells. Cells were lysed 1 hour post-IR and analyzed by doubly phosphorylated S404S406 antibody. **C.** IR-induced Abraxas double phosphorylation is abolished in Abraxas S406A, S404A and S404AS406A double mutants. **D**. DNA damage-induced phosphorylation of Abraxas occurs immediate after IR. Western blot analysis was performed at indicated time-points with pS404pS406 antibody and pS406 antibody. . **E.** IR-induced Abraxas phosphorylation occurs in a dose-dependent manner. *Results were obtained by Dan Su, Ph.D., Wang Lab.*

expressing S404A, S406A as well as S404AS406A double mutant (Figure 6). We tested Abraxas phosphorylation status using the doubly phosphorylated antibody as well as previously generated phosphorylated S406 antibody. As shown in Figure 6, while the band intensity of pS406 antibody did not change after DNA damage; using pS404pS406 antibody we detected Abraxas band intensity increased in a time-dependent manner up to 1 hour post-IR followed by gradual gradually decrease to the basal level at later time-points. Furthermore, we found that pS404pS406 band intensity increased in DNA dose-dependent manner. Since phosphorylation at S406 did not change after IR treatment, these results indicate that phosphorylation at S404 is likely to be IR-induced (87).

2.1.5 DNA damage-induced ATM-dependent phosphorylation of Abraxas at S404

Since the apical kinase ATM plays a crucial role in the IR-induced DNA damage response pathway that recruits BRCA1 and components of the BRCA1-A complex at the sites of DNA damage, we tested whether Abraxas phosphorylation at S404 is ATM-dependent. Cells treated with ATM inhibitor KU55933 showed complete disruption of S404 phosphorylation indicating IR-induced Abraxas phosphorylation at S404 is an ATM-dependent event (Figure 7). On the other hand inhibiting the cells with ATR appeared to have minimal effect on the IR-induced phosphorylation as detected by the pS404pS406 antibody (Figure7) (87).

2.1.6 Crystal structure of BRCA1 BRCT domains in complex with single and double-phosphorylated Abraxas phosphopeptides

To mechanistically dissect the role of S404 phosphorylation in BRCT-Abraxas

26

interaction, we solved the crystal structure of BRCA1 BRCT domain with single (pS406) or double (pS404pS406) phosphorylated phosphopeptide. This work was done in collaboration with Dr. Tom Blundell's lab, University of Cambridge, UK by Dr. Qian Wu (87). The crystal structures of BRCT with both single and double phosphorylated Abraxas phosphopeptides were solved at 3.5 Å resolution. Consistent with previously solved BRCT crystal structure with BACH1 and CtIP, the two BRCT domains of BRCA1 (BRCT1 and BRCT2) associate in a head-to-tail fashion. In each domain, a four-stranded parallel β sheet is surrounded by three α helices. The Abraxas pSPxF motif interacts with BRCT domains in a two-anchor mode where S406 and F409 of the pSPxF interact with residues in the BRCT domains (Figure 8).

Importantly, the crystal structure data of BRCA1 BRCT with single phosphorylated S4046 (termed as BRCT-Ab1p) and double phosphorylated S404S406 (termed as BRCT-Ab2p) revealed unique differences in the conformation of $Y^{403}S^{404}R^{405}$ region, which is located adjacent to the pSPTF motif in Abraxas. Extra electron density corresponding to the phosphate group of phosphorylated S404 and the side chain of Y403 was observed in the case of BRCT-Ab2p but not in the case of BRCT-Ab1p (Figure 8C & D). In addition, unlike BRCT-Ab1p, in the BRCT-Ab2p complex, we found that the pS404 is oriented away from the BRCT domain into the solvent region. The change in pS404 conformation fixes the side chain of Y403 that generates additional interaction with BRCT K1671 residue forming a hydrophobic interaction at the N-terminus of BRCT α1. Additionally, the negative surface region formed by the phosphate group of pS404

27
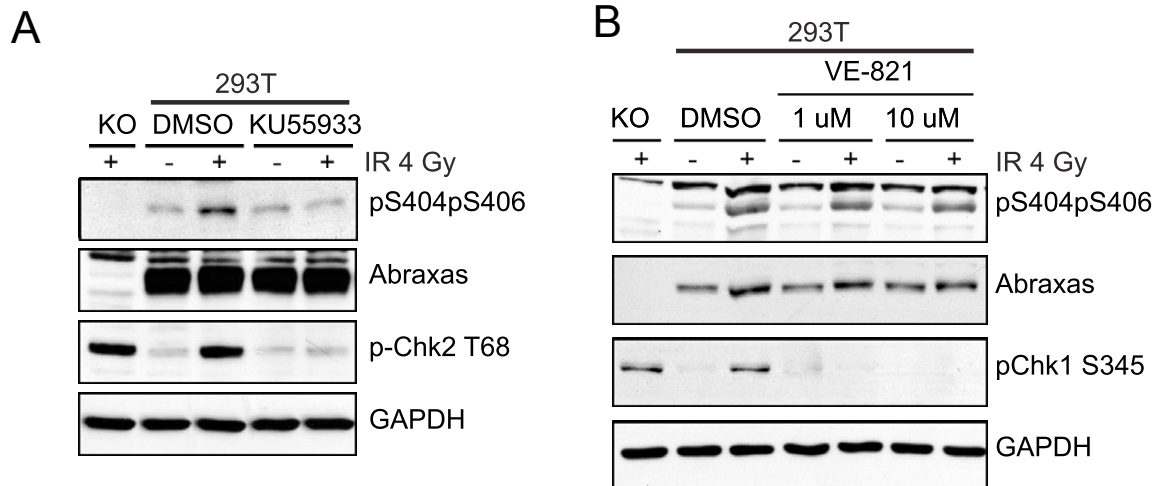
Figure 7. ATM-dependent Abraxas phosphorylation. A. ATM –dependent Abraxas phosphorylation. Cells were treated with ATM inhibitor KU55933 (10 uM) for 2 hours before IR treatment. Abraxas phosphorylation is detected with pS404pS406 antibody. **B.** ATR is not involved in IR-induced Abraxas double phosphorylation. Cells were treated with ATR inhibitor (VE-821) for 2 hours before IR treatment. pS404pS406 antibody was used to detect phosphorylation status of Abraxas.

Results were obtained by Dan Su, Ph.D., Wang Lab.

and side chain E402 leads to cross interaction with BRCT K1671 (Figure 8E) (87).

Collectively, these events promote stable dimerization of the BRCT-Ab2p complex

involving α1 and β2 of the BRCT1 domain and the Ab2p (Figure 9A). α1 of the

BRCT1 domain form hydrophobic interaction between α1 helices (α1- α1) and

extensive hydrogen bonding between the two antiparallel β strands (β2- β2) (Figure

9). At the dimerization interface, we found two of the α1 helices from each BRCT1

domain form isologous interactions burying a hydrophobic patch formed by F1662,

M1663 and Y1666 residues with hydrophobic side chains stacking on each other

(Figure 9B). Importantly, two of three residues (F1662 and M1663) in the BRCT

dimerization interface were identified as BRCA1 germline mutations (F1662S and

M1663K) in the Breast Cancer Information Core database (92) suggesting that

mutations in these residues may disrupt the stable dimer structure and thereby

impairs BRCA1's role as tumor suppressor.

2.1.7 BRCT-Ab2p complex forms a dimer *in vitro*

BRCA1 BRCT-Abraxas dimerization was examined *in vitro* by size-exclusion

chromatography in collaboration with Dr. carol Robinson's lab at the University of

Oxford. The gel filtration analysis obtained from BRCT-Ab1p and BRCT-Ab2p

complexes revealed that compared to the elution peak for BRCT-Ab1p complex,

which aligns with BRCT-Bach1 and BRCT-CtIP complexes, the peak for BRCT-Ab2p

complex shifted to the left of the BRCT-Ab1p suggesting a larger hydrophobic radius

and a possible higher order complex. And according to the protein size markers, the

size of BRCT-Ab2p appeared to be roughly double to that of the BRCT-Ab1p

complex (Figure 10A). Moreover, measuring the exact molecular weight of peak
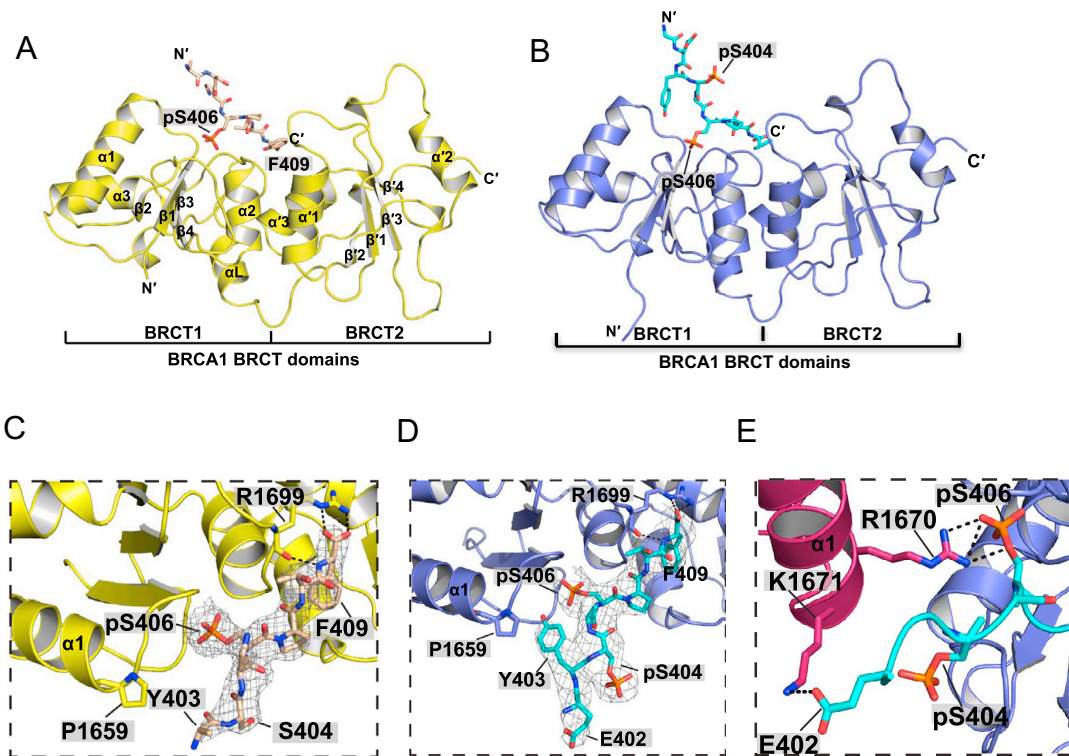
Figure 8. Crystal structure of BRCT in complex with single and doubl phosphorylated Abraxas phosphopeptide. A. Crystal structure of BRCT-Abraxas pS406 complex (BRCT-Ab1p). The BRCT domains are in yellow and the Abraxas pS406 phosphopeptide is in wheat color. **B** Crystal structure of BRCT-Abraxas pS406pS404 complex (BRCT-Ab2p). The BRCT is depicted in blue and pS404pS406 is denoted in cyan. **C & D.** Interface between BRCT and Abraxas phosphopeptide in BRCT-Ab1p (C) and BRCT-Ab2p complexes (D). The 2Fo-Fc electron density (s = 1.0) is shown for Abraxas phosphopeptides. **E.** Interaction between BRCT α1 helix and Ab2p.

Crystal structure data was collected by collaborator Dr. Tom Blundell's group, University of Cambridge.

fractions eluted from size exclusion chromatography by using nano-electrospray mass spectrometry under native conditions showed while BRCT-Ab1p complex appeared to exist predominantly as a 1:1 monomer with a small fraction forming 2:2 dimer, the BRCT-Ab2p was found to exist mostly as 2:2 complexes, indicating a much stable dimer formation. BRCT-Bach1 and BRCT-CtIP were detected as 1:1 monomeric complexes similar to BRCT-Ab1p complex (Figure 10 B-E) **(87)**. Collectively, these findings indeed confirm the crystal structure data that doubly phosphorylated Abraxas phosphopeptide induces stable dimerization of BRCA1 BRCT-Abraxas complex.

2.1.8 Abraxas S404 phosphorylation is essential for stable BRCA1 BRCT-Abraxas complex dimerization

In order to corroborate functional significance of Abraxas S404 phosphorylation in inducing stable dimerization, mutational analyses were performed using S404P and S404D mutants. Size exclusion chromatography with phosphomimetic S404D mutant revealed BRCT-Ab1p (S404D) can maintain 2:2 dimer complex, while BRCT-Ab1p (S404P) led to the formation of 1:1 complex (Figure 11A**)**. These findings highlight the functional significance of S404 phosphorylation. In addition analysis of the N-terminal sequence of the pSPTF motif, which includes GFGEYS^{404}RS^{406}PTF, revealed while GFGE is not absolutely required for the dimer formation, the presence of this sequence stabilizes the dimer structure (data not shown).
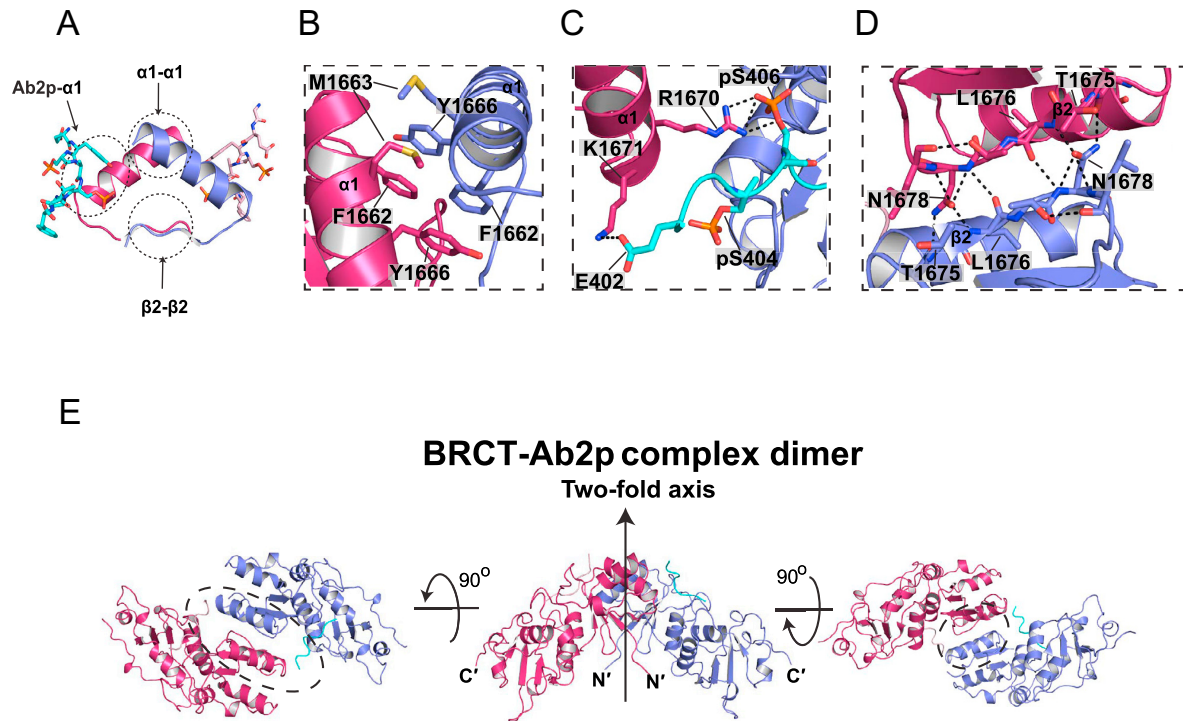
Figure 9. Ab2p induces stable dimerization of BRCT-Ab2p complex. A.
Simplified BRCT-Ab2p dimer interface containing three regions observed in
BRCT-Ab2p crystal structure that contribute to formation of the dimer interface –
N-terminal hydrophobic region of BRCT α1–α1 **(B)**, Extensive hydrogen
bonding by β2–β2 strands **(C)** and N-terminal region of Ab2p including the
phosphorylated S404 interaction with BRCT α1 **(D)**. **E.** Crystal structure of
BRCT-Ab2p complex viewed from three different directions with a two-fold axis.

*In vitro data was collected by collaborators Dr. Tom Blundell's group, University
of Cambridge and Dr. Carol Robinson's group, University of Oxford.*
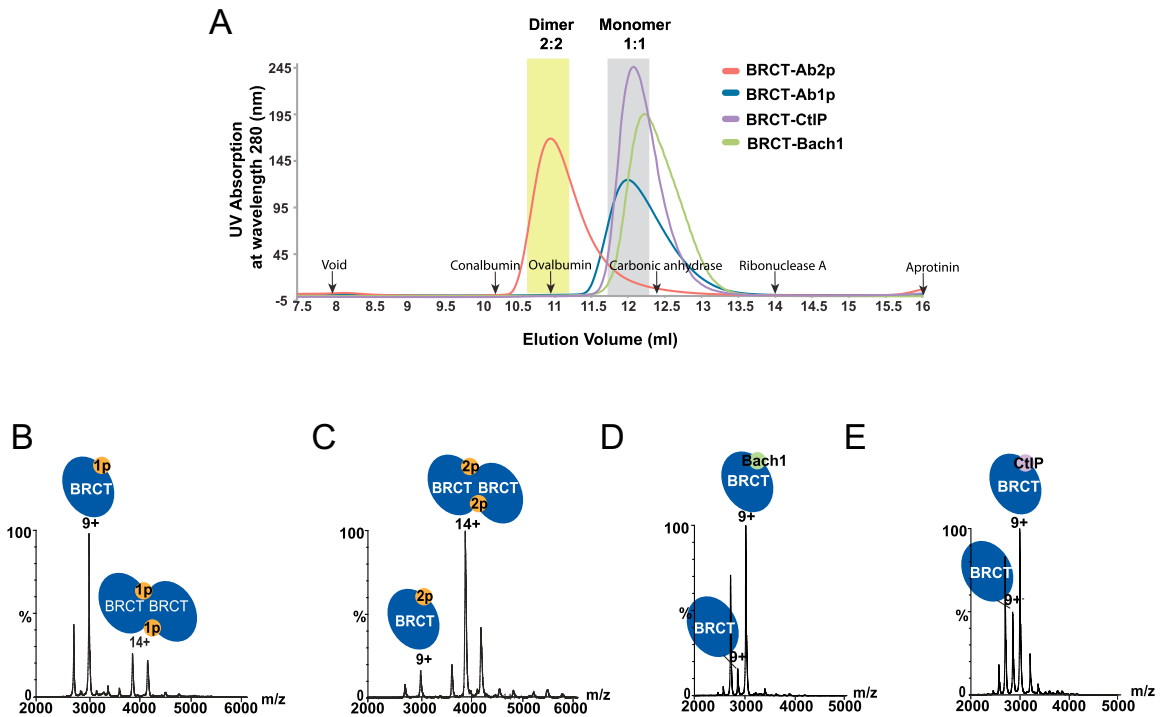
Figure 10. Double phosphorylated Abraxas phosphopeptide induces dimerization of BRCT-Ab2p complex. A. Size exclusion chromatography of BRCT complex with Ab1p, Ab2p, BACH1 and CtIP phosphopeptides. The regions for dimer complex (2:2 complex) and monomer complex (1:1 complex) are high lined in yellow and gray shades. (**B-E)** The native mass spectra of BRCT-Ab1p (B), BRCT-ab2p (C), BRCT-Bach1 (D), and BRCT-CtIP (E) complexes tested at 15 uM.

In vitro data were collected by collaborators Dr. Tom Blundell's group, University of Cambridge and Dr. Carol Robinson's group, University of Oxford.

2.1.9 Germline mutation in the BRCT dimerization interface disrupts stable BRCT-Ab2p complex dimerization *in vitro*

The crystal structure data revealed that the BRCT dimerization involves $\alpha 1$ and $\beta 2$ of the BRCT1 domain forming hydrophobic interaction between $\alpha 1$ helices ($\alpha 1$- $\alpha 1$) and extensive hydrogen bonding between the two antiparallel β strands ($\beta 2$- $\beta 2$) (Figure 9). The $\alpha 1$- $\alpha 1$ dimerization interface consists of hydrophobic patch formed by F1662, M1663 and Y1666 amino acids with aromatic side chains stacking on each other (Figure 9B). As discussed in section 2.1.6, F1662 and M1663 residues were identified as germline mutations as F1162S and M1663K in cancer patients (92). To understand whether $\alpha 1$- $\alpha 1$ interaction contributes more significantly than $\beta 2$- $\beta 2$ interaction in stabilizing the dimer interface, size-exclusion chromatography was carried out with mutants that disrupt the $\beta 2$- $\beta 2$ and $\alpha 1$- $\alpha 1$ interaction. While the BRCT N1678A-Ab2p complex appeared to have minimal effect in destabilizing the dimer structure, the germline mutations F1662S and M1663K led to complete disruption of the dimer formation. BRCT Y1666A mutation did not appear to have much role in the stability of the dimer structure as the elution peak was detected between 2:2 and 1:1 complexes (Figure 11B). Collectively these results support our crystal structure results that F1662S and M1663K mutants disrupt the dimer stability indicating these residues likely play a crucial role in BRCA1's tumor suppressor function (87).
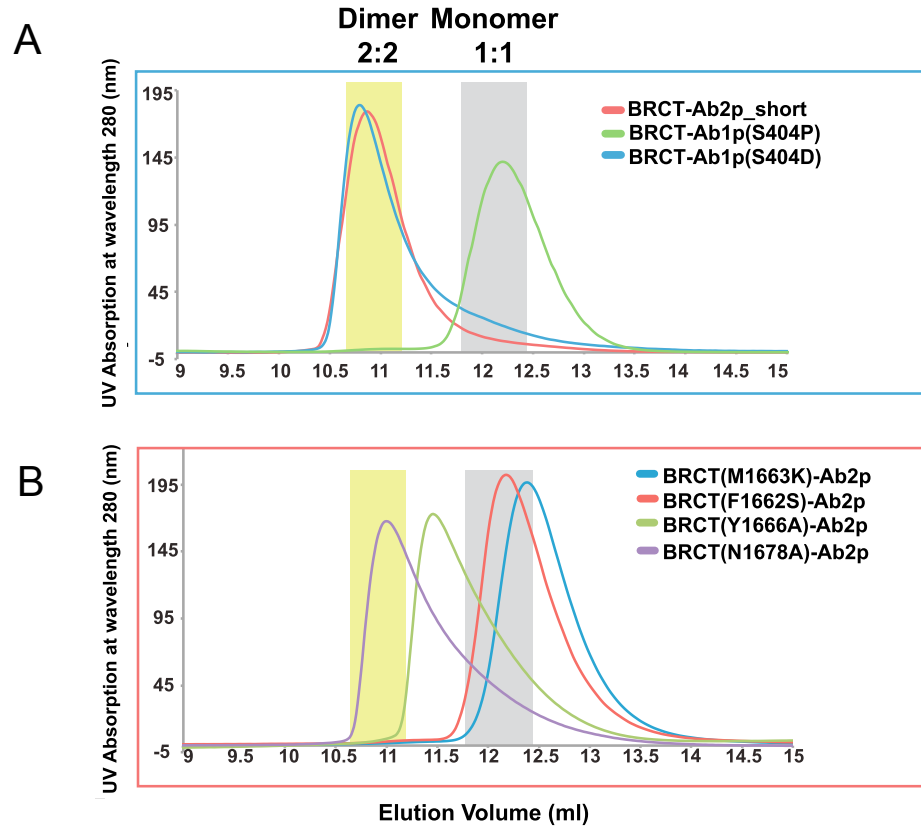
Figure 11. Mutagenesis analysis of BRCT-Ab2p dimer Interface reveal the importance of S404 phosphorylation and residues of BRCA1 germline mutations for stable BRCT/Abraxas dimer formation. A. Gel filtration analysis of BRCT-Ab1p complex containing S404P or phosphomimetic mutant S404D or BRCT-Ab2p complex. **B.** Gel filtration analysis of BRCT-Ab2p complex containing BRCA1 BRCT mutations present in the dimerization interface.

In vitro data were collected by collaborators Dr. Tom Blundell's group, University of Cambridge and Dr. Carol Robinson's group, University of Oxford.

2.1.10 Abraxas dimerization/oligomerization in cells is independent of BRCA1 binding

The findings from this study led us to question whether Abraxas also forms a dimer in which the phosphorylated C-termini of Abraxas in complex with BRCA1-BRCT could be in close proximity for dimerization. To test this, differentially tagged Abraxas molecules, either WT or S404A and S4046A, were immunoprecipitated and detected by western blot analysis. As shown in Figure 12A, both WT and S404A as well as S406A, mutant interact with differentially tagged counterpart suggesting that mutation in S404 or S406 does not disrupt Abraxas dimerization and that Abraxas dimerization is independent of its binding to BRCA1. To further examine the domain required for Abraxas dimerization, Abraxas truncation mutants were generated and tested for binding to its counterpart. Importantly, we found that deletion of the coiled-coil domain in Abraxas disrupts its self-interaction with both WT or coiled-coil deletion mutant (Figure 12B). Taken together, these findings suggest that Abraxas dimerization/oligomerization occurs independently of BRCA1 BRCT dimerization through its coiled-coil domain.

2.1.11 Objective

Although *BRCA1* was cloned more than 20 years ago, the exact mechanism of how it functions as a tumor suppressor still remains to be determined. BRCA1 BRCT domain serves as a phosphopeptide-binding module that recognizes pSPXF motif containing proteins including Abraxas, BACH1, and CtIP, forming three mutually exclusive complexes termed as A, B and C complex, respectively. The

36
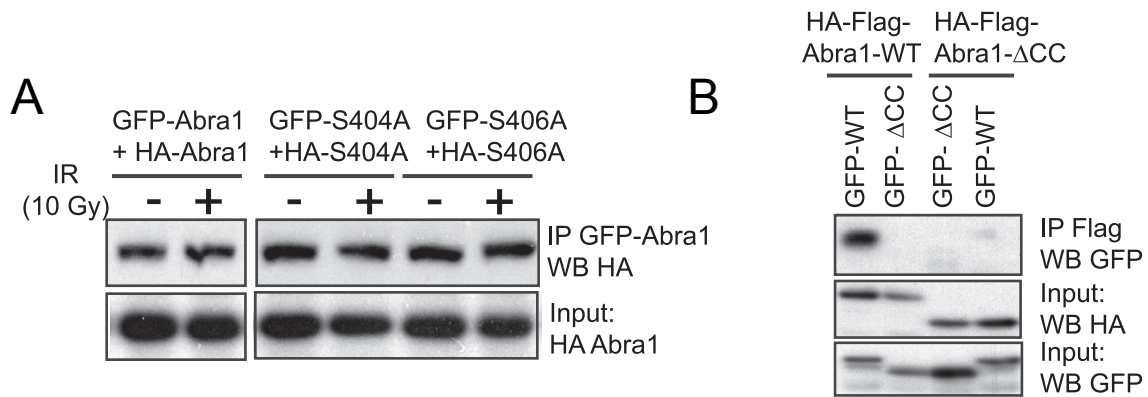
Figure 12. Abraxas dimerization/oligomerization *in vivo* is independent of binding to BRCA1. A. The differentially tagged GFP- and HA-Flag-tagged WT or Abraxas mutants (S404A or S406A) were co-transfected in cells, irradiated (or untreated) followed by GFP immunoprecipitation and interaction between differentially tagged Abraxas mutants was analyzed by immunoblot using HA antibody. **B.** Abraxas dimerizes/oligomerizes through the coiled-coil (CC) domain. The immunoprecipitation was carried out with lysates prepared from cells expressing HA-Flag-tagged WT Abra1 or ΔCC mutant and GFP-tagged WT or ΔCC mutant.

Results were obtained by Dan Su, Ph.D., Wang Lab.

phosphopeptide binding ability of BRCA1 BRCT domain is essential for its tumor suppressor function and has been shown to harbor many clinically important breast and ovarian cancer mutations that lead to early onset of breast cancer in patients (Source: National Cancer Institute) (85, 93, 94). Therefore structural and functional analysis of the BRCA BRCT binding with pSPxF motif containing proteins is essential to understand the tumor suppressor function of BRCA1. Structural analysis of BRCA1-BRCT in complex with other pSPxF motif containing proteins, BACH1 and CtIP, has been solved previously providing a valuable structural framework into this interaction (94-97). However, a detailed structural analysis of BRCA1 BRCT-Abraxas interaction still remains largely unknown. The interaction of Abraxas with BRCA1 is essential for BRCA1 recruitment to DNA damage sites and maintenance of genome stability. The significance of Abraxas pSPxF motif interaction with BRCA1 BRCT in tumor suppression is exemplified by identification of an Abraxas mutation in tumor harboring F409C (55). In this study, we employed in vitro analysis to solve the crystal structure of BRCT-Abraxas complex that showed that phosphorylation at S404 residue induces stable dimerization of BRCT-Abraxas complex. Moreover, at the BRCT dimerization interface we found two germline BRCA1 mutations that destabilized the dimer structure *in vitro*. However, there are several questions that arise from these *in vitro* findings. First, "What is the functional significance of Abraxas S404 phosphorylation in terms of BRCA1 localization to damage sites?" Second, "Does BRCA1 dimerization occur *in vivo* through its BRCT domain?" And third, "Does BRCA1 dimerization *in vivo* in Abraxas-dependent manner?" Addressing these questions will not only validate our *in vitro* findings of BRCT-

Abraxas complex dimerization but will also provide insights into the functional

significance of DNA damage-induced Abraxas S404 phosphorylation in regulating

BRCA1 dimerization at the DNA damaged chromatin, deepening our understanding

of Abraxas and BRCA1 tumor suppressor function to maintain genome stability.

2.2. Materials and Methods

2.2.1 Cell culture

All cell lines were maintained using standardized methodology in sterile

condition. U2OS cells were grown in McCoy's 5A medium (Corning) supplemented

with 10% fetal bovine serum (FBS) and maintained at 37^0C with 5% CO2

atmosphere. HEK293T cells were cultured in DMEM (Corning) supplemented with

10% FBS.

2.2.2 Generation of stable cell lines

To generate Abraxas knockdown cells complemented with WT or mutant

Abraxas, U2OS cells were infected with retrovirus containing shRNAs against

Abraxas followed by selection with puromycin (0.8 ug/ml) for 5 days. The Abraxas

knockdown stable cell line was then complemented with expression of empty MSCV

vector or expression constructs containing HA-tagged WT or mutant Abraxas, and

selected with Blasticidin (9 ug/ml) 1 week for stable expression. Abraxas knockdown

efficiency and complementation with HA-tagged Abraxas was confirmed by western

blot with Abraxas and HA antibodies.

2.2.3 Cell lysis and Western blot

Cell lysis and western blot analyses were performed using established

methodology. Cells were lysed in NETN buffer (50 mM Tris-HCl, pH 8.0, 150 mM NaCl, 1 mM EDTA, 0.5% Nonidet P-40) with protease inhibitors (98) and protein phosphatase inhibitors, 1 mM NaF, and 1 mM Na3VO4. Cells were lysed on ice for atleast 30 minutes followed by brief sonication (Bioruptor) and centrifuged at 13,200 rpm to remove cellular debris. Protein concentration was measured by Bradford assay and 50 μg protein lysate were used for western blot analysis. Samples were run in 10% SDS-PAGE gel and run at 90 volts for 2-3 hours in a Biorad Mini-PROTEAN electrophoresis chamber using running buffer followed by transfer into nitrocellulose membrane using cold transfer buffer. The membranes were blocked with 4% milk for at least 20 minutes followed by incubation with primary and secondary antibodies. Blots were washed at least 4 times after each antibody incubation and developed using ECL-plus chemiluminescent detection reagent (Promega).

2.2.4 Immunofluorescence

Abra1 shRNA knockdown cells complemented with empty vector, wild type or mutants of Abraxas were analyzed for BRCA1 IR-induced foci formation (IRIF). Following 10 Gy irradiation from a ^{137}Cs source, cells were incubated at 37^0C for 2 hours. Cells were then fixed with 3.6% formaldehyde for 10 min, permeabilized with 0.5% Triton X-100 solution, and incubated with primary antibodies for 1 hr at 370C followed by appropriate Alexa 488-conjugated (green; Invitrogen) and Alexa 555-conjugated (red; Invitrogen) secondary antibodies. At least 500 cells were counted for each cell type and cells containing more than 10 foci were counted as positive. All images were obtained with a Nikon TE2000 inverted microscope with a

Photometrics Cool- Snap HQ camera. Quantification of BRCA1 was performed using Imaris software (Bitplane). The DAPI channel was used to select the nuclei of the cells in the field, red and green channel were used for BRCA1 and γH2AX, respectively. For BRCA1 foci intensity measurement, foci were defined as particles bigger than 0.25 µM in diameter with an intensity cut-off value (1200) to eliminate background. At least 50 cells were counted and plotted using GraphPad Prism software. Statistical analysis was performed by student's t-test or ANOVA with Tukey's multiple comparisons test. p-value is as indicated.

2.2.5 Coimmunoprecipitation

Cells were lysed in NETN buffer containing protease inhibitor and phosphatase inhibitor. For Flag IP, cell lysates were incubated with Flag beads (98) overnight with gentle agitation at 4oC. The beads were washed with NETN lysis buffer four times and eluted with 3X sample buffer for Western blot analysis. For analyzing Abraxas dimerization in vivo, GFP-tagged and HF- tagged Abraxas wildtype, S404A, S406A mutant or coiled-coil deletion mutant were transiently transfected to 293T cells. Two days after transfection, cells were either untreated or exposed to 10 Gy IR. 2 hr later, cells were collected for GFP- or Flag- IP and Western blot was probed with either antibodies against HA or GFP. For analyzing BRCA1 dimerization in vivo, Flag- or Myc-tagged BRCA1 full-length wild type or mutants, or HA- and Myc-tagged BRCA1 BRCT fragments were analyzed in a similar way.

2.2.6 Clonogenic survival assay

Abra1 shRNA knockdown cells complemented with empty vector, wild type or

mutants of Abra1 were analyzed for cell survival in response to IR. Stable U2OS cell lines were seeded at low density in 10 cm dishes and irradiated with 4 Gy ionizing irradiation using a 137Cs source. The cells were then cultured at 37°C for 14 days to allow colonies to form. Colonies were stained with 2% methylene blue and 50% ethanol for 10 min. Colonies containing 50 or more cells were counted as positive and statistical data were analyzed by analysis of variance (99) with Tukey's multiple comparisons test.

2.2.7 Chromatin fractionation

Cells were irradiated at 10 Gy followed by 1 hr incubation at 37^0C. For total cell extracts, cells were lysed in NETN150 buffer containing protease inhibitor mixture and analyzed by Western blot. For chromatin fractionation, irradiated cells were washed in PBS and resuspended in Buffer A (10 mM Hepes pH 7.9, 10 mM KCl, 1.5 mM $MgCl_2$, 0.34 M sucrose, 10% glycerol, 5 mM NaF, 1 mM Na_3VO_4 , 1 mM dithiothreitol (DTT), and protease inhibitor mixture) containing 0.1% Triton X-100, and incubated on ice for 5 min for permeabilization. The cytosolic fraction was then separated by centrifugation at 4000 rpm for 5 min at 4°C. The supernatant was discarded and the nuclei pellet was washed once with Buffer A and resuspended in Buffer B (3 mM EDTA, 0.2 mM EGTA, 1 mM DTT, protease inhibitor mixture) and incubated for 30 min on ice. The soluble nuclear fraction was separated by centrifugation at 4500 rpm for 5 min. The chromatin fraction pellet was washed with Buffer B and resuspended in 100 µl Laemmli sample buffer and sonicated for 10 sec before analysis.

2.3 Results

2.3.1 Generation of Abraxas knockdown cells complemented with WT or mutant Abraxas

As discussed in section 2.1.5, while S406 is constitutively phosphorylated even in absence of DNA damage, we found DNA damage triggers ATM-dependent phosphorylation at S404 residue in DNA dose- and time-dependent manner (Figure 13A). To dissect functional significance of S404 phosphorylation in the DDR pathway, I stably knocked down Abraxas in U2OS cells using retrovirus-encoding shRNAs targeting endogenous Abraxas. These cells were then complemented with shRNA-resistant HA-tagged WT, S404A or S406A mutants of Abraxas. The knockdown efficiency and complementation with above-mentioned constructs were confirmed by western blot analysis with Abraxas antibody (Figure 13B). Tubulin was used as loading control.

2.3.2 Increased cellular sensitivity to IR-induced DNA damage of Abraxas-deficient cells expressing mutants of Abraxas.

Since S404 is phosphorylated in DNA damage-dependent manner that likely plays a role in stable BRCT-Abraxas dimerization in cells, I tested whether S404 phosphorylation is critical for the function of Abraxas in response to IR. To test this I measured the cellular sensitivity of Abraxas knockdown cells expressing WT or mutant Abraxas. As shown in Figure 13, I found consistent with previous findings Abraxas depleted cells become hypersensitive to IR-induced DNA damage. Interestingly while complementing these cells with WT Abraxas can rescue the defects in cellular sensitivity, both S404A and S406A mutant expressing cells were

A

Abra1 shRNA

HA-Abra1
Abra1

Tubulin
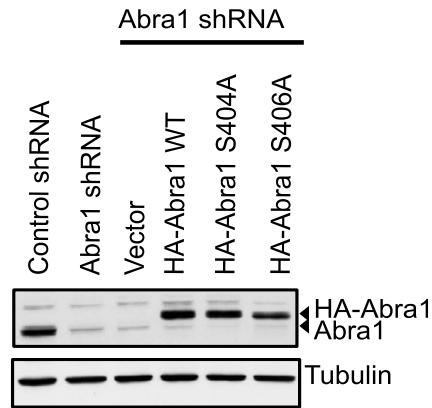
B
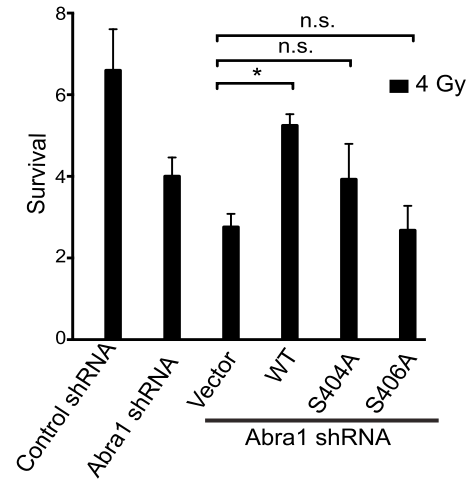
Figure 13. Abraxas phosphorylation at S404 and S406 are both essential for cellular resistance to IR. A. Abraxas stable knockdown cells complemented with vector, WT, S404A or S406A were generated as described in materials and method. Western blot analysis was performed with Abraxas antibody to confirm knockdown efficiency and expression of HA-Abra1 constructs. **B**. Increased cellular sensity to IR-induced DNA damage in Abraxas-deficient cells expressing mutant Abraxas. Colony survival assay was carried out for cells treated with 4 Gy IR. The data represented means ± SD.

were unable to fully rescue the defect. These findings suggest that phosphorylation at plays a role in cellular resistance to IR-induced DNA damage.

2.3.3 Abraxas phosphorylation is essential for efficient recruitment of BRCA1 to DSB sites

Previous findings from our lab showed that Abraxas is essential for efficient recruitment of BRCA1 to DNA damage sites and BRCA1 localization is disrupted in Abraxas KO MEF cells (55). To test whether Abraxas phosphorylation plays any role in BRCA1 recruitment to DNA damage sites, I used Abraxas knockdown cells complemented with WT or S404A and S406A mutants of Abraxas. These cells were irradiated with IR (10 Gy) and immunostained two hours post IR treatment to examine whether IR-induced foci formation (IRIF) of BRCA1. As shown in Figure 14, the BRCA1 foci formation decreased significantly upon Abraxas depletion. While the defect can be rescued by expression of HA-tagged WT Abraxas; S404A or S406A mutants of Abraxas can only partially rescue the defect. Quantification of BRCA1 foci positive cells indicate that compared to WT Abraxas cells showed neither S404A or S406A mutant expressing cells can completely rescue the defects in BRCA1 IRIF. In addition, I measured the intensity of BRCA1 IRIF in these cells. Consistent with reduced foci positive cells, both S404A and S406A expressing cells showed decreased overall BRCA1 foci intensity compared to WT Abraxas expressing cells.

2.3.4 BRCA1 accumulation at damaged chromatin requires both S404 and S406 phosphorylation of Abraxas

To further validate the defects of BRCA1 localization to IR-induced foci in

Abraxas phosphorylation-deficient mutant expressing cells, I isolated chromatin

fraction from Abraxas depleted cells complemented with WT or phosphorylation-

deficient mutants (S404A, S406A or S404AS406A) 1-hour post-IR and analyzed for

accumulation of BRCA1 to damaged chromatin by western blot analysis.

Consistently, I observed that depletion of endogenous Abraxas impaired BRCA1

loading onto damaged chromatin. While expression of WT Abraxas in Abraxas

knockdown cells can rescue the defect, cells expressing S404A and S406A single

mutants or S404AS406A double mutant of Abraxas failed to accumulate BRCA1

onto damaged chromatin (Figure 15). This was not due to change in altered

expression of BRCA1 in these cells since the total BRCA1 protein level was not

affected in Abraxas knockdown cells or knockdown cells complemented with WT or

mutant Abraxas as shown in the total cell lysate (Figure 15 bottom panel). Orc2 was

used as a marker for chromatin fraction. Collectively, these results suggest that DNA

damage-induced Abraxas S404 phosphorylation likely plays a crucial role in BRCA1

accumulation to damaged chromatin.

2.3.5 Abraxas-dependent dimerization of BRCA1 *in vivo*

Our crystal structure data revealed that BRCA1 BRCT dimerizes in presence

of doubly phosphorylated Abraxas phosphopeptide through the BRCT1 domain

(Figure 9). To test whether BRCA1 BRCT dimerizes *in vivo* and whether this

dimerization depends on Abraxas, I co-expressed differentially Myc or Flag-tagged

BRCA1 full-length constructs in 293T parental cells or Abraxas KO cells. These cells

were irradiated, incubated at 37^0C for 1 hour and subjected to co-

immunoprecipitation analysis with Flag beads. To test whether Myc-tagged BRCA1
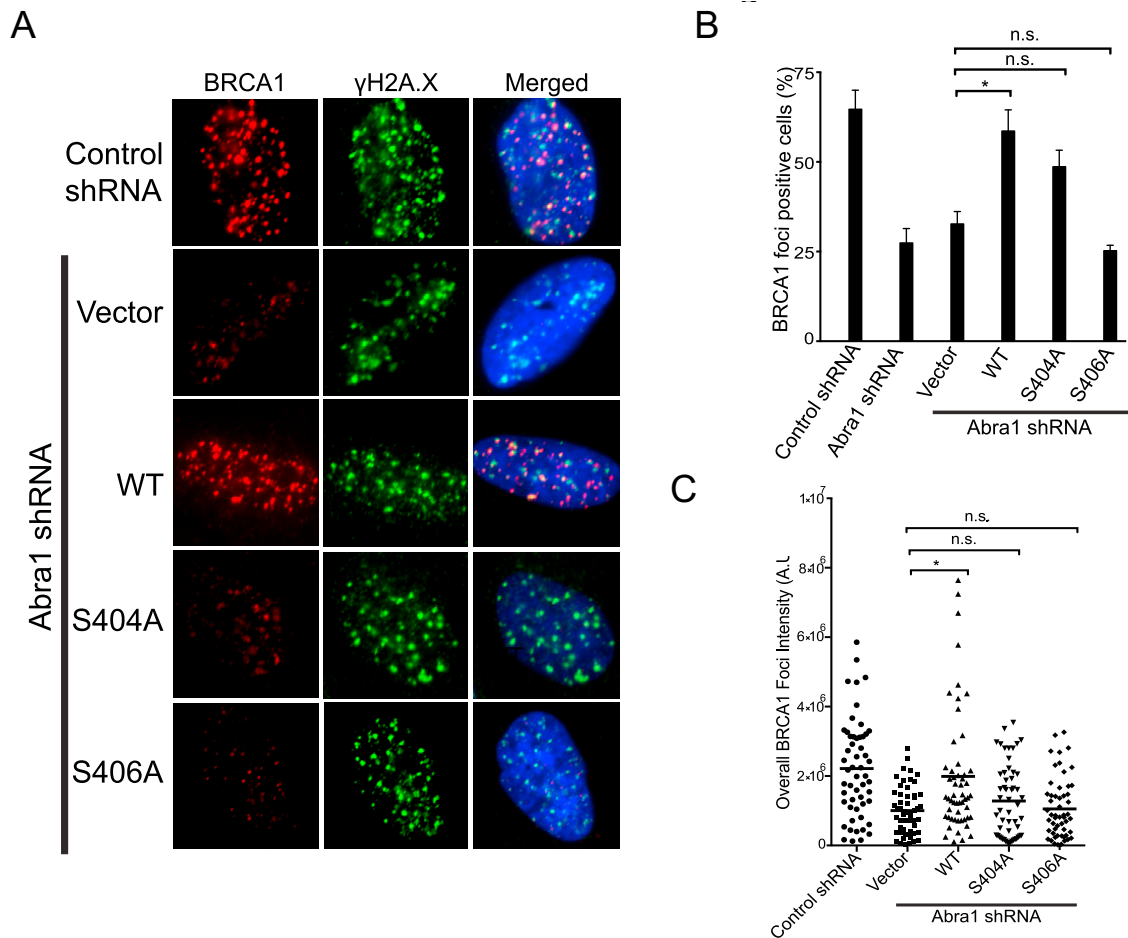
Figure 14. Abraxas phosphorylation at both S404 and S406 are important for BRCA1 accumulation at DNA damage sites. A. Representative image of BRCA1 BRCA1 IRIF in Abraxas knockdown cells complemented with vector, WT, S404A or S406A. Cells were irradiated at 10 Gy, incubated at 37^{0}C for 2 hours followed by immunofluorescence analysis with BRCA1 and γH2A.X antibodies. **B**. The percentage of cells containing more than 10 BRCA1 foci were counted and quantified. At least 300 cells were counted. The data represents means ± SD. **C.** Quantification of intensity of BRCA1 IRIF. The data represents means ± SD.
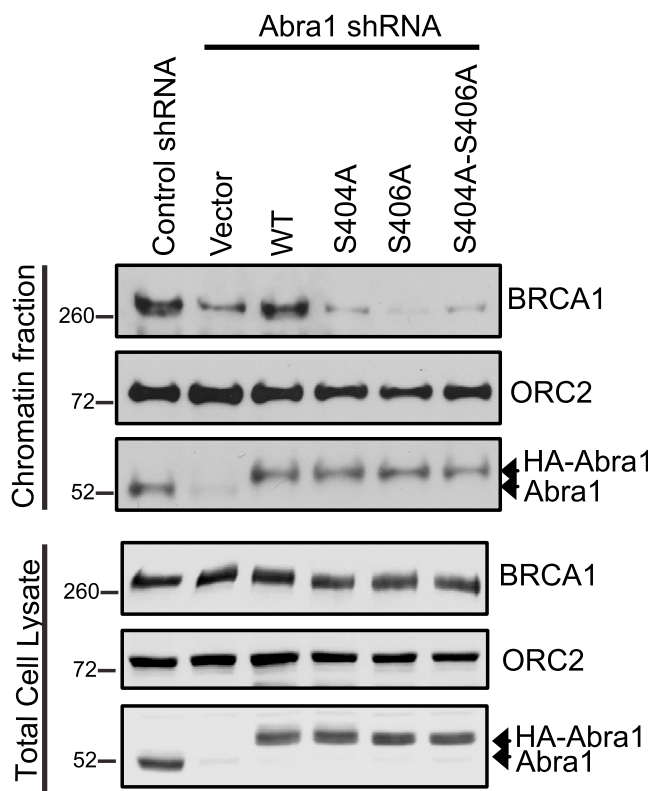
Figure 15. BRCA1 accumulation at damaged chromatin. Depends on both S404 and S406 phosphorylation. Abraxas-deficient cells expressing vector, WT or mutant Abraxas (S404A, S406A or double mutant) were treated with 10 Gy IR followed by 2-hour incubation at 37^{0}C. The cellular fractionation was carried out and the chromatin fraction was analyzed. Orc2 was used as loading control. Bottom panel: total cell lysates were analyzed to confirm BRCA1 protein was not affected in Abraxas knockdown cells and cells complemented with WT or mutant Abraxas.

48

interacts with its Flag-tagged counterpart, I performed immunoblot analysis with Myc antibody to detect BRCA1 dimerization. The findings indicate that BRCA1 indeed dimerizes *in vivo* and this dimerization decreased significantly in Abraxas KO cells indicating that BRCA1 dimerization occurs in an Abraxas-dependent manner (Figure 16A). The Input western blot showed similar expression of BRCA1 constructs in both control and Abraxas KO cells confirming that the decreased BRCA1 dimerization in the KO cells was not due to reduced expression of any of the constructs. The band intensity of myc-BRCA1 was quantified by densitometric analysis using NIH ImageJ software. The normalized value (Immunoprecipitated myc-BRCA1 over Input) was shown in the bar graph.

To further confirm whether this dimerization takes place through the BRCT domain of BRCA1, I performed a similar co-immunoprecipitation experiment with differentially Myc- or HA-tagged BRCT domain only constructs in 293T parental and Abraxas KO cells. In consistent with full-length BRCA1 dimerization, I found that a BRCA1 BRCT domain also dimerizes *in vivo* and this dimerization is also significantly impaired in Abraxas KO cells (Figure 16B). In sum, these findings validate our *in vitro* crystal structure findings that BRCA1 indeed dimerizes *in vivo* in Abraxas-dependent manner.

2.3.6 BRCA1 germline mutations disrupt dimerization *in vivo*

Our crystal structure data revealed that germline mutations in the BRCT dimerization interface, F1662S, and M1663K, disrupt the dimer stability. To test whether these mutations interfere BRCA BRCT dimerization in vivo, I compared the interaction of Myc-tagged full-length BRCA1 and HA-tagged wild-type BRCT fragment with that of

the F1662S or M1663K mutant of BRCA1 and a mutant BRCA1 BRCT fragment with three residues localized in the dimer interface mutated (F1662S/M1663K/R1670E). and performed both Myc-IP and reciprocal HA-IP experiments to confirm if dimerization in impaired when these critical residues in the dimer interface are mutated. Findings from these experiments showed that while the WT BRCA1 and BRCT can efficiently interact, the interaction/dimerization of BRCA1 and BRCT fragment was decreased significantly when these residues were mutated. The band intensity was quantified by densitometric analysis using NIH ImageJ software. The normalized value (IP over Input) was shown in the bar graph (Figure 17). Collectively, these findings suggest that F1662S and M1663K germline mutations interfere with stable dimer formation *in vivo* highlighting the importance of these critical residues in BRCA1 dimerization.

2.4 Discussion

BRCA1 accumulation to DNA damage sites is essential for its function in DNA repair and cell cycle regulation and thereby maintaining genomic integrity. Although phosphorylated S406 residue in the pSPxF motif of Abraxas has been shown to be crucial in interaction with BRCA1, a detailed molecular understanding of Abraxas-BRCA1 BRCT interaction still remained to be determined. In this light, our study provides evidence for DNA damage-induced ATM-dependent mechanism for Abraxas-mediated BRCA1 accumulation to DNA damage sites. In this, IR-induced ATM-dependent phosphorylation of S404 residue adjacent to pSPxF motif acts as a regulatory switch inducing stable dimerization of BRCA1 BRCT-Abraxas complex that is essential for efficient recruitment of BRCA1 to damaged chromatin (Figure 18)
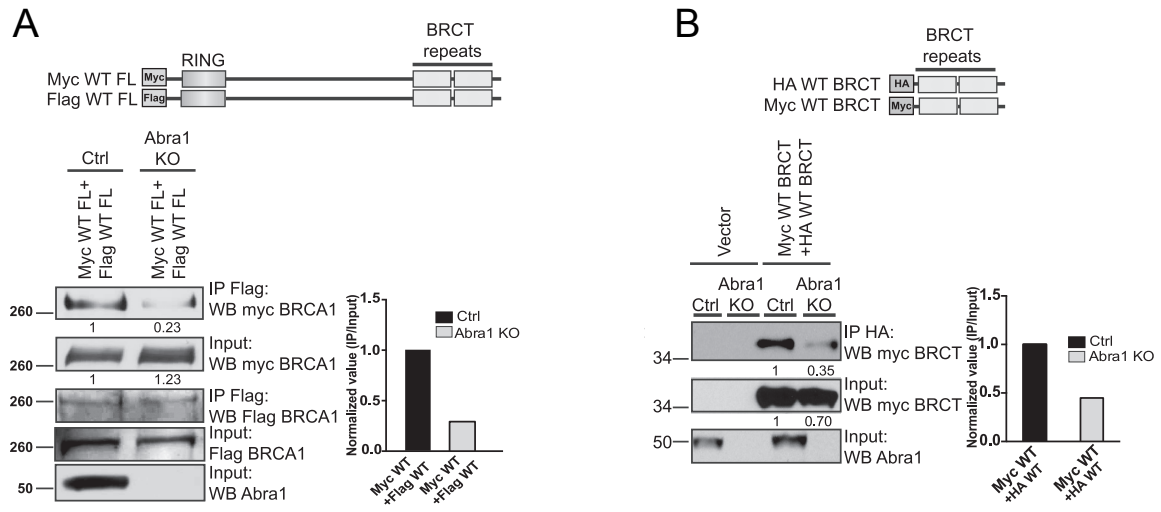
Figure 16. Abraxas-dependent BRCA1 BRCT dimerization. A. Abraxas-

dependent BRCA1 dimerization *in vivo.* The differentially tagged (myc or Flag)

full-length BRCA1 constructs were transiently transfected into parental and

Abraxas KO 293T cells. The lysates from cells treated with 10 Gy IR followed by

1 hour incubation at 37^0C were used for Flag immunoprecipitated followed by

detection with indicated antibodies. The intensity of individual band was

quantified by densitometric analysis using ImageJ software and normalized

value (IPed_mycBRCA1/Input_mycBRCA1) was shown in the bar graph. **B.**

Abraxas-dependent BRCA1-BRCT dimerization *in vivo.* The differentially tagged

BRCA1 BRCT domain constructs were transiently transfected parental or

Abraxas KO 293Tcells and BRCA1 BRCT dimerization was analyzed similarly

as in A. The band intensity was measured by ImageJ and normalized values

were plotted in the bar graph.

Our crystal structure data revealed that while phosphorylated S406 phosphopeptide of Abraxas interacts with BRCT fragment forming a monomeric complex similar to other pSPxF motif containing proteins, doubly phosphorylated Abraxas phosphopeptide (pS04pS406) induces stable dimerization of the BRCT domain, mediated through the BRCT1 domain. The dimerization interface formed by two BRCT1 domains does not interfere with pSPxF motif binding that binds to BRCT domain as "two-anchor mode" where S406 and F409 interact with BRCT1 and BRCT2 domains, respectively. However, the interaction between two BRCT1 domains is not sufficient to form a stable dimer in solution as observed with BRCT domain only or BRCT domain with pS406 Abraxas, BACH1 and CtIP phosphopeptides. On the other hand, under the same condition, in presence of doubly phosphorylated Abraxas phosphopeptide (pS404pS406), BRCT undergoes stable dimerization indicating that residues adjacent to pSPxF motif confer specificity for BRCA1-Abraxas complex dimerization. Consistent with this, we found that along with pS404, the N-terminal region of pSPxF motif (GFGE^{402}Y^{403}pS^{404}RpSPVF) also contributes to stability of the BRCT-Abraxas complex. Therefore, the unique amino acid sequence at the C-terminus of Abraxas allows stable dimerization of BRCT-Abraxas complex but not with pSPxF motif containing BACH1, and CtIP proteins. Because of the symmetric pairing among F1662, M1663, and Y1666 residues of two BRCT1 domains, we refer this interaction as "pair-hugging" mode, where the pS404pS406 phosphopeptide stabilizes the interaction. Consistent with these *in vitro* data, compared to WT Abraxas, expression of S404A and S406A mutants of Abraxas in Abraxas-deficient cells showed decreased BRCA1 accumulation to DSB
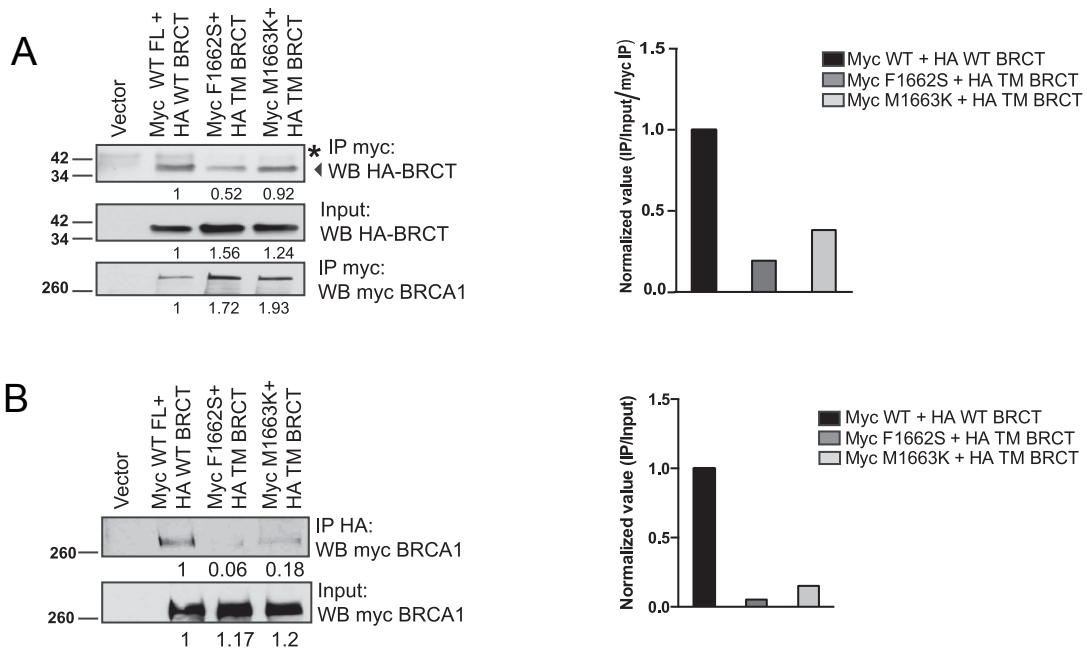
Figure 17. BRCA1 germline mutations at the BRCT dimerization interface disrupt dimerization *in vivo*. BRCA1 germline mutations F1662S and M1663K decrease BRCA1 dimerization in vivo. Myc-tagged BRCA1 full-length (WT-FL) and HA-tagged BRCA1 BRCT (WT-BRCT) or Myc-tagged mutant full-length (F1662S or M1663K) and HA-tagged BRCT triple mutant (TM, F1662S/M1663K/R1670E) were co-expressed in cells. The lysates from cells treated with 10 Gy IR followed by 1 hour incubation at 37 C were prepared for either Myc- immunoprecipitation (A) or reciprocal IP with HA- immunoprecipitation (B). The band intensity was quantified using ImageJ software and normalized value was shown in the bar graph.

sites at IR-induced foci as well as decreased accumulation of BRCA1 to damaged chromatin. With these findings, it is tempting to speculate that S404 phosphorylation-induced BRCA1 BRCT dimerization may lead to increased concentration of BRCA1 at the sites of DNA damage, which is likely essential for efficient DNA damage signaling and repair.

In an attempt to examine how this dimerization takes place *in vivo*, we found that Abraxas forms homodimer through its coiled-coiled domain at the C-terminus. This likely brings two BRCT domains interacting through the pS406 of the pSPxF motif of Abraxas in close proximity and therefore forming an unstable dimer. Since S404 is phosphorylated only in presence of DNA damage in an ATM-dependent manner, IR-induced DNA damage promotes a much more stable dimerization of the BRCT1-Abraxas complex. Of note, Abraxas coiled-coil domain has been shown to form a heterodimer with BRCC36 coiled-coil domain (41). Therefore it appears that in the A complex, BRCC36 and Abraxas form an oligomeric bundle through the coiled-coil domain present in each of them. Detail structural and cellular analysis of the oligomeric complex in future will provide valuable insights into how BRCA1-A complex is assembled at the DNA damage sites.

What is the functional significance of the BRCA1 BRCT dimerization in terms of BRCA1's role as a tumor suppressor? Our *in vitro* and *in* vivo analysis confirmed that the germline mutations in the BRCT dimerization interface destabilize the dimer. While many tumor-derived mutations have been reported in the BRCA1 BRCT domain (72-74), function of large majority of these mutations is still remained to be determined. In this light, our analysis revealed that germline mutations, M1663K,

and F1662S, disrupt the BRCA1 BRCT dimerization and provide an explanation of how these residues play a crucial role in the tumor suppressor function of BRCA1. Future studies examining whether these mutations in the dimerization interface leads to defective DNA repair or inefficient BRCA1 loading onto damaged chromatin will provide valuable insights deepening our understanding of how Abraxas and BRCA1 function in tumor suppression and maintenance of genome stability.

In brief, this study reveals a novel mechanistic view of DNA damage-induced Abraxas phosphorylation-dependent BRCA1 accumulation to DNA damage sites. The structural insights of the BRCA1-Abraxas interaction will aid in designing small molecules in future modulating this interaction for potential therapeutic intervention.

2.5 Future direction

Although BRCA1 was identified as a tumor suppressor almost 20 years ago, the full spectrum of its functional significance is still being elucidated. While mutations in the *BRCA1* gene predisposes women to breast and ovarian cancer along with higher risk of developing other types of cancers, the exact role of BRCA1 in tumor suppression still remains a mystery. Solving this mystery has been a challenge given BRCA1 associates with multiple protein complexes that are involved in various biological processes. Our findings of Abraxas phosphorylation-mediated BRCA1 dimerization at DNA damage sites provides key mechanistic insights into its efficient accumulation to damaged chromatin to repair DNA. However, several important questions still remain to be addressed to understand how BRCA1 dimerization plays an essential role in its tumor suppressor function. Is BRCA1 dimerization important for efficient DNA repair function of BRCA1 and thereby
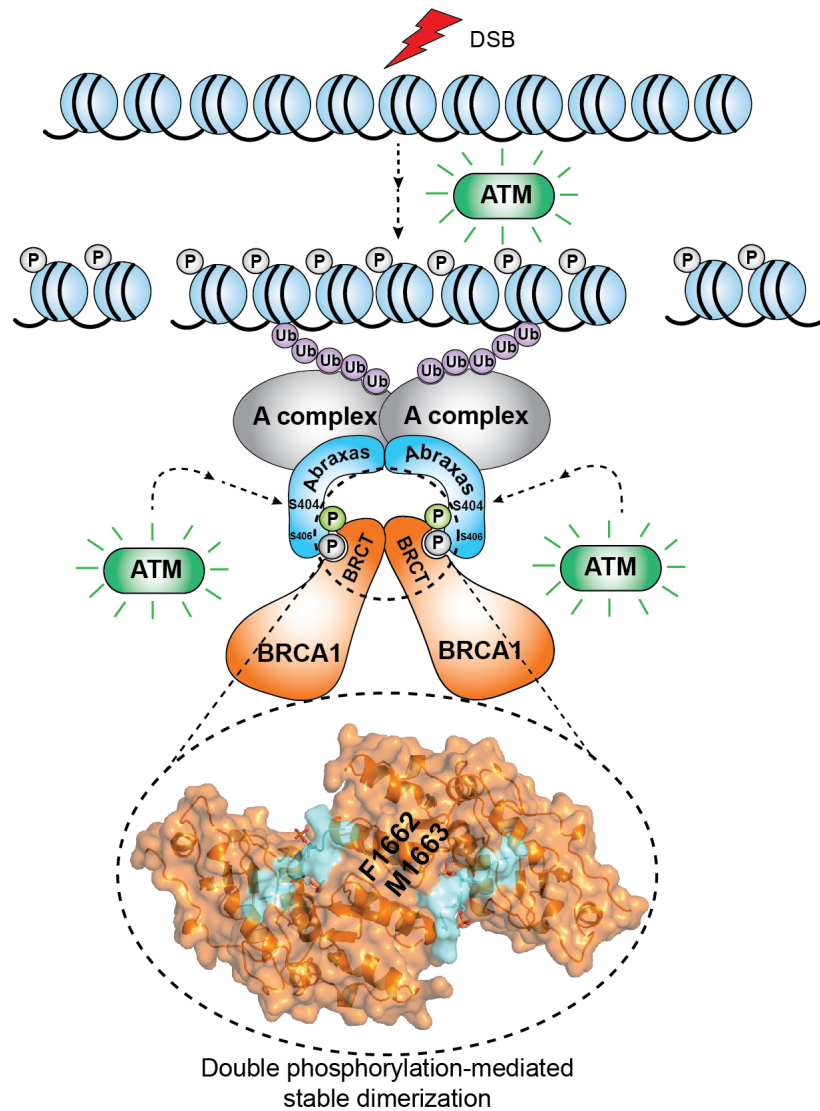
Figure 18. Proposed model showing IR-induced ATM-dependent phosphorylation of Abraxas induces BRCA1 dimerization at sites of DNA damage for efficient BRCA1 accumulation to damaged chromatin. Abraxas C-terminal S404 is phosphorylated in DNA damage dependent manner that promotes stable dimerization of BRCA1 BRCT-Abraxas complex at the sites of damage. S404 phosphorylation is essential for efficient BRCA1 accumulation to damaged chromatin and germline mutations in the BRCA1-BRCT dimerization interface disrupts the dimer formation.

maintaining genome stability? Although I have examined that germline mutations in the BRCT dimerization interface disrupt dimer formation, future study is needed to further examine whether these germline mutations impair BRCA1's role in DNA repair or DNA damage signaling. In addition, whether the dimerization is essential for accumulation of BRCA1 to damaged chromatin and thereby triggering efficient DDR signaling demands further investigation. Another important question that needs to be addressed is identification of the kinase that directly phosphorylates S404 in response to DNA damage. Our findings indicate S404 is phosphorylated ATM-dependent manner. However, proteomic analysis identified more than 700 proteins, including many downstream kinases, as substrates for ATM and ATR (18). Identification of the kinase responsible for S404 phosphorylation will, therefore, broaden our understanding of the damage-induced phosphorylation signaling cascade at the damage site. Answers to these questions will shed light into how Abraxas phosphorylation-mediated dimerization of BRCA1 plays an essential role at the DSB sites to exert its function in the DDR signaling and thereby functioning as a 'master regulator' for maintaining genomic integrity.

CHAPTER 3

INTRODUCTION: ROLE OF LYSINE11-LINKAGE-SPECIFIC UBIQUITINATION IN THE DNA DAMAGE RESPONSE PATHWAY

3.1 Introduction

Ubiquitin is a 76 amino acid long polypeptide that is highly conserved among eukaryotic kingdom identified initially as ATP-dependent protein degradation component in reticulocytes (100-102). However, recent years have witnessed an unprecedented growth in our understanding of the non-proteolytic functions of ubiquitination in cellular signaling (103). Covalent conjugation of ubiquitin molecule to substrate proteins governs a wide range of cellular processes including protein degradation, transcription, cell cycle progression, immune response, and receptor trafficking as well as viral infection. Protein ubiquitination is a three-step enzymatic process mediated by E1 activating enzyme, E2 conjugating enzyme and E3 ligase enzyme (104). Ubiquitin is activated by an E1 activating enzyme in an ATP-dependent manner forming thioester bond between the C-terminal carboxyl group of Gly residue of ubiquitin and the active cysteine residue of the E1 enzyme (105). In the following step, the ubiquitin is transferred to the cysteine residue of the cognate E2 enzyme (106) and subsequently transferred to the ε-amino group of a lysine residue of the substrate forming an isopeptide linkage in presence of an E3 ligase (107). Monoubiquitination of substrates in one or more than one lysine residues (multi-mono ubiquitination) is highly abundant in eukaryotic cells suggesting the functional significance of this modification in cellular signaling (108). For example, (multi) mono-ubiquitination of cell surface receptor proteins plays a crucial role in endocytosis and subsequent degradation of these receptors in lysosomes or recycling back to the cell surface (109).
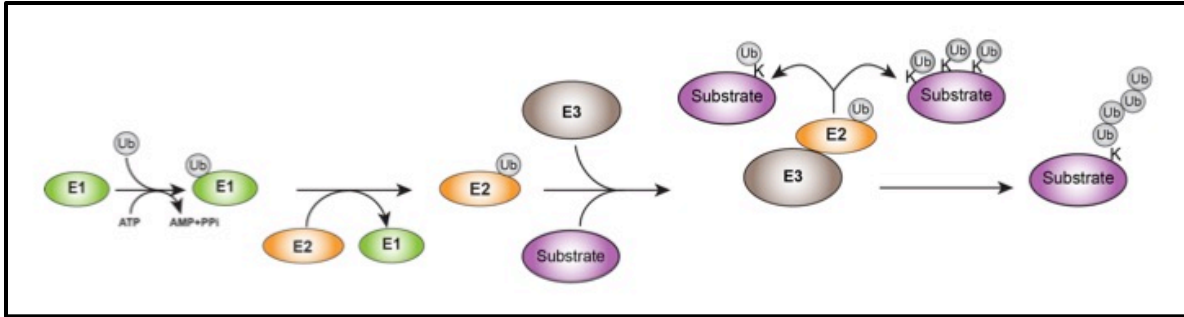
Figure 19: **Schematic of ubiquitin system.** Ubiquitination is an enzymatic process that involves covalent attachment of ubiquitin to target protein catalyzed by E1 activating, E2 conjugating and E3 ligase enzymes. These enzymes not only transfer ubiquitin to protein substrates at single or multiple lysine residues, but also promote the formation of long polyubiquitin chains through one of seven lysine residues of ubiquitin as shown here in blue forming polyubiquitin chain of distinct linkages.

Interestingly, unlike phosphorylation, ubiquitin machinery can also add further ubiquitin molecules through one of the seven lysine residues in substrate-conjugated ubiquitin molecule synthesizing polyubiquitin chain of distinct lineages forming polyubiquitin chain of distinct linkages (110, 111). In addition, recent findings indicate the existence of an eighth kind of ubiquitin chain formed through the N-terminus of ubiquitin, also known as 'Met1-linked' or linear chains, demonstrating the magnitude of complexity of the 'ubiquitin code' (112). Proteomic approaches have shown the existence of all seven lysine residue-linked as well as Met1-linked linear ubiquitination in cells (108, 113-115). Since different ubiquitin chains adopt a distinct structure that can be recognized by specific ubiquitin-binding domain (UBD) containing proteins, ubiquitin chain with different length and topology trigger vastly different molecular signals *in vivo* (116, 117). Chain specificity is an intrinsic property of E2 enzymes; and E3 ligases interact with different E2 enzymes generating different linkage-specific ubiquitin chains on substrate proteins (106, 118). In eukaryotes, there are approximately 35 E2s and more than 500 E3 enzymes have been reported to date. Given the vast number of different E2-E3 combinations, this provides an additional layer of regulation for assembly of linkage-specific ubiquitination. Furthermore, similar to other post-translational modifications, cellular ubiquitination is also reversible process, in which enzymes known as deubiquitinases or DUBs cleave the polyubiquitin chain on substrates, thereby recycling and maintain free ubiquitin pool in the cell. There are around 100 DUB enzymes encoded by the human genome that oppose the function of E3 ligases and thereby regulating the ubiquitin signaling in cells (89). Therefore, precise balance

and coordination among 'writer', 'reader' and 'eraser' for the 'ubiquitin code' propagates specific cellular signaling *in vivo* essential for cellular homeostasis.

3.1.1 Linkage-specific ubiquitination:

Among different lysine residue-linked ubiquitination, canonical Lys48-linked ubiquitination was first identified and assumed to be the only linkage type targeting proteins for degradation (119, 120). Over the following years, Lys63-linked ubiquitination was identified as a non-proteolytic signal involved in DNA repair in yeast *Saccharomyces cerevisiae* (121). Since then Lys63-linked ubiquitination has been extensively studied in the DNA damage response pathway as well as other non-proteolytic pathways including vesicular traffic, endocytosis, and NF-kB pathways (122-125). However, our knowledge of the role of other linkage-specific ubiquitination in cellular signaling pathways remained limited. One of the major challenges in the field of linkage-specific ubiquitination is the detection of different lysine residue-linked ubiquitin conjugation in cells due to varying degree of chain abundance and rapid turnover of ubiquitin chains by different DUB enzymes. Nonetheless, advancement in mass-spectrometry-based proteomic approaches such as Absolute QUantitative Analysis (AQUA) as well as Protein Standard Absolute Quantification (PSAQ), paves the way to gain further insights into the unexplored world of different linkage-specific ubiquitination in cells (108, 111, 113, 114, 126-129). Although different groups have reported a varying abundance of linkage-specific ubiquitin chains, findings from these studies suggest the presence of all different chain types in yeast and mammalian cells.

3.1.2 Linkage-specific polyubiquitination in the DNA damage response pathway:

Although mass-spec analysis identified the existence of all seven lysine residue-linked ubiquitination in cells, the functional significance of these different chain types in various cellular signaling pathways in cells still remains to be determined. Given the heterogeneity of ubiquitin code and complexity of the DNA damage response signaling, it is not tempting to speculate that many of these ubiquitin chains exist at the damaged chromatin. Indeed seminal studies done by different groups had conclusively shown that Lys63-linked ubiquitin conjugation is predominant at DNA damage sites modifying histone proteins at damaged chromatin and regulating downstream DDR factor recruitment such as 53BP1 and components of the BRCA1-A complex (37-39, 41, 43-45). Along with Lys63-linked ubiquitination, several biochemical studies and mass-spec analysis identified existence of other Lys residue-linked ubiquitination including Lys6, 27, 29, 33 and 48 at damaged chromatin and the abundance of this ubiquitin chains can alter dramatically in response to DNA damage. Together these findings indicate that ubiquitin signaling at the damage sites is much more complex than anticipated before.

3.1.3 Lys63-linked ubiquitin chain:

DNA damage-induced Lys63-linked ubiquitin conjugation is the most well characterized linkage-specific ubiquitination involved in the DNA damage response pathway. In one of the seminal articles, Finley and colleagues first reported existence of the Lys63-linked ubiquitin conjugates in yeast *Saccharomyces cerevisiae* (121). Although yeast strains carrying K63R mutant ubiquitin were

proficient in growth and efficient in turning over of cellular proteins, K63R mutation

conferred hypersensitivity to DNA damaging agents such as methyl

methanesulfonate (MMS), UV, X-rays providing key evidence that nonproteolytic

Lys63-linked ubiquitination is involved in the DDR signaling pathway. Subsequent

studies identified Ubc13/Mms2 heterodimer assembles Lys63-linked polyubiquitin

chain *in vitro* and in yeast (122, 130). To identify the E3 ubiquitin ligase involved in

the Lys63-linked ubiquitination, *Plans et al* performed yeast two-hybrid screening

using Ubc13 (also known as Ube2N) as bait and identified human Ring finger protein

8 (RNF8) as an E3 ligase that interacts and co-localizes with human Ubc13 in cells.

Further analysis demonstrated that RNF8 functions as a self-ubiquitin ligase that is

polyubiquitinated in Lys63-linked manner mediated by Ubc13 (131).

Although these early findings provided the key insights into the enzymatic

machinery catalyzing non-proteolytic Lys63-linked ubiquitination, the functional role

of this ubiquitination in the DDR signaling was still missing until 2007 when

independent studies demonstrated Lys63-linked polyubiquitin conjugate enrichment

at damaged chromatin by elegant biochemical approaches (37-39, 41). These

studies have conclusively shown that a phosphorylation-dependent ubiquitin

signaling cascade at the DSB sites orchestrates the DNA damage response

signaling by functioning as a molecular scaffold to recruit downstream DDR factors.

Upon DNA damage, ATM-mediated phosphorylation of adaptor protein MDC1

recruits RNF8 to DSBs flanking chromatin. Once recruited, RNF8, in association with

Ubc13, initiates non-proteolytic Lys63-linked ubiquitination of histones H2A and

H2A.X. The assembly of the Ubc13-RNF8 complex is further facilitated by another

E3 ligase, HERC2, which is phosphorylated by ATM upon DNA damage and interacts with RNF8 FHA domain (40). Later studies demonstrated that initial Lys63-linked ubiquitin polymer generated by Ubc13-RNF8 enzymes is recognized by ubiquitin binding domain of another E3 ligase, RNF168 that functions in concert with Ubc13 and amplifies the Lys63-linked ubiquitin chain on H2A and H2A.X generating polyubiquitin chain of Lys63 lineage (43-45). Ubc13-RNF8-RNF168-mediated Lys63-linked ubiquitination of core histones and other unidentified non-histone proteins at damaged chromosomes is crucial to transduce the DDR signal by recruiting the DDR mediator proteins, BRCA1 and 53BP1 to DSB sites. As shown by our lab and several other groups, Lys63-linked polyubiquitin conjugates at DSB sites is recognized by ubiquitin interacting motif (UIM) of Rap80 protein that recruits Abraxas and subsequently the entire BRCA1-A complex, which includes Abraxas, Rap80, NBA1, BRE and BRCC36 (41, 47, 49, 51, 132, 133). Recruitment of these factors to DNA damage sites is essential for efficient DNA repair and checkpoint signaling indicating the functional significance of these enzymes in the DDR pathway. Although these studies showed core histone proteins, H2A and H2A.X are modified by Lys63-linked ubiquitination; it is likely that other non-histone proteins at damaged chromatin are also modified by this modification. Identification and characterization of these proteins will broaden our understanding of the complexity of the DDR signaling.

In addition to BRCA1, Lys63-linked ubiquitination on nucleosome also recruits another mediator protein 53BP1 to the sites of DNA damage. Earlier studies have demonstrated that 53BP1 localization to damaged chromatin is mediated by

recognition of dimethylated histone H4K20 (H4K20me2) by tandem Tudor domain of 53BP1 (134). However, impaired recruitment of 53BP1 in RNF8 and RNF168 depleted cells raised the possibility that Ubc13-RNF168 catalyzed Lys63-linked ubiquitination at damaged chromatin may also promote its recruitment to IR-induced foci (37-39, 43). Consistent with this idea, recent experimental evidence by Durocher group have shown that in addition to its Tudor domain, 53BP1 also harbors a C-terminal extension, termed as ubiquitination-dependent recruitment (UDR) motif that specifically recognizes ubiquitinated histone H2A on lys15 (H2AK15ub) (135). Together these findings propose a model of 53BP1 recruitment to DNA damage sites as a bivalent reader recognizing both H4K20me2 and Ubc13-RNF8-RNF168 mediated H2AK15ub.

Although the seminal studies provided key evidence of histones H2A and H2A.X as major substrates for Lys63-linked ubiquitination, the full-spectrum of substrates modified by Lys63-linked ubiquitination still remained largely unknown. In this light, it is of interest that a recent study identified H1-type linker histone as a key substrate modified by the Ubc13-RNF8 complex in DNA damage-dependent manner forming Lys63-linked ubiquitin chain. The lys63-linked chain functions as an interacting module for RNF168 through its N-terminal ubiquitin-dependent DSB recruitment module 1 (UDM1). Once recruited, the Ubc13-RNF8-RNF168 enzymatic machinery then catalyzes Lys63-linked ubiquitination of core histone proteins. Consistently, depletion of linker histone impairs Lys63-linked ubiquitin conjugation and accumulation of DDR factors at damage sites including BRCA1. These findings propose a model where Ubc13-RNF8 complex and RNF168 function as writer and

reader, respectively of the Lys63 ubiquitinated linker histone H1 protein expanding the 'histone code' in the DNA damage response pathway (136).

3.1.4 Lys6-linked ubiquitin chain:

In the DNA damage response pathway, Lys6-linked ubiquitination was initially identified as polyubiquitin chain catalyzed by heterodimeric BRCA1/BARD1 E3 ubiquitin ligase complex. Both *in vitro* and *in vivo* analysis have shown that BRCA1/BARD1 ligase complex catalyzes autoubiquitination of BRCA1 in Lys6-linked polyubiquitin chain that is recognized but not degraded by the 26S proteasome (81-84). In addition to BRCA1 autoubiquitination, BRCA1/BRAD1 ligase complex has been shown to ubiquitinates RPB8, a subunit of RNA polymerase holoenzyme, upon UV-induced DNA damage. While retaining its function as a subunit of RNA polymerase complex, the Lys6-linked polyubiquitin-resistant RPB8 mutant showed UV hypersensitivity in cells emphasizing the role of Lys6-linked ubiquitination in the DDR pathway (137). These findings have been validated further by recent global profiling of the ubiquitin species in cells showing that enrichment of Lys6-linked polyubiquitin conjugates after UV treatment but not irradiation (IR)-induced DNA damages (138). BRCA1 has been shown to localize to UV-induced foci and functions in a DNA replication-dependent manner to facilitate post-replicative repair (139).

In addition to BRCA/BARD1, another RING domain E3 ligase, RNF8, has been shown to catalyze Lys6-linked ubiquitination of Nbs1, a component of the MRN (MRE11-Rad50-Nbs1) protein complex that senses the DNA double-strand breaks. The E2 conjugating enzyme UbcH5c and E3 ligase RNF8-mediated Lys6-linked

ubiquitination of Nbs1 is essential for efficient recruitment of Nbs1 to damaged chromatin to promote HR repair (140). Consistent with these findings mass-spectrometry analysis have confirmed no significant enrichment of Lys6-linked polyubiquitin conjugates upon treatment with proteasomal inhibitor MG132 indicating unlike Lys48-linked ubiquitination, Lys6 polyubiquitin chain is involved in non-proteolytic functions in cells (141, 142).

3.1.5 Lys27-linked ubiquitin chain:

Lys27-linked ubiquitination has emerged recently as another 'atypical ubiquitination' involved in the DNA damage response pathway. In their recent findings Penengo and colleagues have analyzed different lysine residue-linked ubiquitination in cells overexpressing RING E3 ligase, RNF168, which has been shown previously to catalyze Lys63-linked ubiquitination at the damage sites (43-45, 143). Selected reaction-monitoring mass spectrometry (SRM) analysis revealed that overexpression of RNF168 leads to Lys27-linked polyubiquitin conjugation in cells. In addition their findings indicate histone proteins, H2A and H2A.X, were modified by RNF168-mediated Lys27-linked polyubiquitination. Furthermore, Lys27-linked chromatin ubiquitination is essential for efficient recruitment of DDR mediators such as BRCA1, 53BP1, Rap80, RNF168, RNF169 to DSB sites and therefore is required for optimal activation of the DDR signaling (56). Taken together, these findings revealed new roles of linkage-specific ubiquitination induced by genotoxic stress providing insights into the complexity of 'ubiquitin code' at the DNA damage site.

3.1.6 Lys29 and Lys33-linked ubiquitin chain:

While functions of Lys29-and Lys33-linked ubiquitination in DNA damage

response still remain largely elusive, findings from recent studies provide evidence

of these linkage-specific ubiquitination in various other signaling pathways such as

Wnt/β-catenin signaling and protein trafficking, respectively (110, 111). Both these

modifications have been shown to be enriched upon treating the cells with

proteasomal inhibitor MG132 suggesting proteolytic functions of these chain types in

cells (113, 142). Interestingly recent quantitative proteomic analysis of global

ubiquitination profile in mammalian cells by Elledge and colleagues showed a

marked increase (about 2 fold) in endogenous Lys33-linked ubiquitination upon UV-

induced but not IR-induced DNA damages (138). Although functional significance of

these preliminary findings demand further investigation, given the complexity of the

DDR signaling and 'ubiquitin code', it is tempting to speculate that these

modifications play potential roles in the DNA damage response pathway.

3.1.7 Lys48-linked ubiquitin chain:

Although degradation-linked Lys48 ubiquitination has been extensively

studied in various cellular signaling, its role is obscured in the DDR pathway. Since

DDR factor retention at the sites of DNA damage needs to be tightly regulated, it is

likely that many of the DDR factors are modified with Lys48 ubiquitin chain to ensure

removal of these factors from sites of DNA damage in a timely manner. In one of the

earliest studies using *Xenopus* egg extract coupled to tandem Mass-spectrometry,

Funabiki and colleagues showed that among different DDR factors, Ku80, a crucial

factors in the NHEJ repair pathway, is modified with Lys48-linked ubiquitin chain

upon binding to DBS containing DNA by Skp1–Cul1–F-box (SCF) E3 ligase

complex. Strikingly, although proteasome targets for lys48 ubiquitin decorated Ku80

once it is released from DSB, the proteasome activity is not required for Ku80 removal from DSBs (144, 145). Another study by *Shi et al* showed that MDC1 is heavily ubiquitinated with the Lys48-linked chain in DNA damage-dependent manner and subsequently degraded by the proteasome that is essential for disassembly of MDC1 protein from the sites of DNA damage (146). Similar to MDC1, BRCA1 has also been shown to be ubiquitinated and degraded following a high dose of irradiation (IR)-induced DNA damage, independent of its autoubiquitination E3 ligase activity and is required for IR-induced apoptosis (147, 148). More recently, RNF8 E3 ligase, which has been identified as an E3 ligase catalyzing Lys63-linked ubiquitination in concert with the Ubc13 E2 enzyme at damaged chromatin, has shown to function with another E2 conjugating enzyme, UbcH8, to catalyze Lys48-linked ubiquitin chain at the damage sites. RNF8-mediated Lys48-linked ubiquitination of Ku80 regulates its turnover at the sites of DNA damage regulating NHEJ-mediated DNA repair (57, 58). Kinetic analysis of Lys48 and Ly63-linked ubiquitination at the sites of DNA damage using linkage-specific antibody showed that Lys48-linked ubiquitin chain is assembled at the DSBs immediately after DNA damage, while Lys63-linked ubiquitin conjugation occurs at much slower rate at the damaged chromatin facilitating coordinated recruitment of DDR factors (57, 149). These observations suggest that Lys48-linked ubiquitin conjugation and proteasome are the essential elements of the DDR signaling that regulate orchestration of DDR factors.

3.1.8 Lys11-linked ubiquitination:

Lys11-linked ubiquitination was first identified as novel ubiquitin chain type

catalyzed by Ube2S (also known as E2-EPF) in 1996 (150). Later studies identified another E2 conjugating enzyme Ube2C (also known as UbcH10) that along with Ube2S catalyze Lys11-linked ubiquitin chain on substrates in presence of APC/C E3 ubiquitin ligase (151-155). APC/C is a large multisubunit E3 ligase complex that in association with Ube2S and Ube2C modifies mitotic and G1 phase cell cycle proteins including CyclinB1 and securin, with Lys11-linked ubiquitin chain and target proteasomal degradation (156). In recent years, Ube2S/Ube2C and APC/C-mediated Lys11-linked ubiquitin chain assembly has emerged as a major regulatory player in proper cell cycle progression. Importantly, recent studies identified an OUT family deubiquitinase (DUB), Cezanne (also known as OTUD7B), which preferentially cleaves Lys11 ubiquitin chain (157, 158). Interestingly, although a proteomic study identified Lys11-linked ubiquitination as one of most abundant ubiquitin chain types in cells (114), the role of Lys11-linked ubiquitination in the DDR pathway still remains to be elucidated.

3.1.9 Objective:

Chromatin modification at DNA damage sites constitutes an immediate component of the cellular response to DNA damage for signaling and repair. While proteomic analysis of global ubiquitination profiling revealed assembly of all seven lysine residue-linked ubiquitination in a varying degree of abundance in both yeast and mammalian cells (113, 114, 159), function and characterization of non Lys63-linked ubiquitin conjugation at the DSB sites still demands further investigation. Since the DNA damage response signaling encompasses a vast number of molecules, depending on the type of DNA lesions experienced by the cell, it is not

71

surprising that DDR factors are modified with non Lys63-linked ubiquitin chains as well to regulate the DDR signaling and facilitate efficient repair. Although recent findings by above-mentioned studies showed promising evidence of the existence of different types of ubiquitin linkages in UV- and IR-induced DNA damage sites, much is still missing for understanding the role of linkage-specific ubiquitin chains in the regulation of DNA damage response and repair. Therefore, in this study, I aim to explore existence and functional significance of non-lys63-linked ubiquitin conjugation at the DNA damage sites. Findings from this study will broaden our understanding of the complexity of ubiquitin signaling at the damage sites.

3.2. Materials and Methods

3.2.1 Cell Culture, Transfection, Antibodies and Reagents

U2OS and HEK293T cells were grown in McCoy's 5A and DMEM medium respectively with 10% fetal bovine serum (FBS) and maintained at 37°C with 5% CO_2. For generation of stable knockdown cell lines, cells were infected with retrovirus containing shRNAs against Ube2S, Ube2C or CDH1 followed by selection with puromycin (0.8 µg/ml) or blasticidin (9 µg/ml) according to the selection marker of the construct. For generation of Ube2S/Ube2C double knockdown cell line, Ube2S-knockdown cells were further infected with retrovirus containing Ube2C shRNA followed by selection with blasticidin. For transient transfection, cells were transfected with PEI (polyethylenimine) or Lipofectamine 2000 (Invitrogen). Antibodies used in this study are listed in Table 1. Other regents used are listed in Table 2.

3.2.2 Plasmids, shRNAs and siRNAs

Retroviral constructs expressing GFP-Ube2S, GFP-Ube2C, Flag-RNF8 were generated using MSCV vector. Flag-tagged histone plasmids were kindly provided by Dr. Yuzuru Shiio (160), University of Texas Health Science Center at San Antonio. HA-tagged WT and K0 ubiquitin plasmids (pRK5-HA-ubiquitin) were obtained from Addgene (161) and lysine-only ubiquitin mutants were generated by site-directed mutagenesis. His-Biotin (HBT)-WT ubiquitin (pQCXIP HB-Ubiquitin) was used to generate His-biotin-K11 ubiquitin mutant through site-directed mutagenesis. The shRNAs and siRNAs used in this study are listed in Table 3. GFP-tagged siRNA1-resistant Ube2S clone was generated by inserting three nucleotide mismatches underlined (TCTTCCCAAATGAGG) into Ube2S sequence by site-directed mutagenesis using the primers described in the Table for resources and subsequently recombining into pDEST-MSCV-GFP vector.

3.2.3 Immunofluorescence

Immunofluorescence was carried out as described previously (55). Briefly, cells were fixed with 2% formaldehyde for 10 min at room temperature, permeabilized with 0.5% Triton X-100 solution (25 mM HEPES pH 7.4, 50 mM NaCl, 1 mM EDTA, 3 mM $MgCl_2$, 300 mM Sucrose, 0.5% triton-X) at 4°C for 5 min and incubated with primary antibodies at 37°C for 1 hr. Appropriate secondary antibodies conjugated with Alexa 488-conjugated (green; Invitrogen) and Alexa 555-conjugated (red; Invitrogen) were used. For endogenous Ube2S immunostaining following laser micro-irradiation, cells were pre-extracted with ice-cold pre-extraction buffer (10 mM PIPES, pH 7, 100 mM NaCl, 300 mM Sucrose, 3 mM MgCl2, 0.2% Triton-X100) for

5 min at room temperature before fixation and permeabilization. Images were obtained by Nikon confocal microscope.

3.2.4 Cell Lysis and Immunoprecipitation

Cells were lysed in NETN buffer (50 mM Tris-HCl, pH 8.0, 150 mM NaCl, 1 mM EDTA, 0.5% Nonidet P-40, 1 mM DTT) with protease inhibitors, 1 mM PMSF,1 mM NaF, 1 mM Na_3VO_4 and 20 mM N-Ethylmaleimide (NEM) (freshly prepared). For Flag immunoprecipitation, Flag beads (98) were added to cell lysates and incubated overnight with gentle agitation at 4°C. The beads were washed four times with NETN lysis buffer before elution with 2X sample loading buffer. For Flag-immunoprecipitation under denaturing condition, cells were harvested and washed with PBS, cell pellets were resuspended in denaturing lysis buffer (20 mM Tris, pH 7.4, 50 mM NaCl, 0.5% NP-40, 0.5% sodium deoxycholate, 0.5% SDS, 1 mM EDTA, 20 mM N-Ethylmaleimide (NEM) and protease inhibitors). The lysates were sonicated, centrifuged and immunoprecipitated with Flag-beads overnight at 4°C with gentle agitation. The beads were then washed with denaturing lysis buffer four times before elution with 2X sample buffer.

3.2.5 Chromatin fractionation

Chromatin fractionation was carries out as described previously (87). The chromatin fraction pellet was resuspended in NETN lysis buffer containing 20 mM NEM and protease inhibitors. After sonication and centrifugation at 15000 rpm for 10 min, the supernatant was collected as chromatin fraction and protein concentration was measured by Bradford assay. 10 μg of total chromatin fraction protein was used for western blot analysis.

3.2.6 Laser-induced DNA Damage and Live Cell Imaging

U2OS cells were cultured in glass-bottomed dish or 8-well chambers (Mattek Cultureware). BrdU (BD Biosciences) was added to medium with a final concentration 10 µM 24 hour prior to laser irradiation. Nikon TE2000 inverted microscope coupled with a MicroPoint laser system with a UV laser (364 nm) and 60X water lens was used with laser energy output set to 20-30% and number of pulses set to five (total of 335 ms). Following laser ablation, cells were either fixed for immunostaining at indicated time points or monitored by live cell imaging with images captured at 30 seconds intervals. Live-cell imaging was taken and analyzed with Metamorph software.

3.2.7 Clonogenic survival assay

The assay was performed as described previously (87). Briefly, U2OS cells were plated at low density and treated with 4 or 6 Gy IR (or left untreated). The cells were then incubated at 37^0C for two weeks to form colonies. Colonies were fixed and stained with 2% methylene blue and 50% ethanol. Colonies with 50 or more cells were counted as positive.

3.2.8 Nascent transcript detection at DNA damage sites

U2OS cells were transfected with control or Ube2S/Ube2C siRNAs. 48 hr post-transfection, cells were subjected to laser-microirradiation. 5-ethynyl uridine (5-EU) was added to the media immediately after laser treatment to a final concentration of 1 mM followed by incubation at 37^0C for 1 hr. Cells were then fixed, permeabilized and incorporation of 5-EU was detected by Click-iT RNA imaging kit (Invitrogen) following manufacturer's instruction and IF staining of γH2AX was

75

carried out after Click-it reaction. Relative 5-EU intensity along the laser track was quantified using Nikon Elements software and normalized to γH2A.X mean intensity along the same region.

3.2.9 Histone acid extraction

U2OS cells harvested and washed with 1X PBS were resuspended in freshly prepared cytosolic extraction buffer (10 mM HEPES pH 7.9, 10 mM KCl, 1.5 mM $MgCl_2$, 0.34 M sucrose, 10% glycerol, 5 mM NaF, 1 mM Na_3VO_4 , 1 mM dithiothreitol (DTT), 0.5% Triton-X, 20 mM NEM) with protease inhibitors at a concentration of 10^7 cells/ml and incubated on ice for 10 min followed by centrifugation at 4000 rpm for 5 min at 4°C. Cell pellet was washed once with cytosolic extraction buffer and then resuspended in 0.25N HCl at a cell density of $4X10^7$/ml and incubated at $4°C$ for 3 hr followed by centrifugation at 12,000 rpm for 5 min at $4°C$. The supernatant was then collected and 1 ml ice-cold acetone was added for overnight at -20°C. Following centrifugation at 12,000 rpm for 5 min at $4°C$, the pellet was rinsed with acetone once, air-dried at room temperature, and dissolved in 25 μl 50 mM Tris, pH 7.4 buffer. 5-10 μg of acid-extracted histones was used for western blot analysis.

3.2.10 Streptavidin beads pull-down

HeLa cells stably expressing His-Biotin-K11 ubiquitin were grown in media supplemented with 2 μg/ml Biotin for 36 hr before treatment with 10 Gy IR. After irradiation, cells were incubated at 37°C for 30 min, then lysed in denaturing buffer (8M Urea, 300 mM NaCl, 0.5% NP-40, 50 mM Na_2HPO_4, 50 mM Tris, pH 8, 1 mM PMSF, 20 mM NEM). Lysates were sonicated and pull-down with Streptavidin beads was carried out overnight at room temperature. Beads were washed 4 times with

denaturing buffer and bound proteins were eluted with sample buffer and analyzed by SDS-PAGE and western blot using ubH2A antibody.

2.2.11 *In vitro* ubiquitination assay

For *in vitro* ubiquitination assay, 1 μg histone H2A (New England Biolabs) or 2 μg mononucleosome or 1 μg H2A/H2B dimer was incubated with 50 ng E1 (Boston Biochem), 50 or 100 ng of each of Ube2S and Ube2C (Abcam), 2 μg ubiquitin (Boston Biochem) and purified Flag-RNF8 in 20 μl reaction mixture buffer (50 mM Tris, 5 mM KCl, 5 mM MgCl2, 0.5 mM DTT, 200 mM Creatine phosphate (Calbiochem), 2 μg/μl Creatine Phosphokinase (Calbiochem), 2 mM ATP(New England Biolabs) at 32°C for 2 hr. The reaction was stopped by addition of sample buffer and resolved by SDS-PAGE. Flag-RNF8 was purified from HEK293T cells expressing Flag-tagged RNF8. Flag immunoprecipitation was carried out by incubating Flag-beads with cell lysates overnight at 4°C with gentle agitation. The beads were then washed by NETN buffer followed by elution with 3X Flag peptide (98). For RNF8 autoubiquitination assay, Flag-RNF8 was incubated with purified ubiquitin (2 μg), E1 activating enzyme (50 ng), 50 or 100 ng of each of Ube2S and Ube2C in the reaction mixture buffer at 32°C for 2 hr. For recombinant GST-RNF8 in vitro autoubiquitination assay, 500-1000 ng of purified GST-RNF8 was used. Reaction was stopped by addition of 2X sample loading buffer and analyzed by western blot with FK2 antibody.

77

Table 1: List of Antibodies:

Antibody	Company/Source	Catalogue number
BRCA1	Santa Cruz	Cat#sc-6954
γ-tubulin	Sigma Aldrich	Cat#T3559
HA	Cell Signaling	Cat#C29F4
Ube2S	Cell Signaling	Cat#9630
Ube2C	Sigma Aldrich	Cat#WH0011065M1
Flag	Sigma Aldrich	Cat#F7425
H2A	Abcam	Cat#Ab13923
H2AX	Abcam	Cat#Ab11175
H3	Abcam	Cat#ab1791
H2B	Abcam	Cat#ab1790
phospho H3	Millipore	Cat#06-570
53BP1	Upstate	Cat#05-726
γ-H2A.X	Upstate	Cat#05-636
γ-H2A.X	Millipore	Cat#07-164
ubH2A	Millipore	Cat#05-678 (lot 22424)
GFP	Invitrogen	Cat#A11122
FK2	Biomol	Cat#PW8810
Cyclin B1	Santa Cruz	Cat#SC245
ATM	Cell Signaling	Cat#2873S
ATR	SantaCruz	Cat#sc-1887
Ubc13	Zymed Laboratories	Cat#37-1100
Rap80	Bethyl	Cat#A300-763A
Rpb1	Santa Cruz	Cat#sc-899
PCNA	Santa Cruz	Cat#sc-56
OTUD7B	Santa Cruz	Cat#sc-514402
Abraxas	Wang et al., 2007	N/A
Cdh1	NeoMarkers	Cat# MS-1116-P0
MDC1	Stuart et al., 2003	N/A

Table 2: List of chemicals, recombinant proteins and reagents:

Chemicals (Inhibitors), Purified protein, reagents	Company	Catalogue number
MG132	Thermo Scientific	Cat#NC9819784
NEM	Thermo Scientific	Cat#128-53-0
proTAME	Boston Biochem	Cat#I-440
Purified GST-RNF8	Ubiquigent	Cat#63-0021-025
Purified Ube2S	Abcam	Cat#ab87756
Purified Ube2C	Abcam	Cat#ab151891
Recombinant Human Mononucleosome	EpiCypher	Cat#16-0009
Recombinant Human H2A/H2B dimer	EpiCypher	Cat#15-0311
Recombinant Human histone H2A	NEB	Cat#M2502S

Table 3: List of shRNA and siRNA sequences:

Ube2S shRNA - TGGAGGTCTGTTCCGCATG		
Ube2C shRNA - GGAGCAGCTGGAACAGTAT		
Cdh1 shRNA - GGGAAGAAGCTGTCCATGT		
Ube2S siRNAs (siRNA1-GGUCUUUCCCAACGAGGAG, siRNA2-CAAGGAGGUGACGACACUG, siRNA3-CAUGCUGGCGAGCGCGAUA)	Invitrogen	
Ube2C siRNAs (siRNA1-CCUACUCAAAGCAGGUCAC, siRNA2-GUGUCGUCUUUUUAAUUUU)	Invitrogen	
ATM siRNAs (siRNA1-GCGCAGTGTAGCTACTTCTTCTATT, siRNA2- GGGCCTTTGTTCTTCGAGACGTTAT, siRNA3-GCAACATTTGCCTATATCAGCAATT)	Invitrogen (Stealth siRNA)	
ATR siRNAs	Invitrogen (Stealth siRNA)	HSS100876, HSS100877, HSS100878
MDC1 siRNAs	Invitrogen (Stealth siRNA)	HSS114445, HSS114446, HSS114447
RNF8 siRNAs (siRNA1-GGGUUUGGAGAUAGCCCAAGGAGAA, siRNA2-GCAGCAAGAAGGACUUUGAAGCAAU, siRNA3-GGAGAAUGCGGA- GUAUGAAUAUGAA)	Invitrogen (Stealth siRNAs	
Ubc13 siRNAs (siRNA1-UUCUGGAAGGAAUAGUUCAAGUUUA, siRNA2-UUCCCAACUUGUCUACAUUAGGAUG, siRNA3-AUUGGGAGCACUUAACAAGGCCUGG)	Invitrogen (Stealth siRNAs	
Cezanne (OTUD7B) siRNAs (siRNA1 – AGGUCUCUCUCUAUGAAGC, siRNA2 – CUUCUGUGUAUACCAGCCC)	Invitrogen	
H2AX siRNAs	Invitrogen stealth siRNAs	HSS142372, HSS142373, HSS142374
Apc2 siRNAs (siRNA1 – GAGAUGAUCCAGCGUCUGUUU, siRNA2 –GACAUCAUCACCCUCUAUAUU)	Dhamrmacon	

3.3. Results

3.3.1 Analysis of linkage-specific ubiquitin mutant conjugation at DNA damage sites

As described in section 3.1, all seven lysine residues in ubiquitin molecule can serve as conjugate sites for additional ubiquitin molecules forming polyubiquitin chain of distinct lineages. To test whether different linkage-specific ubiquitin conjugation occurs at the site, GFP-tagged single lysine only ubiquitin mutants (K6-, K11-, K27-, K29-, K33-, K48- and K63-), in which all lysine residues except one were mutated to arginine, as well as a lysine-less mutant with all lysine residues mutated (K0) were generated (Figure 20A). Stable U2OS cells expressing GFP-tagged WT or lysine only and K0 ubiquitin mutants were generated by infecting WT U2OS cells with retroviral constructs expressing WT or abovementioned ubiquitin mutants. Western blot analysis confirmed GFP-WT or mutant Ub was expressed at a similar level and was able to form polyubiquitin conjugates indicated by higher molecular weight bands in the western blot with GFP antibody. (Figure 20B). To test conjugation of different lysine only ubiquitin mutants at the DNA damage sites, a laser ablation system equipped with live-cell imaging was utilized to induce DNA damage at a particular region in the nucleus and conjugation of different ubiquitin mutants as the damage sites were monitored by time-lapse microscopy. As shown in Figure 21A, GFP-WT and GFP Lys63 Ub were deposited at laser-induced DNA damage tracks immediately after laser treatment, in consistent with an established role of ubiquitin conjugation occurring at DNA damage
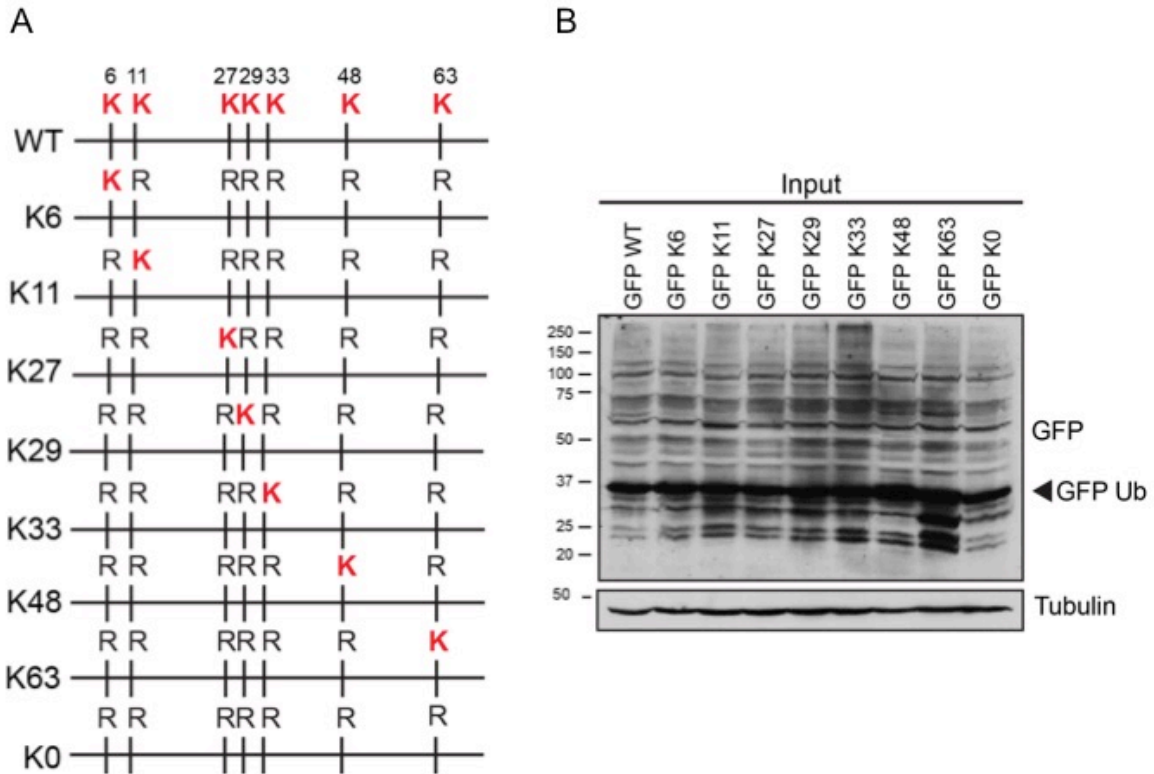
Figure 20 :**Generation of lysine only ubiquitin mutants. A** Schematic

representation of different lysine only ubiquitin mutants.

linkages. **B.** Western blot analysis of cell lysates from U2OS cells stably

overexpressing GFP-tagged WT or lysine only ubiquitin mutants. Expression of GFP-

ubiquitin was detected by GFP antibody. (*) indicates a non-specific band used as

loading control.

sites (37-39, 41, 43-45, 162). Interestingly, GFP-K11 Ub was observed accumulating at laser-irradiated tracks robustly with similar kinetics as that of GFP-K63 Ub or K48 Ub (Figure 21A and B). Compared to WT, GFP-K63, -K48, and -K11; accumulation of GFP-K6, K27, K29, K33, and K0 Ub to laser tracks were mild during the time frame of imaging. These findings suggest that mono-ubiquitination or polyubiquitin conjugation with linkages other than Lys11, 48 and 63 does not occur as robustly at least in the early time points in response to laser-induced DNA damage. Since GFP-Ub can be incorporated into chains of endogenous Ub, it is also possible that GFP-Ub K11/K48/K63 mutant are more efficient than other mutants to be incorporated into endogenous Ub chain. Nevertheless, the accumulation of GFP-K11 Ub to laser tracks suggests that Lys11-linkage ubiquitination may occur at DNA damage sites. This led us to characterize Lys11-linked ubiquitination in the DNA damage response pathway.

3.3.2 Recruitment of ubiquitin Lys11-linkage-catalyzing E2 conjugating enzymes to DNA damage site

Conjugation of Lys11-linkage ubiquitination at DNA damage sites indicates that the corresponding E2 conjugating enzyme and E3 ligase may also accumulate to DNA damage sites for assembly of the Lys11-linkage ubiquitin chains. Lys11-linked polyubiquitination was first identified as a product of an E2-conjugating enzyme Ube2S (also known as E2-EPF) (150). Ube2S and Ube2C (also known as UbcH10) works in concert with the anaphase promoting complex/cyclosome (APC/C) to assemble Lys11-linked ubiquitin chain, in which Ube2C initiates and Ube2S elongates Lys11-linked polyubiquitin chain on APC/C

	GFP-WT Ub	GFP-K63 Ub	GFP-K48 Ub	GFP-K11 Ub	GFP-K6 Ub	GFP-K27 Ub	GFP-K29 Ub	GFP-K33 Ub	GFP-K0 Ub
t=3 min									

Time post-laser	10 sec	1 min	3 min	6 min
GFP – WT Ub				
GFP – K63 Ub				
GFP – K11 Ub				
GFP – K0 Ub				
GFP				
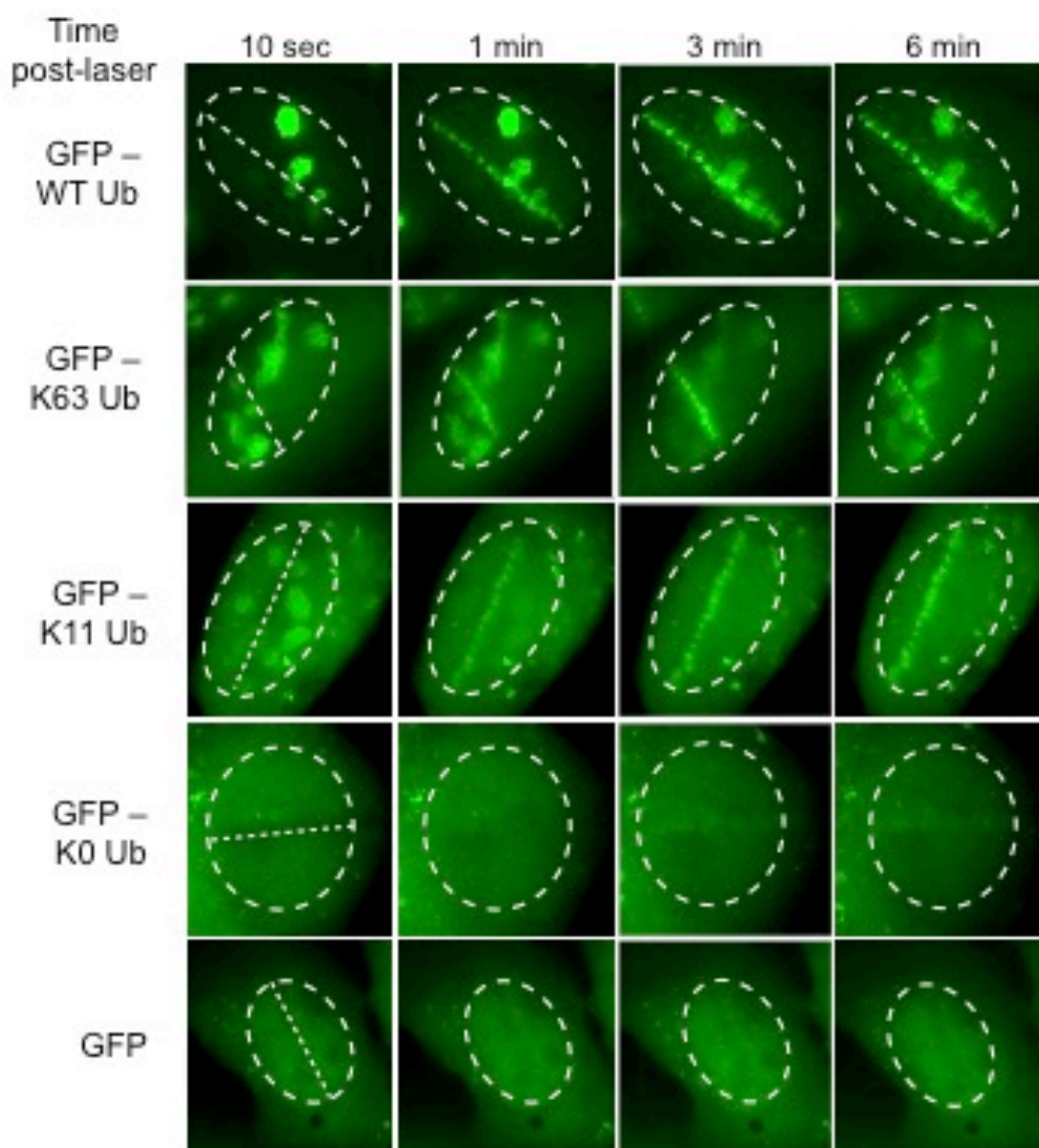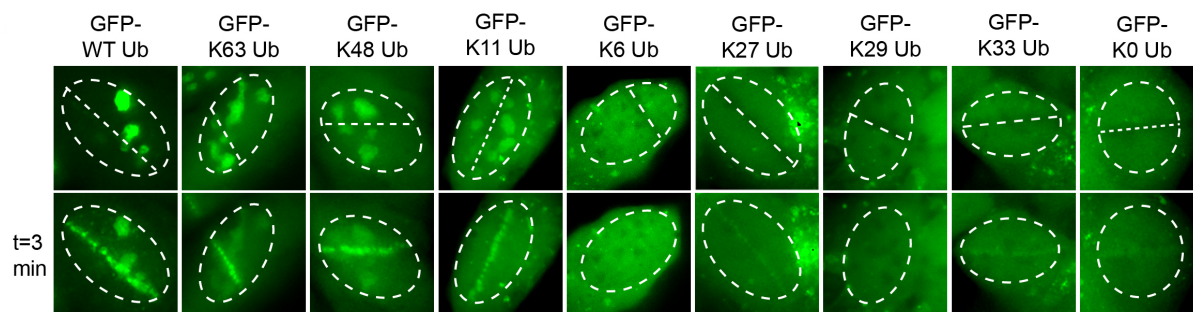
Figure 21: **Linkage specific ubiquitin conjugation in response to DNA damage. A** U2OS cells stably overexpressing either GFP-tagged-WT or Lys only ubiquitin mutants were subject to laser micro irradiation with a UV laser. Live-cell imaging was performed immediately after laser damage for 6 minutes with 30 seconds interval. Dotted line in the first image indicates laser micro irradiated regions across the cell nuclei. Shown here are t=0 and t=3 minutes post-laser micro irradiation. **B.** Lys11-linked ubiquitin conjugation at DNA damage sites. Live-cell imaging of GFP-WT or -Lys63, Lys11 or Lys0 ubiquitin mutants at indicated time-points post-laser micro irradiation. U2OS cells expressing GFP was used as negative control.
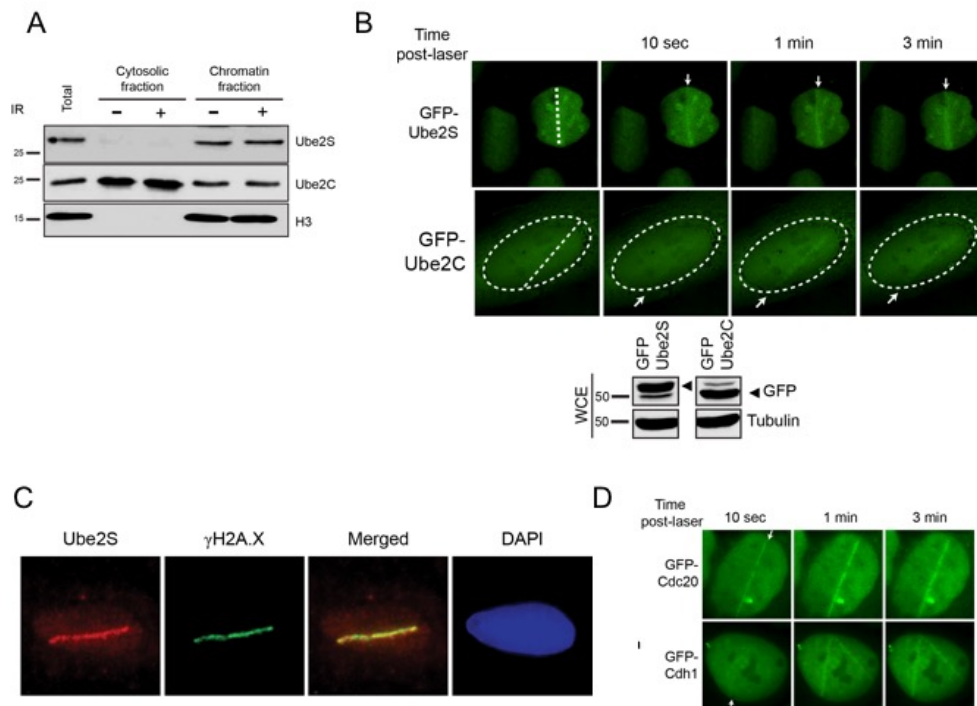
Figure 22 : **Lysine11 ubiquitin conjugation enzymes localize to DNA damage sites. A.** Ube2S and Ube2C are associated with chromatin. Cell fraction analysis was carried out with U2OS cells treated or not treated with 10 Gy IR followed by 30 min incubation at 37°C. **B.** Ube2S and Ube2C accumulate to DNA damage sites. Images of U2OS cells stably expressing GFP-Ube2S or GFP-Ube2C were laser microirradiated and live cell imaging was performed at indicated time points. Western blot analysis of GFP-Ube2S or Ube2C expression levels was shown with tubulin expression as a loading control. **C.** Ube2S co-localizes with γH2AX at DNA damage sites. U2OS cells 5-10 min after laser-micro-irradiation were treated with pre-extraction buffer and immunostained with antibodies to Ube2S and γH2AX. **D.** Cdc20 and Cdh1 localization to DNA damage sites. U2OS cells stably expressing GFP-Cdc20 or Cdh1 were subjected for laser micro-irradiation followed by live cell imaging. Images at indicated times are shown.

substrates (151-154, 163). APC/C is a large multisubunit RING-finger E3 ligase complex including a catalytic core along with two additional co-activators Cdc20 and Cdh1 that recruit substrates to the APC/C ligase complex during mitosis and G1 phases respectively. It plays a major function during cell cycle progression targeting mitotic and G1 cell cycle specific regulators for proteasomal degradation (164, 165). More recently studies done by Komander group identified an OTU family deubiquitinase (DUB), Cezanne (also known as OTUD7B), which preferentially cleaves Lys11-linked ubiquitin chain (157, 158). I first determined whether Ube2S/Ube2C or the APC/C E3 ligase components accumulate to DNA damage sites. Cell fractionation analysis showed that Ube2S and a portion of Ube2C are associated with chromatin (Figure 22A). In addition, using live-cell imaging following laser ablation in cells stably expressing GFP-tagged Ube2S and Ube2C, I observed that GFP-Ube2S and to a lesser extent GFP-Ube2C were recruited to laser-induced DNA damage tracks immediately after damage (Figure 22B). To further confirm recruitment of Ube2S, I used a Ube2S-specific antibody to detect localization of endogenous Ube2S to laser-induced DNA damage sites in U2OS cells and found that endogenous Ube2S accumulates to damage sites marked with the DNA damage marker γH2AX (Figure 22C). APC/C coactivators, CDC20 and CDH1 were also appeared to be recruited to damage tracks after laser treatment (Figure 22D).

3.3.3 Ube2S/Ube2C dependent Lys11-linkage ubiquitin conjugation of chromatin-bound proteins

Next, I examined whether Lys11-linkage ubiquitination occurs to chromatin-bound proteins on damaged chromatin. To test this, I utilized biochemical approach

by isolating chromatin fraction from cells transiently expressing HA-K11 Ub. Analysis of chromatin-enriched fraction isolated from these cells showed that chromatin ubiquitination by K11 Ub increased significantly upon IR-induced DNA damage and was further enhanced by treatment with a proteasomal inhibitor, MG132 (Figure 23A). In addition, by comparing cells expressing HA-WT or mutant (K63, K48, and K11) Ub, I found that ubiquitin modification by K11 Ub was at a level similar to that of K63 or K48 Ub (Figure 23B). These findings confirm live-cell imaging data indicating that Lys11-linked ubiquitination at damaged chromatin is as abundant as Lys63 and Lys48-linked ubiquitination. A ubiquitin K0G76V mutant that cannot be conjugated to substrates was included in the experiment as a negative control and showed no conjugation of chromatin-bound proteins with this mutant ubiquitin (Figure 23B).

To determine whether Lys11-linkage chromatin ubiquitination is mediated by Ube2S/Ube2C conjugating enzymes at DNA damage sites, I depleted endogenous Ube2S and Ube2C using siRNAs from cells expressing HA-K11 Ub. Analysis of chromatin fraction isolated from these cells showed significant impairment of K11-linked ubiquitination of chromatin-bound proteins in Ube2S/Ube2C siRNAs (Figure 24A). Additionally, I found depletion of Ube2S alone impaired Lys11-linked chromatin ubiquitination to a large extent (Figure 24B), suggesting that Ube2S catalyzes K11-linkage ubiquitin chain formation on damaged chromatin. In order to exclude any possibility of siRNA off-target effects, these results were further confirmed with three different Ube2S siRNAs and as shown in Figure 24C, all three Ube2S siRNAs impaired Lys11-linked chromatin ubiquitination. Moreover, to validate Ube2S–mediated chromatin ubiquitination by K11 ubiquitin chain, I used siRNA-
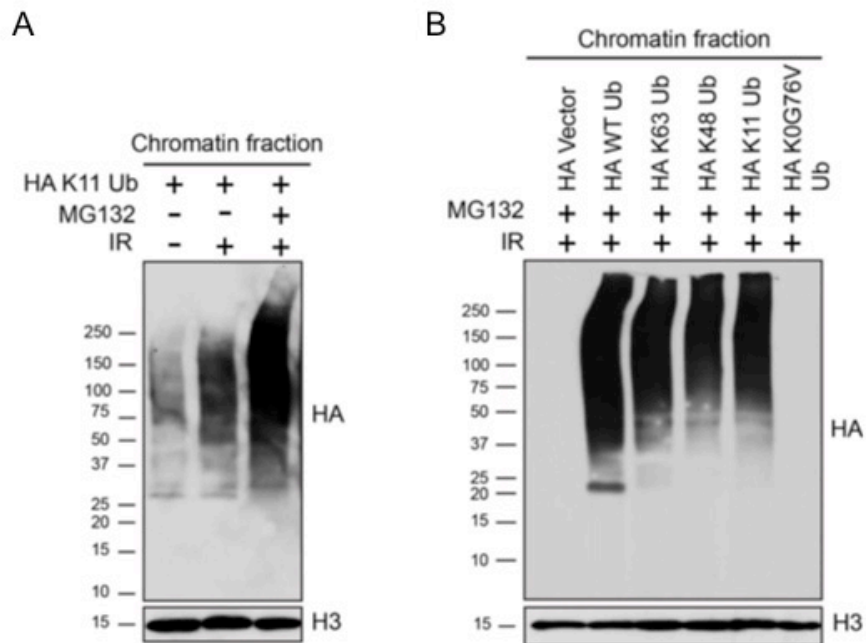
Figure 23 : **IR-induced Lys11-linkage ubiquitination at damaged chromatin A**

IR-induced Lys11-linkage chromatin ubiquitination. U2OS cells expressing HA-K11

Ub were either treated or not treated with 10 Gy IR followed by 1hr incubation at

37°C. MG132 (10 μM) was added 5 hr before IR.

B. Linkage-specific ubiquitination on chromatin in response to IR. U2OS cells

expressing HA-Ub WT or mutant were treated with IR similarly as in (A).
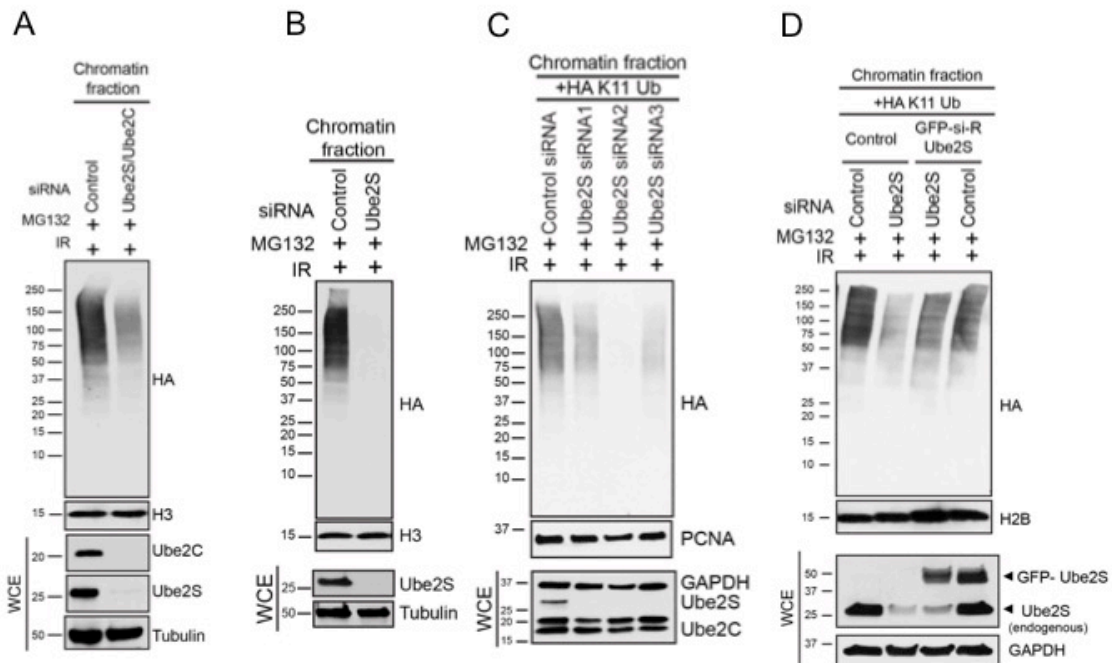
Figure 24: **IR-induced Lys11-linkage chromatin ubiquitination depends on Ube2S/Ube2C enzyme A** Ube2S/Ube2C are required for Lys11-linkage chromatin ubiquitination. Cells expressing HA-K11 Ub were treated with control or Ube2S/Ube2C siRNAs. 48 hours post transfection, cells were treated with MG132 and IR and chromatin fraction was isolated for HA antibody analysis. Whole cell lysate (WCE) was used for western blot for assessing knockdown efficiency. **B.** Ube2S depletion alone impairs Lys11-linked chromatin ubiquitination. U2OS cells expressing HA-K11 Ub were transfected with siRNA targeting Ube2S. Chromatin fraction was analyzed as in A. **C.** Three independent Ube2S siRNAs decreases Lys11-linked chromatin ubiquitination. **D.** Ube2S catalyzes Lys11-linkage chromatin

ubiquitination. Cells expressing HA-K11 Ub were transfected with control or

Ube2S siRNA along with GFP vector or GFP-tagged siRNA-resistant Ube2S, as

indicated. Chromatin fraction was isolated and analyzed with HA antibody. Whole

cell extract was used to detect knockdown efficiency.

resistant Ube2S construct in the Ube2S-depleted cells and found that expression of

siRNA-resistant GFP-Ube2S can restore Lys11-linked chromatin ubiquitination in

Ube2S-depleted cells (Figure 24D). Together, these results indicate that chromatin-

bound proteins are modified with Lys11-linked ubiquitin modification in Ube2S-

dependent manner.

3.3.4 APC/C E3 ligase-independent Lys11-linked chromatin ubiquitination

Since Ube2S/Ube2C functions with APC/C E3 ligase to catalyze Lys11-linked

ubiquitination on substrates that regulate cell cycle progression such as cyclin B, I

tested whether APC/C is required for Lys11-linkage modification on chromatin in

response to DNA damage. To test this, I depleted Apc2, a core component of the

APC/C E3 complex, in cells expressing HA-K11 Ub. While depletion of Apc2

abrogated APC/C's E3 ligase function leading to stabilization of Cyclin B1 and an

increase of mitotic cells as marked by increased phospho-histone H3, this had

minimal effect on K11-linked chromatin ubiquitination in response to IR (Figure 25A).

Inhibition of APC/C by proTAME, an inhibitor to APC (166), also did not decrease

K11 Ub modification on damaged chromatin (Figure 25B). Moreover, knockdown of

the APC/C co-activator Cdh1 also did not result in a decrease of chromatin-level

K11-linked ubiquitin conjugation (Figure 25C). Together, these findings indicate that

Ube2S-catalyzed Lys11-linkage chromatin ubiquitination in response to DNA

damage is independent of APC/C E3 ubiquitin ligase.
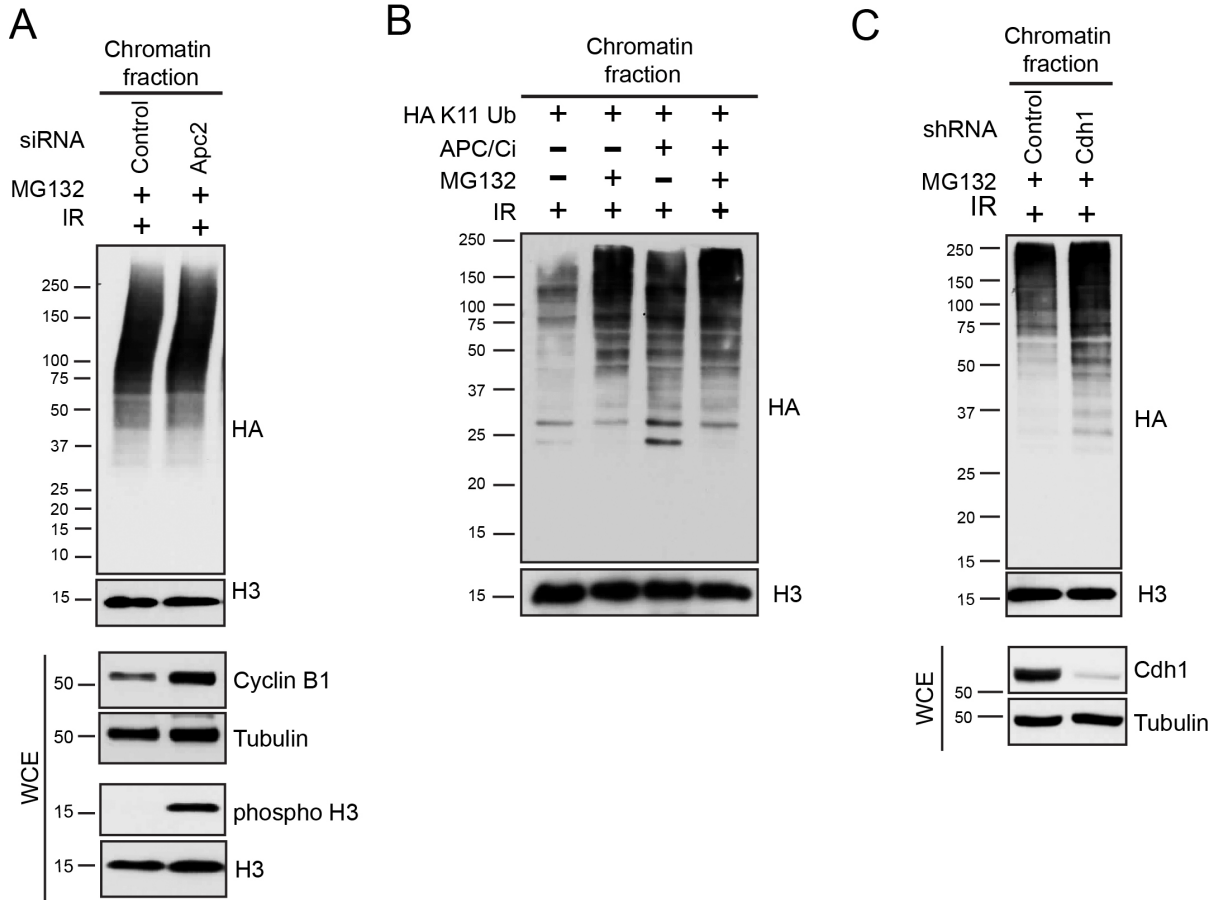
Figure 25 : **APC/C-independent Lys11-linkage chromatin ubiquitination.**

A. U2OS cells expressing HA-K11 Ub were transfected with control or Apc2

siRNAs. 48 hours post-transfection, cells were treated with MG132, irradiated and

chromatin fraction was isolated for western blot analysis with HA antibody. Total

cell lysates were blotted with indicated antibodies to confirm abrogation of APC/C's

function in Apc2 knockdown cells. **B.** U2OS expressing HA-K11 Ub were treated

with APC/C inhibitor (proTAME 25 µM) for 18 hours before treatment with MG132

(or untreated) and IR. Chromatin fraction was isolated and analyzed with HA

antibody. H3 was used as loading control. **C.** Knockdown of Cdh1 does not

decrease Lys11-linkage chromatin ubiquitination. U2OS cells stably expressing

control shRNA or shRNA targeting Cdh1 were transfected with HA-K11 Ub. 48 hr

post-transfection, chromatin fraction was isolated and analyzed by western blot

with HA antibody. Total cell lysates were analyzed to confirm knockdown

efficiency.

3.3.5 Lys11-linked chromatin ubiquitination is dependent on ATM kinase and upstream DDR factors

In response to IR-induced DNA damage, ATM-mediated phosphorylation of histone H2AX (γH2AX) recruits MDC1 to DNA damage sites that initiates the subsequent recruitment of RNF8 and RNF168 E3 ubiquitin ligases and Ubc13 E2 conjugating enzyme for Lys63-linkage ubiquitin chain assembly on histones H2A and H2AX (37-39, 41, 43, 45, 143). Given the pivotal role of ATM kinase in triggering DDR response immediately after DNA damage, I investigated whether the Lys11-linkage ubiquitin modification on damaged chromatin is also regulated by ATM signaling. Cells treated with siRNAs to ATM but not ATR greatly impaired K11-linked ubiquitination on damaged chromatin to levels resembling those of Ube2S/Ube2C depleted cells (Figure 26A), indicating that Lys11-linkage ubiquitin modification occurs on damaged chromatin in an ATM-dependent manner. I further tested whether depletion of other upstream DDR factors such as MDC1 as well H2A.X had any effect in Lys11-linked chromatin ubiquitination. Interestingly, I found that knockdown of MDC1 and H2AX also led to significant impairment of K11-linked chromatin ubiquitination (Figure 26A and B).
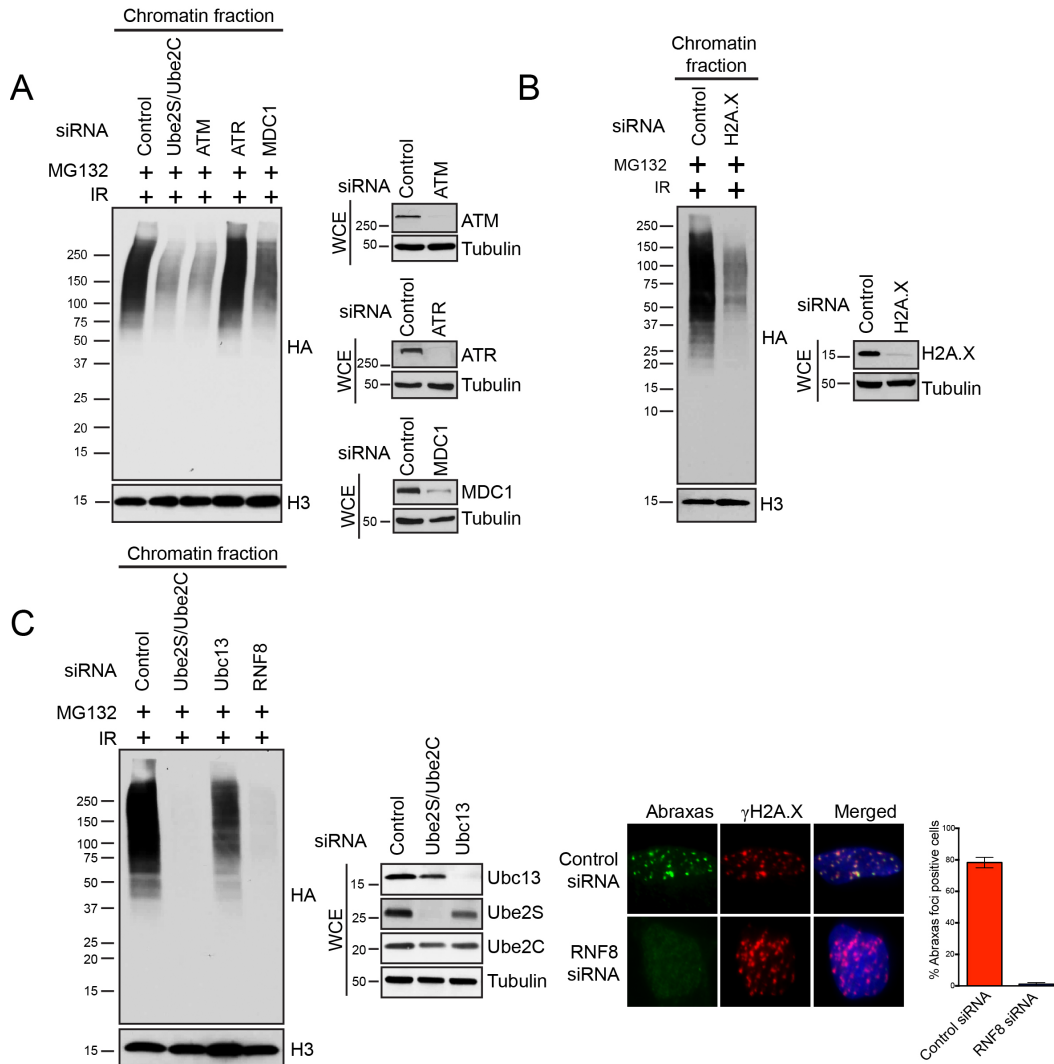
Figure 26 : **Lys11-linkage chromatin ubiquitination is regulated by ATM, MDC1 and RNF8 A.** ATM and MDC1, but not ATR is required for Lys11-linkage ubiquitination on chromatin in response to IR. U2OS cells treated with control or Ube2S/Ube2C, ATM, ATR or MDC1 were transfected with HA-K11 Ub. 48 hours post-transfection, chromatin fractions were extracted and analyzed with HA antibody. Histone H3 was used as a loading control. Whole cell extracts were analyzed with indicated antibodies to confirm knockdown efficiency **B.** H2AX is

required for Lys11-linkage ubiquitination on damaged chromatin. Chromatin fraction was isolated from cells transfected with control or H2A.X siRNAs and HA K11 Ub and treated similarly as in A **C.** RNF8 regulates Lys11-linkage ubiquitination on chromatin. Cells transfected with indicated siRNAs and HA K11 Ub were treated and analyzed similarly as in A. RNF8 knockdown efficiency is measured by decrease of Abraxas IRIF. U2OS cells transfected with control or RNF8 siRNAs treated with IR at 10 Gy followed by 2 hours incubation at 37°C were analyzed by IF with Abraxas and γH2AX antibodies. More than 500 cells were counted for quantification and cells containing more than 10 foci were counted as positive. The data represents means± SD.

3.3.6 RNF8 functions as an E3 ligase catalyzing Lys11 ubiquitin chain that is deubiquitnated by the DUB Cezanne

Since my findings indicate that Lys11-linked chromatin ubiquitination occurs in a manner independent of APC/C E3 ligase, I examined other enzymes known to play role in catalyzing ubiquitination at damaged chromatin. To this end, I examined whether Ubc13 and RNF8, enzymes known to catalyze Lys63-linked ubiquitination at DNA damage sites, also regulate K11-linked ubiquitin conjugation on damaged chromatin. Interestingly while depletion of Ubc13 appeared to have minimal effects on Lys11-linked chromatin ubiquitination, I found that depletion of RNF8 completely abrogated K11-linked chromatin ubiquitination to a level similar to that of the Ube2S/Ube2C knockdown cells (Figure 26C), indicating that RNF8 may function as an E3 ligase in catalyzing Lys11-linkage ubiquitination at DNA damage sites independent of Ubc13. Of note, as described in sections 3.1.2 and 3.1.6, RNF8 has been shown to catalyze both Lys63 and Lys48-linked ubiquitination by interacting with distinct of E2 enzymes, Ubc13, and UbcH8, respectively. RNF8 is a RING domain E3 ligase and one characteristic feature of many of the RING domain E3 ligases is to catalyze substrate-independent autoubiquitination (167). RNF8 has been shown to undergo substrate-independent autoubiquitination synthesizing both Lys63 and Lys48-linked chains by interacting with distinct E2 enzymes, Ubc13 and UbcH8, respectively (57, 58). I hypothesized that if RNF8 indeed catalyzes Lys11-linked ubiquitin chain in concert with Ube2S, it might also undergo Lys11-linked autoubiquitination. To test this, I co-expressed Flag-RNF8 along with HA-K11,
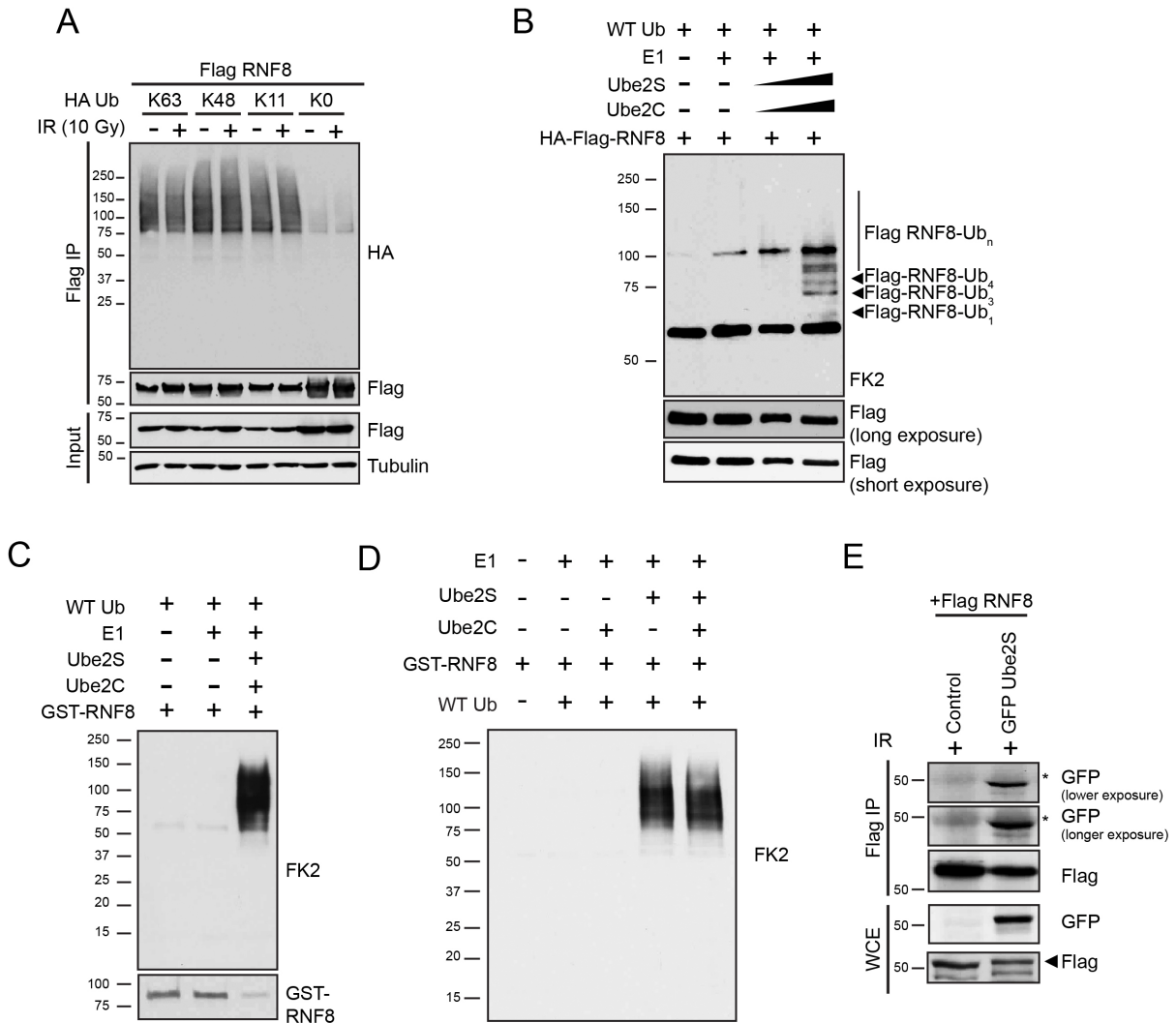
Figure 27: RNF8 functions as an E3 ligase for Lys11-linked ubiquitination.

A. RNF8 autoubiquitination by Lys11-linkage modification. HEK293T cells were co-transfected with Flag-RNF8 and HA-K63, -K48 or -K11 Ub. 48 hours post-transfection, cells were irradiated with 10 Gy IR (or left untreated) followed by 30 min incubation at 37°C. Flag-immunoprecipitation was carried out under denaturing condition. **B.** Lys11-linkage autoubiquitination of RNF8 *in vitro*. Purified HA-Flag-RNF8 was eluted from Flag-beads after immunoprecipitation from lysates of HEK293T cells expressing HA-Flag-RNF8. Equal amount of eluted Flag-RNF8 was

reaction mixtures containing purified ubiquitin, E1 and increasing amount of purified

Ube2S and Ube2C as indicated. **C.** Lys11-linkage autoubiquitination of RNF8 *in vitro*

using recombinant GST-RNF8. **D.** Ube2S alone can promote RNF8

autoubiquitination *in vitro*. *In vitro* autoubiquitination assay was performed in

presence of recombinant Ube2C (lane 4) or Ube2S (lane 5) or both (lane 6) and

GST-RNF8 similarly as in C. **E.** RNF8 interacts with Ube2S. HEK293T cells were co-

transfected with Flag-RNF8 and GFP-Ube2S before treatment with IR.

K63, K48 or K0 Ub in cells and examined linkage-specific RNF8 self-ubiquitination under denaturing condition. This analysis revealed that in addition to previously reported K63- and K48-linked autoubiquitination; RNF8 is also modified by Lys11-linked polyubiquitin chain, suggesting that RNF8 may act as an E3 ligase for Lys11-linked ubiquitination (Figure 27A). To validate RNF8's role as an E3 ligase that in concert with Ube2S/Ube2C catalyzes Lys11-linkage ubiquitination, I tested whether Ube2S/Ube2C assist in autoubiquitination of RNF8 *in vitro*. Purified RNF8 eluted from Flag-immunoprecipitates from cell lysates (Figure 27B) or recombinant GST-RNF8 was incubated *in vitro* with ubiquitin in the presence of purified E1 and Ube2S/Ube2C E2 enzymes (Figure 27C). The findings obtained from this *in vitro* ubiquitination assays showed that Ube2S/Ube2C facilitated self-ubiquitination of RNF8 *in vitro*. Moreover, I tested whether Ube2S alone can facilitate RNF8 autoubiquitination. As shown in Figure 27D, *in vitro* RNF8 autoubiquitination assay in presence of Ube2S or Ube2C or both confirmed that Ube2S alone can catalyze RNF8 autoubiquitination under this condition. Furthermore, I reason that if Ube2S and RNF8 coordinate with each other to catalyze Lys11-linked ubiquitination, they might also interact with each other. Since endogenous E2-E3 interaction is difficult to detect due to transient nature of this interaction (106, 168), I co-expressed Flag-RNF8 with GFP-Ube2S or GFP-Ube2C in HEK293T cells. Co-immunoprecipitation analysis showed that Flag-tagged RNF8 interacted with GFP-tagged Ube2S (Figure 27E) but not Ube2C (data not shown) in the presence of IR; consistent with the idea that RNF8 E3 ligase works with Ube2S to assemble Lys11-linked chains.
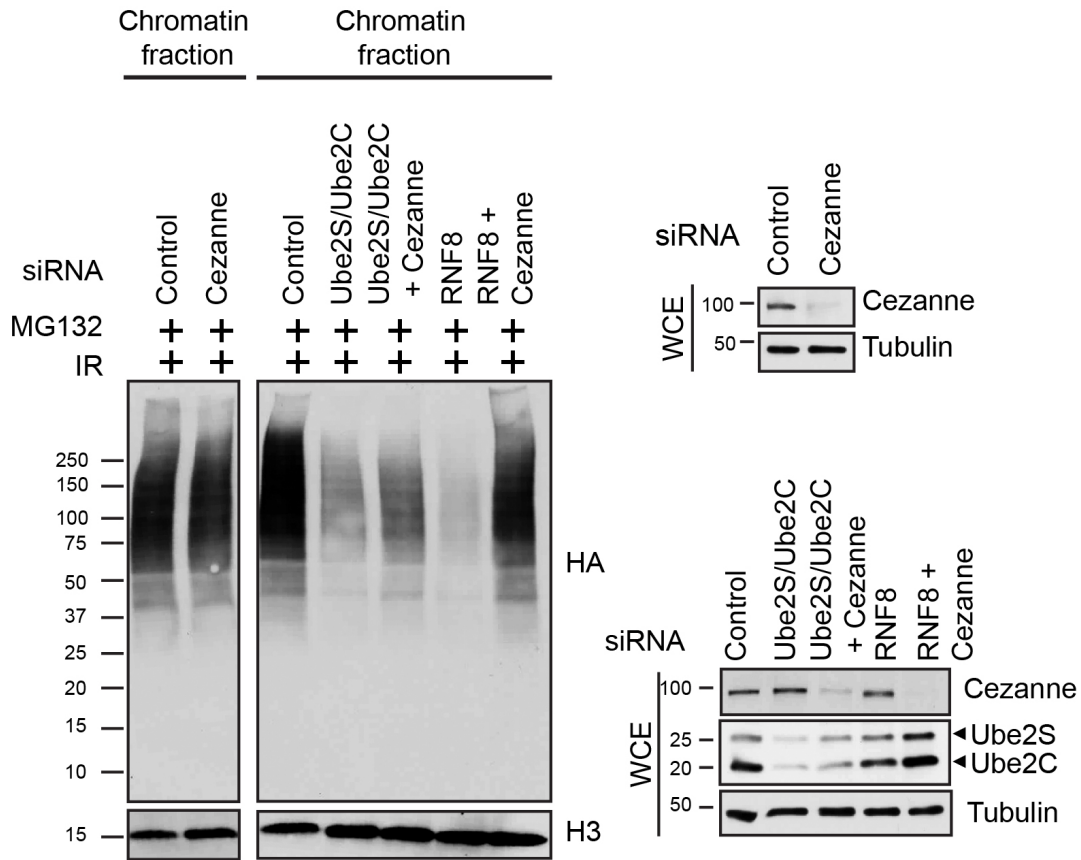
Figure 28 : **RNF8-dependent Lys11-linkage ubiquitination is antagonized by Cezanne.** U2OS cells were transfected with indicated siRNAs individually or in combination, followed by transient transfection of HA-K11 Ub. 48 hours post-transfection, cells were treated with MG132, irradiated and chromatin fraction was isolated for western blot analysis with HA antibody. Knockdown efficiency of individual gene was confirmed by western blot analysis of whole cell lysate with indicated antibodies (right panel).

Finally, to further confirm that RNF8 promotes Lys11-linkage ubiquitin modification, I examined whether Cezanne, a DUB that specifically cleaves the Lys11-linkage ubiquitin conjugates (157), antagonizes the activity of RNF8 in Lys11-linkage ubiquitin modification of chromatin-bound proteins. Indeed, while knockdown of RNF8 decreased the Lys11-linkage ubiquitin modification, depletion of Cezanne in RNF8-deficient cells significantly reversed the decrease of Lys11-linkage ubiquitination, indicating that RNF8 and Cezanne function in the same pathway to modify Lys11-linkage ubiquitin conjugation on damaged chromatin (Figure 28). Taken together, these findings conclusively suggest that RNF8 acts as an E3 ligase that in association Ube2S E2 conjugating enzyme catalyzes Lys11-linked chromatin ubiquitination at the damaged chromatin.

3.3.7 Histone H2A/H2A.X are modified with Lys11-linked ubiquitin conjugates in DNA damage-dependent manner

My findings indicate that chromatin-bound proteins undergo Lys11-linked ubiquitination by Ube2S-RNF8 enzymes in DNA damage-dependent manner. Because histone proteins are the fundamental unit of chromatin structure and are subjected to extensive post-translational modifications including ubiquitination, I examined whether histones are modified by Lys11-linkage ubiquitin conjugates. To test this, I undertook multiple biochemical approaches. First, I used acid extraction to isolate all histone proteins from cells expressing HA-tagged WT or Lys only mutant Ub. Acid extraction of highly basic histone proteins is a standard procedure to isolate histone proteins from chromatin. Robust ubiquitination of acid-extracted proteins,
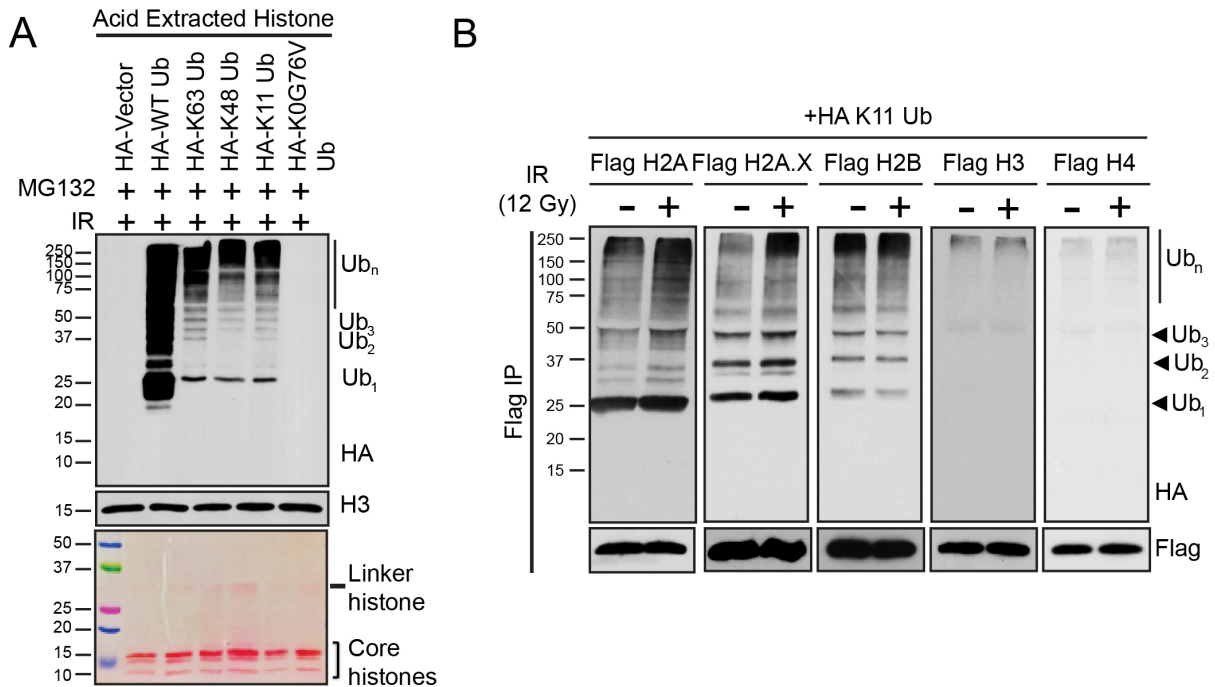
Figure 29 : **Histone proteins are modified with Lys11-linked ubiquitination.** Linkage-specific ubiquitination of acid-extracted histone faction. U2OS cells expressing HA-WT or mutant Ub were treated with MG132, irradiated followed by acid extraction to isolate highly basic histone proteins. Histone H3 was used as loading control. Bottom panel: Ponceau staining of acid-extracted histones is shown. **B.** DNA damage-induced Lys11-linkage ubiquitination of histone H2A/H2AX. HEK293T cells co-transfected with Flag-H2A or -H2AX and HA-K11 Ub were irradiated at 12 Gy and incubated at 37°C for 1 hour. Flag-immunoprecipitation was carried out under denaturing condition as described in material and methods. Bottom panel: Flag immunoblot showing immunoprecipitated Flag-tagged histone proteins.

presumably mainly histones, by HA-WT Ub could be seen with western blot. Interestingly, the level of ubiquitin modification by K11 Ub was similar to that of K63 and K48 Ub, suggesting that Lys11-linkage formation occurs as extensively as the Lys63- or Lys48-linkage formation on histones (Figure 29A). These findings again corroborate my live-cell imaging data of Lys11-linked ubiquitination at damaged chromatin (Figure 21). Second, to examine which histone protein(s) is modified with Lys11-linked ubiquitination, I co-expressed Flag-tagged individual histone proteins, including H2A, H2AX, H2B, H3, and H4 along with HA-K11 Ub in HEK293T cells and treated the cells with IR to induce DNA damage. Analysis of Flag-immunoprecipitation done under denaturing condition revealed that among all histone proteins, histone H2A and H2AX were modified with K11 Ub in a DNA damage-dependent manner. Analysis of Lys11-linkage ubiquitin modification on other histone proteins showed that H2B was also modified by K11-linked ubiquitin but the modification was independent of IR and that H3 and H4, on the other hand, did not show modification by K11-linked ubiquitin (Figure 29B).

I then set out to confirm whether endogenous histone H2A/H2A.X are modified by Lys11-linkage ubiquitination upon DNA damage. Utilizing a previously published system expressing a tandem hexahistidine-biotin tag (HBT-tag) fused to ubiquitin for purification of ubiquitinated proteins under fully denaturing conditions (113), I generated HeLa cells stably expressing HBT-K11 Ub. Analysis of streptavidin beads pull-down proteins under complete denaturing condition (8M Urea) and by western blot with antibodies to ubH2A, H2A or γH2A.X revealed that
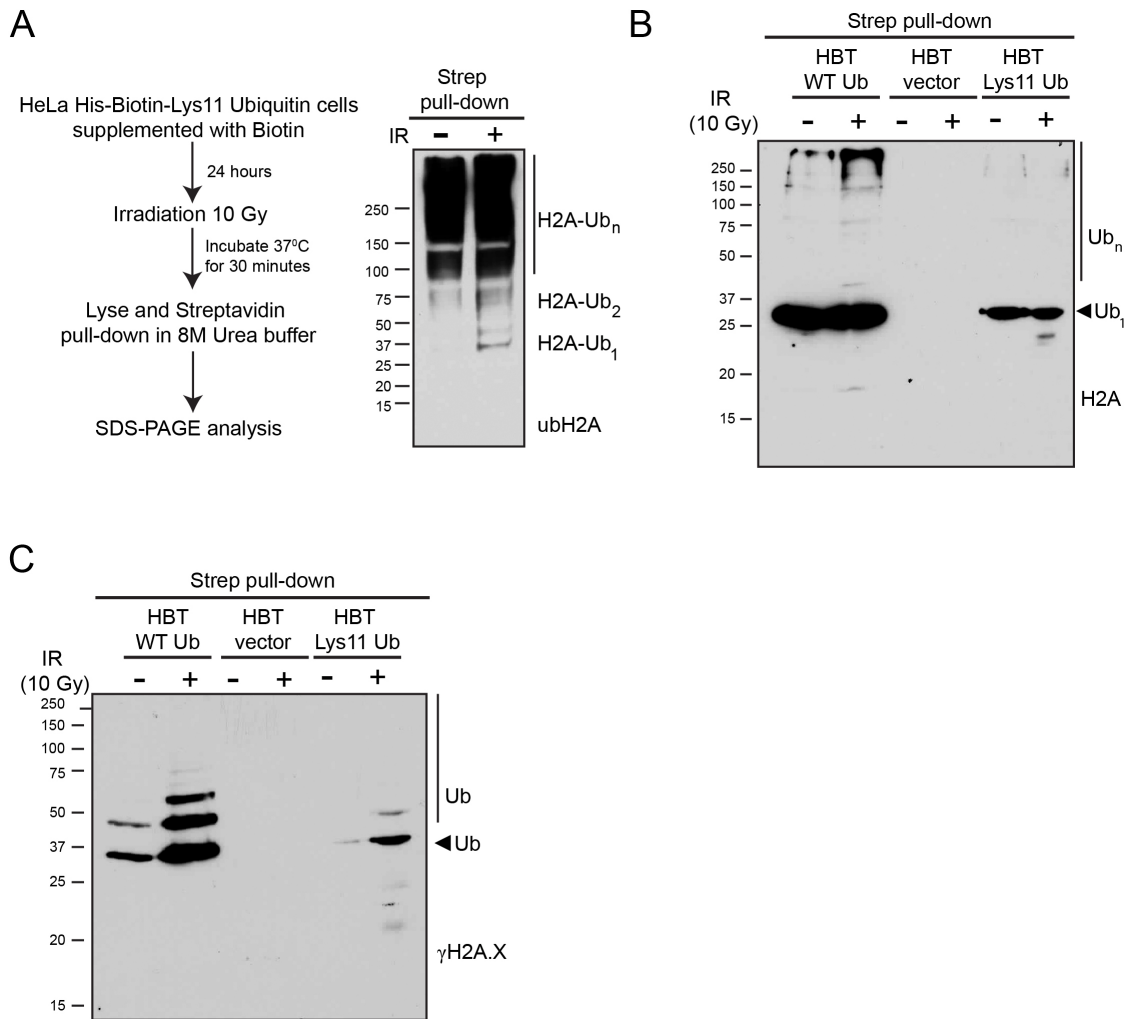
Figure 30 : **Endogenous histone H2A/H2A.X are modified with Lys11-linked ubiquitination. A.** Left panel: Schematic for detection of endogenous histone H2A modification with Lys11-linked ubiquitin conjugates under denaturing condition. Right panel: Streptavidin pulldown proteins were analyzed with western blot using antibodies to ubiquitinated H2A (ubH2A). **B and C.** Hela cells expressing His-Biotin-K11 Ub were subjected to treatment as described in Figure A and were analyzed with antibodies again H2A (B) and γH2A.X (C).
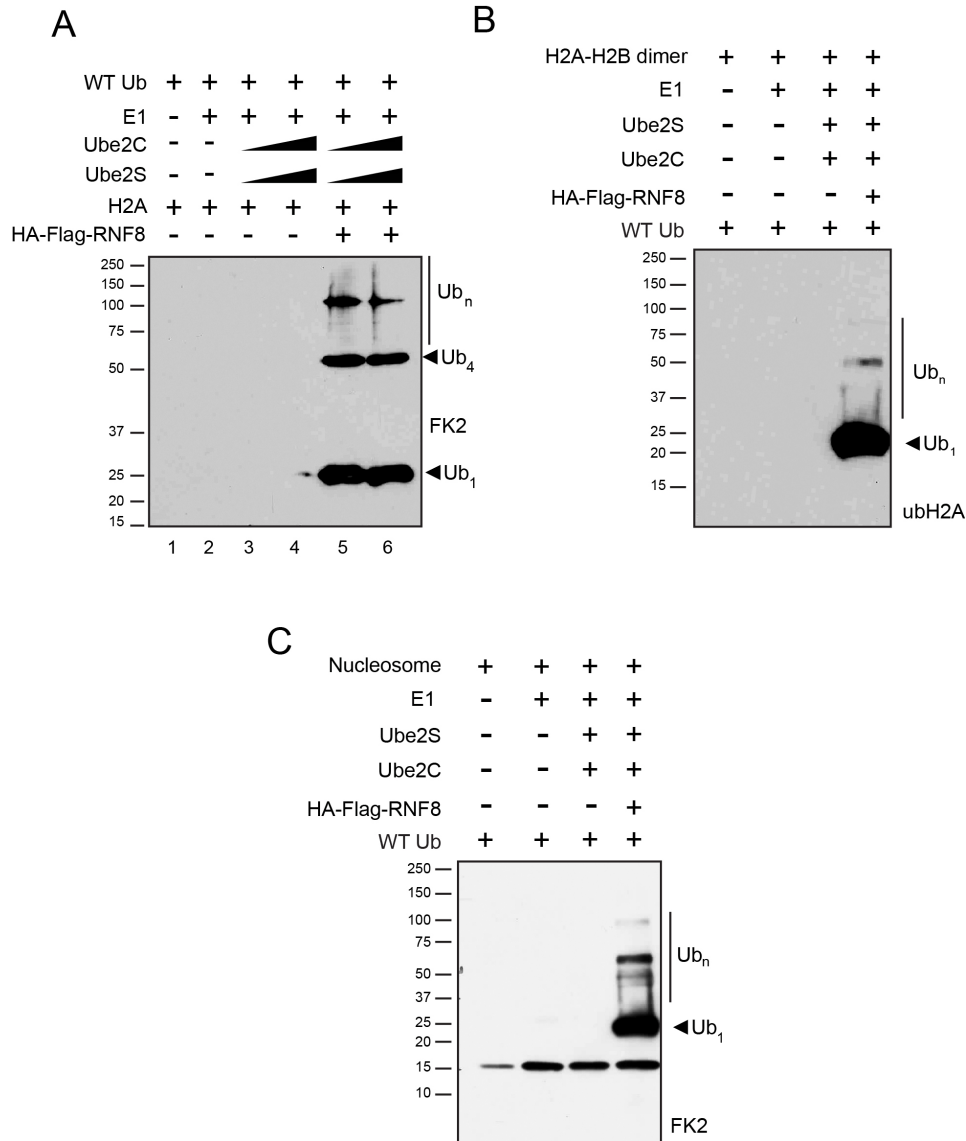
Figure 31: **RNF8 and Ube2S/Ube2C catalyze histone H2A ubiquitination *in vitro*. A.** Recombinant histone H2A was incubated with a reaction mixture containing purified ubiquitin, E1, increasing amount of Ube2S/Ube2C (lanes 3-4 and 5-6), in the presence (lane 5 & 6) or absence (lanes 1-4) of purified HA-Flag-RNF8. Reaction mixtures were analyzed by western blot with FK2 antibody. **B.** H2A ubiquitination *in vitro.* H2A/H2B dimer was used in the reaction as described in (A). The western blot was carried out with ubH2A antibody. **C.** *In vitro* ubiquitination by RNF8 and Ube2C/Ube2S using nucleosome as substrates.

107

endogenous histone H2A/H2AX could be modified by K11-Ub conjugates and this modification was somewhat enhanced in response to IR (Figure 30). Finally, I tested whether histone H2A is a substrate directly modified by RNF8 and Ube2S/Ube2C using *in vitro* ubiquitination assay. I incubated purified H2A with ubiquitin, E1, Ube2S/Ube2C and HA-Flag-RNF8 and examined the conjugation of ubiquitin on H2A by the FK2 antibody or ubH2A antibody. It showed that polyubiquitination of H2A was triggered when purified RNF8 was present, suggesting that H2A is a direct substrate of RNF8 (Figure 31A). Ubiquitination of H2A recognized by ubH2A antibody was also shown when histone H2A/H2B dimer was used in the reaction (Figure 31B). Similar findings were also observed when I used nucleosome as substrate for *in vitro* ubiquitination reaction (Figure 31C)*.* Together, these findings confirm that RNF8 functions with Ube2S to assemble Lys11-linkage ubiquitin chains on substrates including H2A.

3.3.8 RNF8 and Ube2S catalyze Lys11-linked H2A ubiquitination in DNA damage-dependent manner

Next, I tested whether Ube2S and RNF8 are required for Lys11-linkage ubiquitin modification of H2A. I depleted Ube2S or RNF8 in HEK293T cells expressing Flag-tagged H2A and HA-K11 Ub. My findings indicate that depletion of Ube2S or RNF8 by siRNAs led to a marked decrease of K11-linked polyubiquitination of H2A, indicating that Ube2S and RNF8 are required for catalyzing Lys11-linkage ubiquitination of H2A in response to IR (Figure 32A). Since Lys11-linked ubiquitination was identified as a proteolytic signal for mitotic proteins, I tested whether modification of histones H2A and H2A.X triggers degradation of
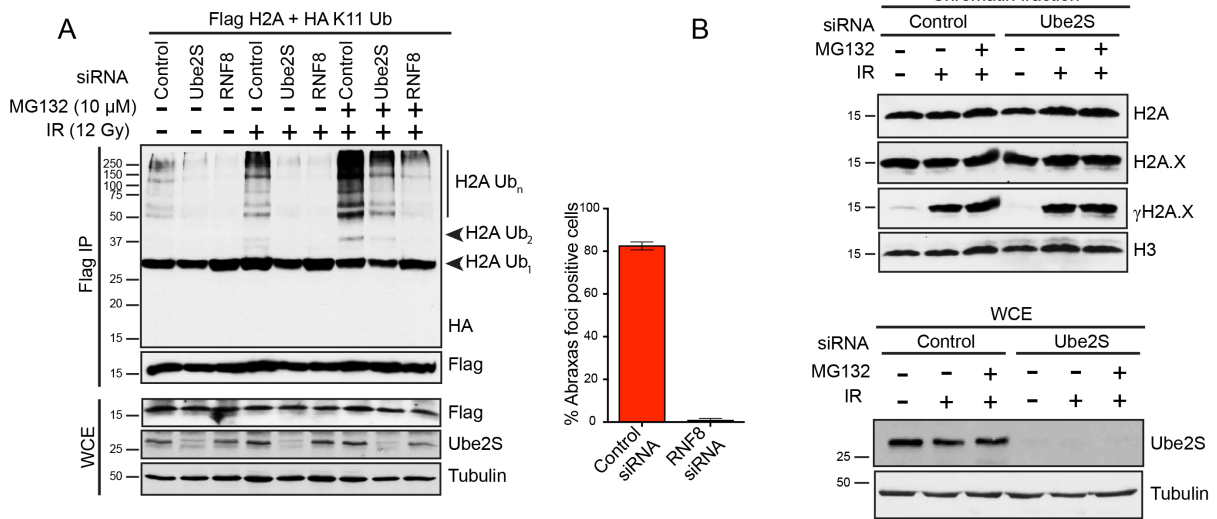
Figure 32: **Ube2S and RNF8-dependent Lys11-linkage ubiquitination of histone H2A/H2AX in response to DNA damage. A.** HEK293T cells depleted of Ube2S or RNF8 were co-transfected with Flag-H2A and HA-K11 Ub. 48 hours post-transfection, cells were treated with MG132 (or left untreated), irradiated at 12 Gy (or untreated) followed by lysis and Flag-immunoprecipitation under denaturing condition and western blot analysis with indicated antibodies. Whole cell extracts were immunoblotted with indicated antibodies to confirm knockdown efficiency. Right panel: Confirmation of RNF8 knockdown efficiency. U2OS cells transfected with control or RNF8 siRNAs were analyzed by IF for Abraxas IRIF formation. Cells containing 10 or more foci were counted as positive and the data represents means± SD. **B.** Endogenous H2A/H2AX protein levels are not affected in Ube2S-deficient cells. Chromatin fraction from U2OS cells transfected with control or Ube2S siRNAs was analyzed by western blot with indicated histone antibodies. PCNA protein level was used as a loading control. Total cell lysates were analyzed by western blot for knockdown efficiency.

these proteins. Analysis of endogenous histones H2A and H2A.X in presence or absence of DNA damage and/or proteasomal inhibitor MG132 revealed no alteration in chromatin-bound histone protein level in control and Ube2S depleted cells indicating Lys11-linked ubiquitination of histone is not a proteolytic signal (Figure 32B).

3.3.9 Lys11-linkage ubiquitination does not interfere with Lys63-linked ubiquitination-dependent recruitment of 53BP1 and BRCA1

We reason that, if RNF8 functions with Ube2S/Ube2C, but not Ubc13, in regulating Lys11-linkage ubiquitin modification, knocking down Ube2S/Ube2C should not interfere with the Ubc13-dependent Lys63-linkage ubiquitin conjugation at damaged chromatin that recruits 53BP1 and BRCA1 to DNA damage sites. To test this, I utilized multiple approaches. First, I examined whether depletion of endogenous Ube2S impairs chromatin-bound proteins modification by Lys63-linked ubiquitin. Isolating chromatin fraction from Ube2S depleted cells showed that Ube2S depletion had minimal effect on Lys63-linked chromatin ubiquitination (Figure 33). In addition, I tested IR-induced foci formation (IRIF) of 53BP1 and Abraxas/BRCA1-A complex (41, 47) components in Ube2S/Ube2C depleted cells. Consistent with a role of Ube2S in forming DNA damage-induced ubiquitin conjugates at DNA damage sites, IF staining with the FK2 antibody that detects ubiquitin chains showed a significant decrease of ubiquitin foci formation in Ube2S/Ube2C (Figure 34). However, knockdown of Ube2S/Ube2C did not appear to have a major effect on affecting IRIF of 53BP1, BRCA1, Abraxas, or Rap80 (Figure 35), indicating that Lys11-linkage ubiquitin modification does not directly interfere with the Lys63-linkage
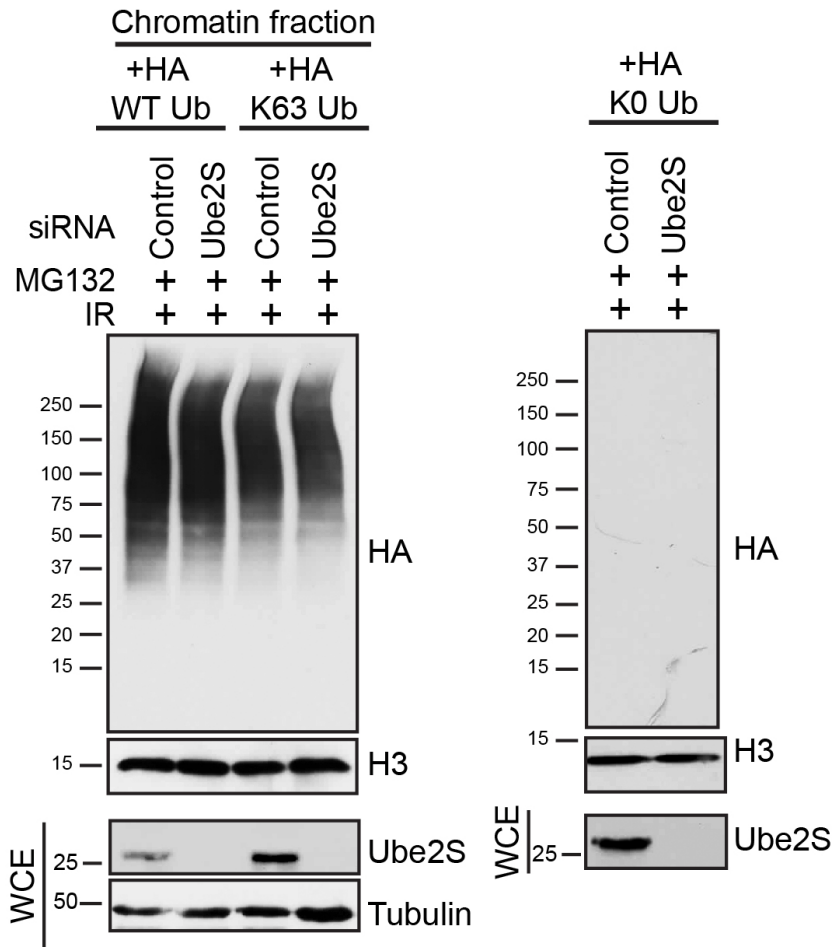
Figure 33: **Ube2S knockdown effect on chromatin ubiquitination modified by HA-WT, K63 or K0 Ub.** U2OS cells treated with control or Ibe2S siRNAs were transfected with HA-K11 Ub. 48 hours post-transfection, chromatin fractions were extracted and analyzed with HA antibody. Histone H3 was used as a loading control. Whole cell extracts were analyzed with indicated antibodies to confirm knockdown efficiency.
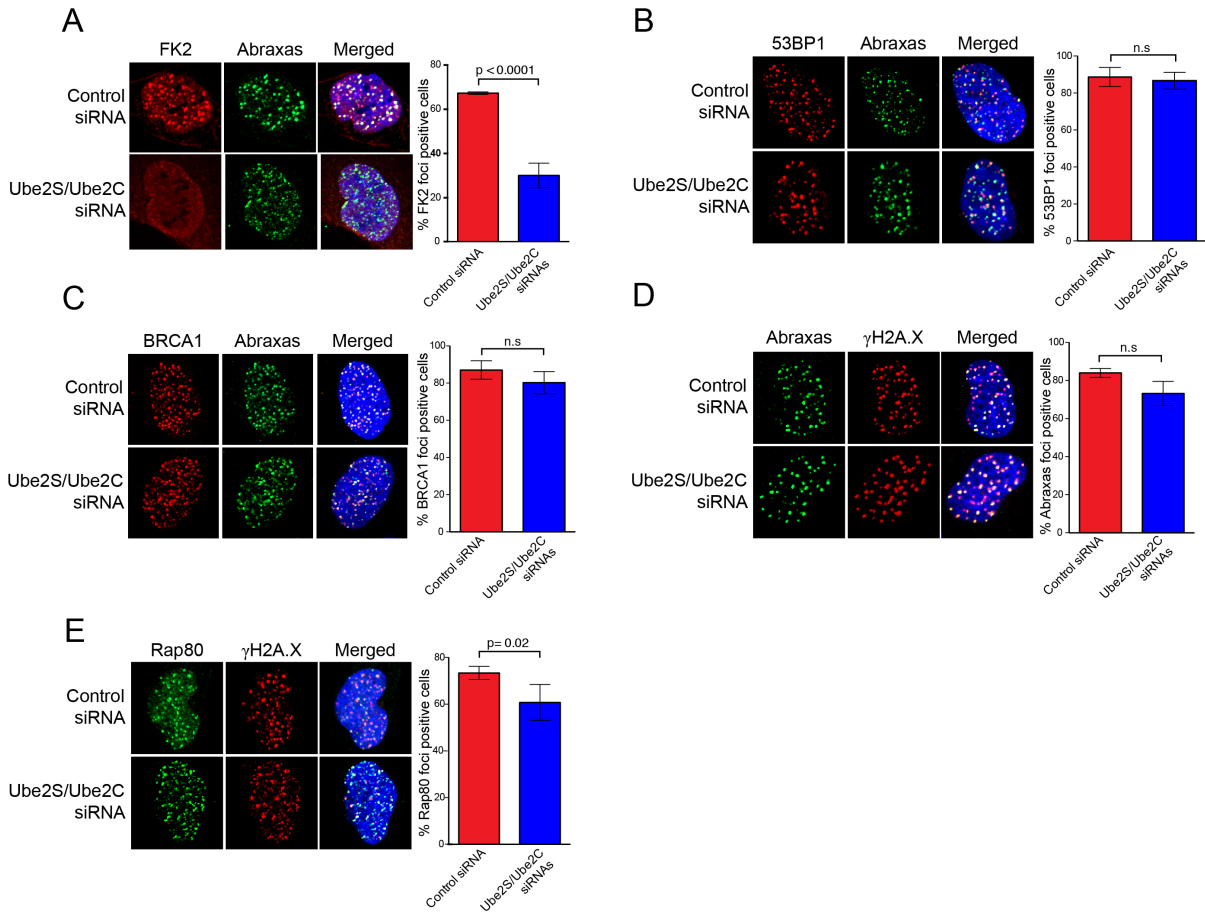
Figure 34 : **Lys11-linkage ubiquitination is dispensable for recruitment of DNA damage repair proteins 53BP1 and BRCA1-A complex proteins.**

U2OS cells were transfected with control siRNA or siRNAs targeting Ube2S/Ube2C. 48 hr post-transfection, cells were irradiated with 10 Gy IR, incubated for 2 hr at 37°C followed by immunostaining with antibodies to conjugated ubiquitin (FK2 antibody) **(A),** 53BP1 **(B),** BRCA1 **(C),** Abraxas (**D**), or Rap80 **(E).** Percentage of foci-positive cells (cells containing more than 10 foci) was quantified and indicated as means± SD with p-value indicated. The experiments were repeated three times with more than 500 cells counted each time, and representative images are shown.
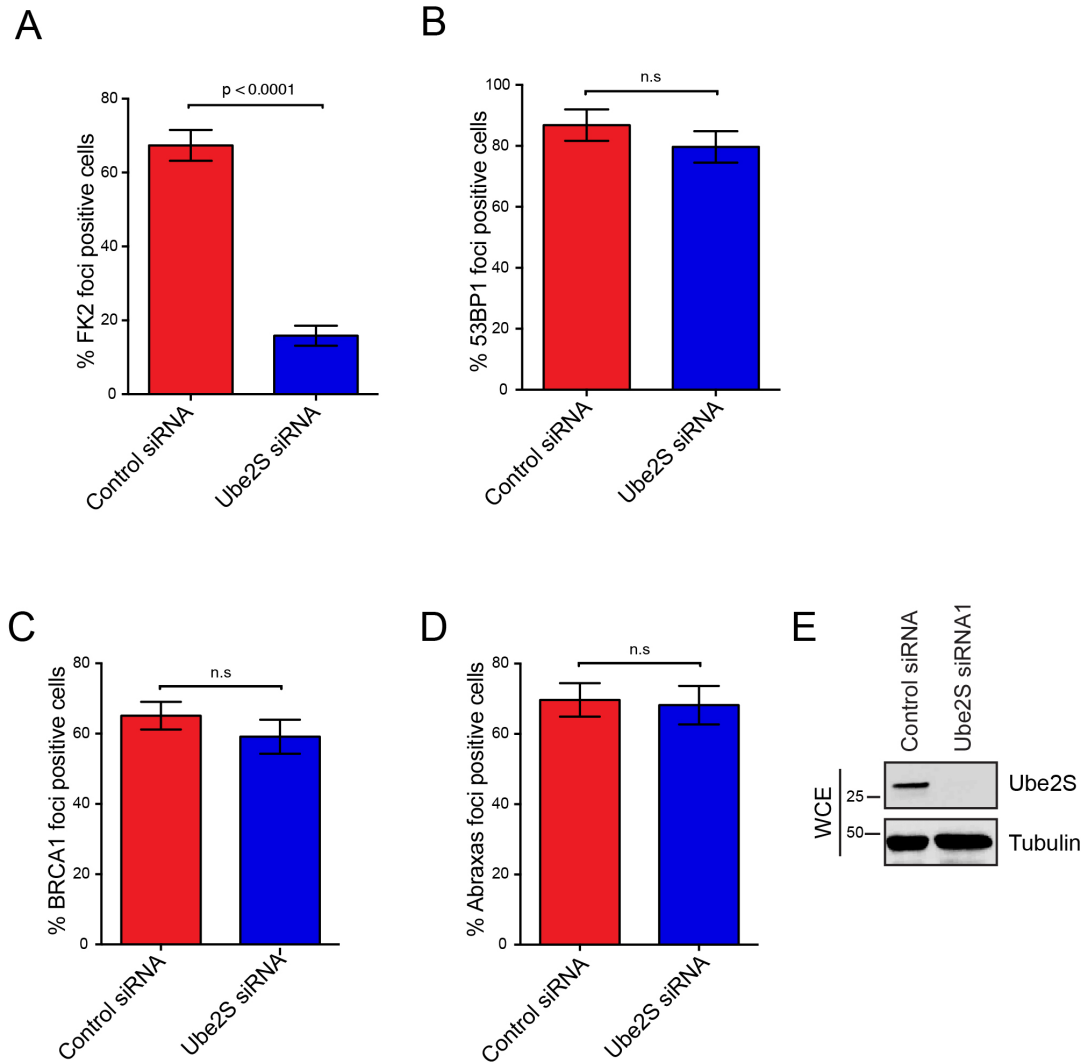
Figure 35: **Lys11-linkage ubiquitination is dispensable for recruitment of DNA damage repair proteins 53BP1 and BRCA1 in Ube2S depleted cells.** U2OS cells were transfected with control or siRNAs targeting Ube2S (siRNA#1). 48 hr post-transfection, cells were irradiated with 10 Gy IR followed by 2 hr incubation at 37°C followed by immunostaining with antibodies to conjugated ubiquitin (FK2 antibody) **(A),** 53BP1 **(B)**, BRCA1 **(C)**, Abraxas **(D)**. Percentage of foci-positive cells (cells containing more than 10 foci) was quantified and indicated as means± SD with p-value indicated. **E**. Whole cell extracts were analyzed for Ube2S knockdown efficiency. Tubulin was used as a control.

ubiquitin conjugation-mediated recruitment of 53BP1 and Abraxas/BRCA1-A complex. Since Ube2C has been shown to catalyze Lys63, Lys48 and Lys11-linked ubiquitination, while Ube2S is Lys11-Ub specific E2 conjugating enzyme, I further confirmed the IRIF of 53BP1 and of BRCA1-A complex components in Ube2S only depleted cells. And as shown in Figure 35, depletion of Ube2S alone appeared to have a similar phenotype as dual depletion of Ube2S and Ube2C. Taken together, these data, suggest that the role of RNF8 in regulating Lys11-linkage modification is independent of its role in catalyzing Lys63-linkage ubiquitin conjugation at DNA damage sites.

3.3.10 Lys11-linked ubiquitination at damaged chromatin is required for regulation of DNA damage-induced transcription silencing

Histone ubiquitination is often associated with transcription regulation (169-172). In addition, a recent study by Greenberg and colleague showed that RNF8 plays an essential role in inducing transcription inhibition at DSBs (67). To find out the functional significance of Ube2S-RNF8-mediated Lys11-linked chromatin ubiquitination, I tested whether Lys11-linkage ubiquitination is involved in regulating transcriptional silencing at the sites of DNA damage. To examine this, I utilized the Click chemistry-based imaging to measure the nascent transcript production at the sites of DNA damage induced by laser micro irradiation as described by *Gong et al*, 2015 and depicted in Figure 36A. In this assay system, I monitored nascent RNA transcript production at laser micro irradiated DNA damage sites using 5-ethynyl uridine (EU), a nucleoside analog of uracil, which is incorporated into nascent RNA during active transcription (173). Using this system I first confirmed whether RNF8
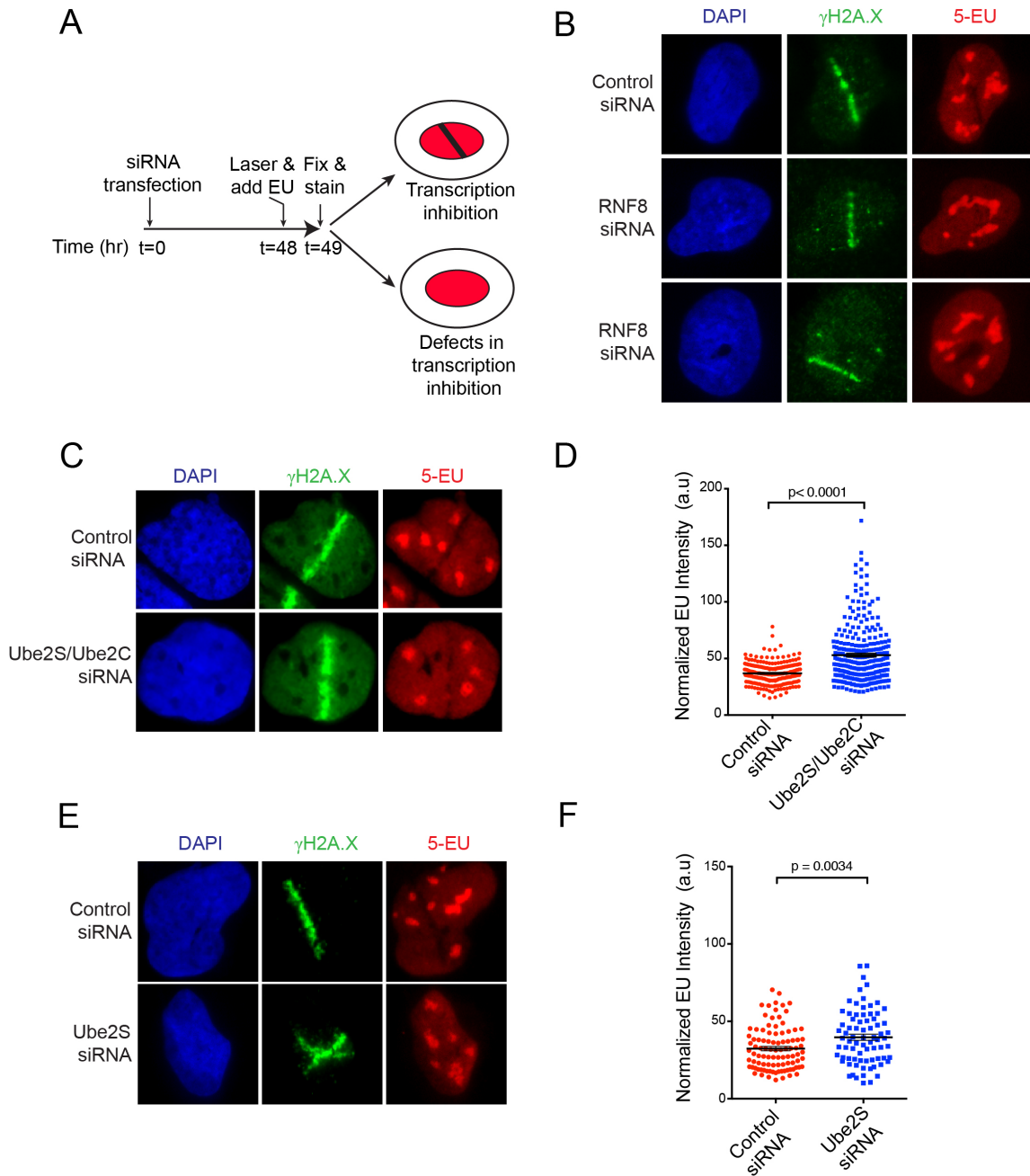
Figure 36: **Lys11-linkage ubiquitination regulates DNA damage-induced transcription silencing. A.** A scheme for examining DNA damage-induced transcription inhibition as described in materials and method section. **B.** Detection of 5-EU labeling and gH2AX staining 1 hr post laser-microirradiation in control and RNF8 siRNA-transfected U2OS cells. **C.** Ube2S/Ube2C-deficient cells are defective

in DNA damage-induced transcription inhibition. **D.** Quantification of 5-EU

intensity normalized by γH2AX intensity in the laser-damaged region. **E.** Ube2S-

deficient cells are defective in DNA damage-induced transcription inhibition. EU

labeling and γH2AX staining was performed similarly as in B and C. **F.**

Quantification of E. 5-EU intensity was measured along the laser tracks and

normalized by γH2AX intensity along the same laser-damaged region.

depletion had any effects in transcription silencing as reported by Shanbhag et al, 2012. Consistent with previous findings, I found compared to control siRNA transfected cells, transcription silencing was significantly impaired in RNF8 depleted cells as indicated by enrichment of EU intensity along the γH2A.X marked damaged region Figure 36B. These findings corroborate previous findings of RNF8's role in transcription silencing at the sites of DNA damage. Interestingly compared to that in control cells in which nascent transcript production was inhibited at laser micro irradiation-induced DNA damage sites, in Ube2S/Ube2C depleted cells, transcriptional silencing after DNA damage is significantly reduced (Figure 36C). Quantification of EU intensity normalized over γH2AX intensity showed significant enrichment of EU labeling along the damage region of the chromatin in Ube2S/Ube2C siRNA transfected cells (Figure 36D). Moreover, to test whether depletion of Ube2S alone can impair transcription silencing at damaged chromatin, I measured nascent transcript production in Ube2S depleted cells. Quantification of EU intensity normalized to γH2AX intensity showed that Ube2S deficiency alone can affect transcription silencing at DNA damage sites (Figure 36E and F).

To further validate these findings, I tested RNAPII phosphorylation status. RNAPII transcribing activity correlates with the phosphorylation status of RNA polymerase II carboxy-terminal domain (CTD) in hepta-repeats YSPTSPS. Active transcription is associated with hyperphosphorylation of the C-terminal domain (CTD) of RNA polymerase II (RNAPII), whereas it remains hypophosphorylated in non-elongating RNAPII complexes (174-177). To test the effect of Ube2S/Ube2C depletion in RNAPII phosphorylation status, I monitored the phosphorylation state of
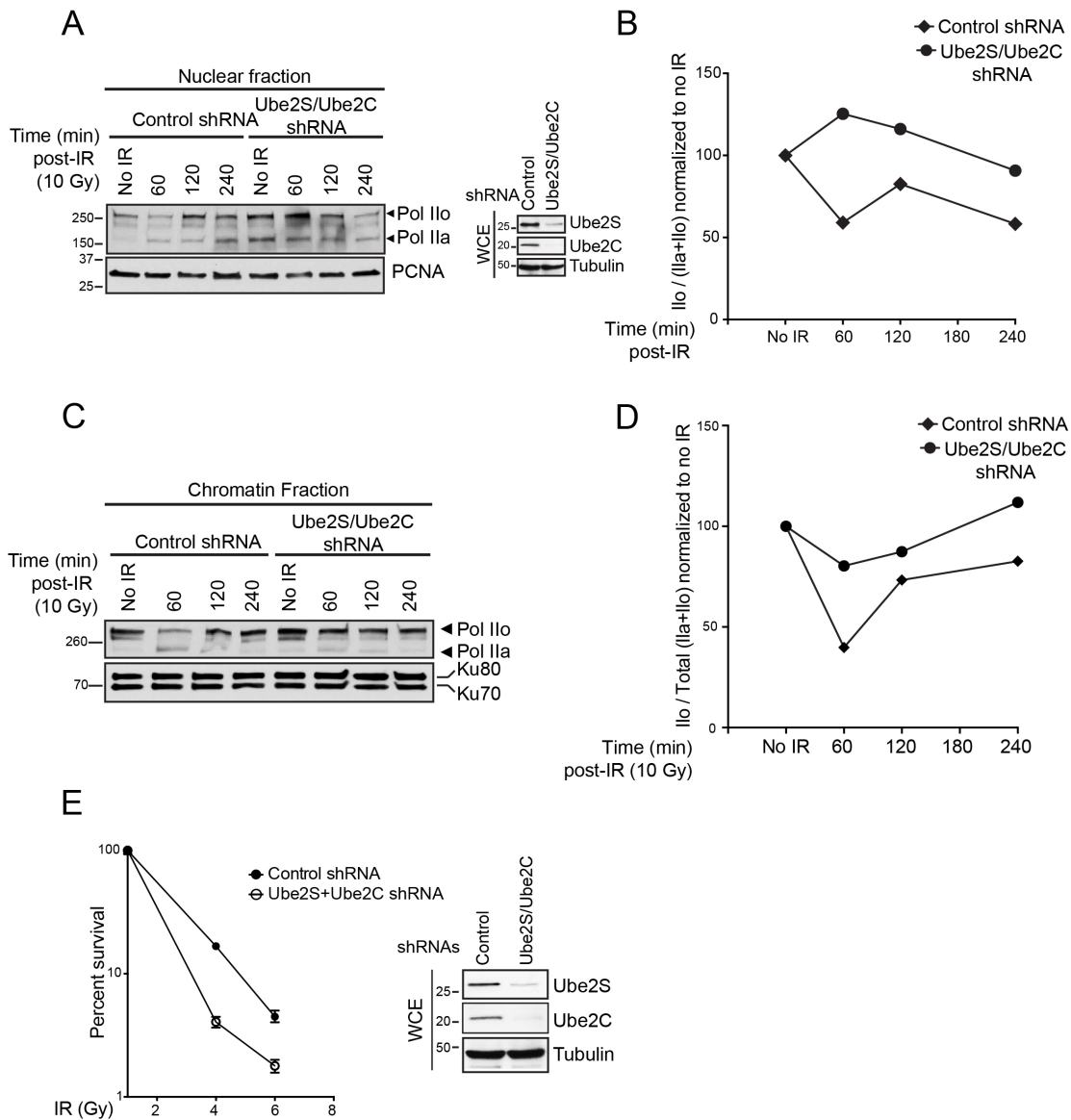
Figure 37: **Increased RNAPII phosphorylation and IR sensitivity in**

Ube2S/Ube2C depleted cells in response to IR. A. Increased RNAPol II

hyperphosphorylation in Ube2S/Ube2C-deficient cells. U2OS cells stably

expressing indicated shRNAs were irradiated with 10 Gy IR, harvested at indicated

time-points and nuclear fractions were isolated for western blot analysis. IIo and IIa

designate hyperphosphorylated and hypophosphorylated forms of the large subunit

Rpb1 of RNA Pol II respectively. **B.** Quantification of Rpb1 hyperphosphorylation

in Ube2S/Ube2C-deficient cells. Hyperphosphorylated Rpb1 and hypophosphorylated Rpb1 (IIa) band intensities were measured by ImageJ and normalized to untreated samples. **C.** Chromatin fraction analysis of increased RNAPII hyperphosphorylation in control and Ube2S/Ube2C deficient cells. **D.** Quantification of C. **E.** Increased cellular sensitivity of Ube2/Ube2C-deficient cells to IR. Percentage of survival in the clonogenic survival assay is quantified and presented as means ± SD.

RNAPII by using an antibody that recognizes both hyperphosphorylated and Hypophosphorylated (IIa) forms of RNAPII. As shown in Figure 37A analysis of nuclear fraction showed that hyperphosphorylation of RNAPII decreased significantly in control cells after 1 hour post-IR-induced DNA damage followed by recovery at later time points, indicating silencing of active transcription at damaged chromatin after DNA damage. Interestingly, compared to control cells, hyperphosphorylation status of RNAPII in Ube2S/Ube2C-deficient cells did not decrease particularly at 1 hour after IR treatment, indicating that active transcription is not efficiently inhibited in Ube2S/Ube2C-deficient cells in response to IR (Figure 37A and B). This was also confirmed when chromatin fraction was analyzed for RNAPII phosphorylation state (Figure 37C and D). Collectively, these data indicate that Ube2S/Ube2C-mediated Lys11-linkage ubiquitination plays a crucial role in promoting transcriptional silencing on the damaged chromatin. In consistent with a role of Lys11-linkage ubiquitination in the DDR, I also found that depletion of Ube2S/Ube2C led to a marked increase in cellular sensitivity to IR (Figure 37E). Thus Lys11-linkage ubiquitination is likely to play a critical role in the cellular response to DNA damage.

Collectively, in this study, we report ubiquitin Lys11-linkage conjugation as a new platform of ubiquitin landscape on damaged chromatin in the cellular response to DNA damage. I show that Lys11-linkage ubiquitination occurs on damaged chromatin and is regulated by ATM-dependent signaling. I identify the corresponding ubiquitin modifying enzymes responsible for the Lys11-linkage ubiquitin events at DNA damage sites including Ube2S/Ube2C E2 conjugating enzymes, RNF8 E3 ligase and Cezanne deubiquitinating enzyme. Moreover, I find that histone

H2A/H2AX is a target of this modification on damaged chromatin. Importantly, I show that Lys11-linkage ubiquitin conjugation plays a critical role in the regulation of DNA damage-induced transcription silencing, distinct from the role of Lys63-linkage ubiquitin in the recruitment of 53BP1 and BRCA1 DNA damage repair proteins.

3.4 Discussion

Chromatin modification at DNA damages sites constitutes an immediate component of the cellular response to DNA damage for signaling and repair. Proteomic analysis of global ubiquitination profiling reveals assembly of all seven lysine residue-linked ubiquitination in a varying degree of abundance in both yeast and mammalian cells (113, 114, 159). However, much is still missing for understanding the role of linkage-specific ubiquitin chains in the regulation of DNA damage response and repair. My findings in this study, for the first time, reveals a connection between Lys11-linkage ubiquitination, one of the most abundant ubiquitin linkages (114), to DNA damage response. It provides evidence that Lys11-linkage ubiquitin chains occur extensively at DNA damage sites in an ATM-dependent manner with kinetics and degree of conjugation similar to that of Lys63- and Lys48-linkages, putting Lys11-linkage ubiquitin modification as a yet another important aspect of the ubiquitin landscape at sites of DNA damage (Figure 38).

In this study, I have identified the ubiquitin enzymatic machinery that assembles and disassembles Lys11-linkage ubiquitin modification at the DNA damage sites. I found that E2 conjugating enzyme Ube2S and E3 ligase RNF8 catalyze Lys11-linked Ub modification at damaged chromatin. Ube2S was identified as a bona fide E2 enzyme that functions in concert with APC/C E3 ligase complex to

elongate the Lys11-linked ubiquitin chain initiated by Ube2C, another cognate E2 conjugating enzyme that can also assemble Lys63 and Lys48-linked ubiquitin chains substrates (129, 151-154, 163, 178). Although APC/C has been extensively shown to partner with Ube2S and Ube2C in catalyzing Lys11-linked ubiquitination during mitosis and G1 phases of the cell cycle, in our analysis I found Ube2S does not partner with APC/C to assemble Lys11-linked polyubiquitin conjugates. While depletion of Ube2S alone abrogates Lys11-linked chromatin ubiquitination, it is largely unaffected by APC/C inactivation. Instead, my findings identify RNF8 as a new partner E3 ligase that works with Ube2S for the DNA damage-induced Lys11-linkage ubiquitin conjugation on chromatin-bound proteins including histone H2A both *in vitro* and *in vivo*. RNF8-deficient cells abolish both Lys11-linked chromatin and histone H2A ubiquitination to the same degree as Ube2S depleted cells indicating that these two enzymes work in concert to catalyze Lys11-linked polyubiquitin conjugates at damaged chromatin. In addition, I found that Ube2S and RNF8 interact with each other and RNF8 is self-ubiquitinated in Ube2S-dependent manner. Since Ube2S has specificity to assemble only Lys11 ubiquitin chain, these findings confirm that RNF8 is autoubiquitinated by Lys11 ubiquitin. Interestingly, it has been shown that RNF8 is capable of interacting with several different E2 conjugating enzymes in response to DNA damage, including Ubc13 for Lys63-linkage (37-39, 41), UbcH5C for Lys6-linkage (140) and UbcH8 for Lys48-linkage (57, 58) ubiquitination. This is consistent with the notion that chain specificity is an intrinsic property of E2 enzymes and E3 ligases interact with different E2s generating linkage-specific ubiquitin chains (106, 118). Therefore, RNF8 appears to

function as a 'master E3 ligase' at the DNA damage sites generating different Lys

residue-linked ubiquitination by interacting with different E2 conjugating enzymes.

One question that arises from these observations is "how these different types of

ubiquitin chains are coordinated at the DNA damage sites?" Although we are still

away from understanding the full spectrum of the complexity of ubiquitin signaling at

the damage sites, it is tempting to speculate that many of the E3 ligases, previously

known to catalyze single type of ubiquitin chain, may interact with other E2 enzymes

at the damage sites to assemble different linkage-specific ubiquitination. Along with

RNF8's role to generate multiple different chain types, as discussed in section 3.1.4,

recent findings from Penengo and colleague showed that RNF168 is also involved in

catalyzing Lys27-linked ubiquitination at DNA damage sites (56). Together, E3 ligase

interaction with the distinct E2 enzyme is likely to be a central mechanism for

coordination of linkage-specific ubiquitination at sites of DNA damage.

Ubiquitin conjugation is a dynamic enzymatic activity that is regulated by the

precise balance between enzymatic activities of the ligase and DUB that cleaves the

polyubiquitin chain and thereby regulates downstream signaling (89). Ubc13-

mediated Lys63-linked polyubiquitin chain at damage sites is disassembled by

BRCC36, a DUB present in the BRCA1-A complex (41, 54, 88, 91). In this study, we

identify that Cezanne, a DUB that has been shown to preferentially deubiquitinate

Lys11-linked ubiquitin chain (157), regulates DNA damage-induced Lys11-linkage

ubiquitination, antagonizing the RNF8- and Ube2S-dependent assembly of Lys11-

linkage chains. Thus, our data illustrates Lys11-linkage modification as an

independent posttranslational modification utilizing distinct E2 conjugating enzyme,

123

E3 ligase and DUB for assembly and disassembly of ubiquitin chains at DNA damage sites.

Chromatin ubiquitination plays a crucial role in the DNA damage response (4, 162). Functional significance of linkage-specific ubiquitination at DSBs has just begun to emerge. The best-illustrated example is Lys63-linkage ubiquitination in response to DNA damage and activation of ATM. The RNF8/RNF168- and Ubc13-catalyzed Lys63-linkage ubiquitin chains assembled on damaged chromatin provide docking sites for the recruitment of 53BP1 and BRCA1-A complex (4, 162). The study done by Penengo group indicates that Lys27-linked ubiquitination of H2A/H2AX generated by RNF168 adds an additional layer of regulation by linkage-specific ubiquitination facilitating the accumulation of 53BP1 and BRCA1 forming IRIF (56). Lys48-linkage formation, on the other hand, modifies Ku80 and regulates its abundance at DNA damage sites for modulation of non-homologous end joining repair (57). Thus, the type of ubiquitin linkage is likely to determine the functional outcome of the modification. In this report, I found that although disruption of Lys11-linkage formation significantly decreased the ubiquitin conjugates detected by the FK2 antibody at DNA damage-induced foci, it has minimal effect on the recruitment of 53BP1 or BRCA1, distinct from the role of Lys63- or Lys27-linkage ubiquitin chains. Rather, Ube2S- and RNF8- mediated Lys11-linkage formation plays an important role in regulating DNA damage- induced transcriptional silencing. Transcription in regions near DNA damage site is temporarily inhibited in an ATM- and DNAPK-dependent manner for proper DNA repair and transcription activities to

maintain genome stability (67, 179). However, how the transcriptional silencing is achieved at DSB sites still remains elusive. Our study uncovers a novel role of Lys11-linked chromatin ubiquitination in promoting transcriptional repression at DSBs. It is possible that Lys11-linked ubiquitin modification of H2A/H2AX directly contributes to the recruitment of transcriptional repressor complexes or adopting a chromatin environment that enhances repression of transcription locally at sites of damage. In fact, histone ubiquitination has been implicated extensively in transcriptional regulation (180). Ubiquitination of histone H2A (uH2A) accumulates at DNA damage sites and is correlated with transcriptional repression (169-172). It is also indicated that ATM- and RNF8-dependent ubiquitination of H2A promotes DNA damage-induced transcription repression (67). Our study expands this knowledge and suggests that RNF8 may regulate the DNA damage-induced transcriptional silencing through catalyzing Lys11-linkage ubiquitin modification of H2A/H2AX. Alternatively, additional substrates of Lys11-linkage modification may be involved in promoting transcriptional silencing through additional mechanisms such as influencing the phosphorylation of RNA polymerase II.

Lys11-linked chain type has been considered as a degradative chain type, along with Lys48-linked ubiquitin polymers, promoting proteasome-dependent degradation of substrates. The Lys11-linkage ubiquitin chain assembly on APC/C substrates Cyclin B1 and Securin during mitosis and G1 phases leads to their degradation and regulating cell cycle progression (151-154). Although the study of
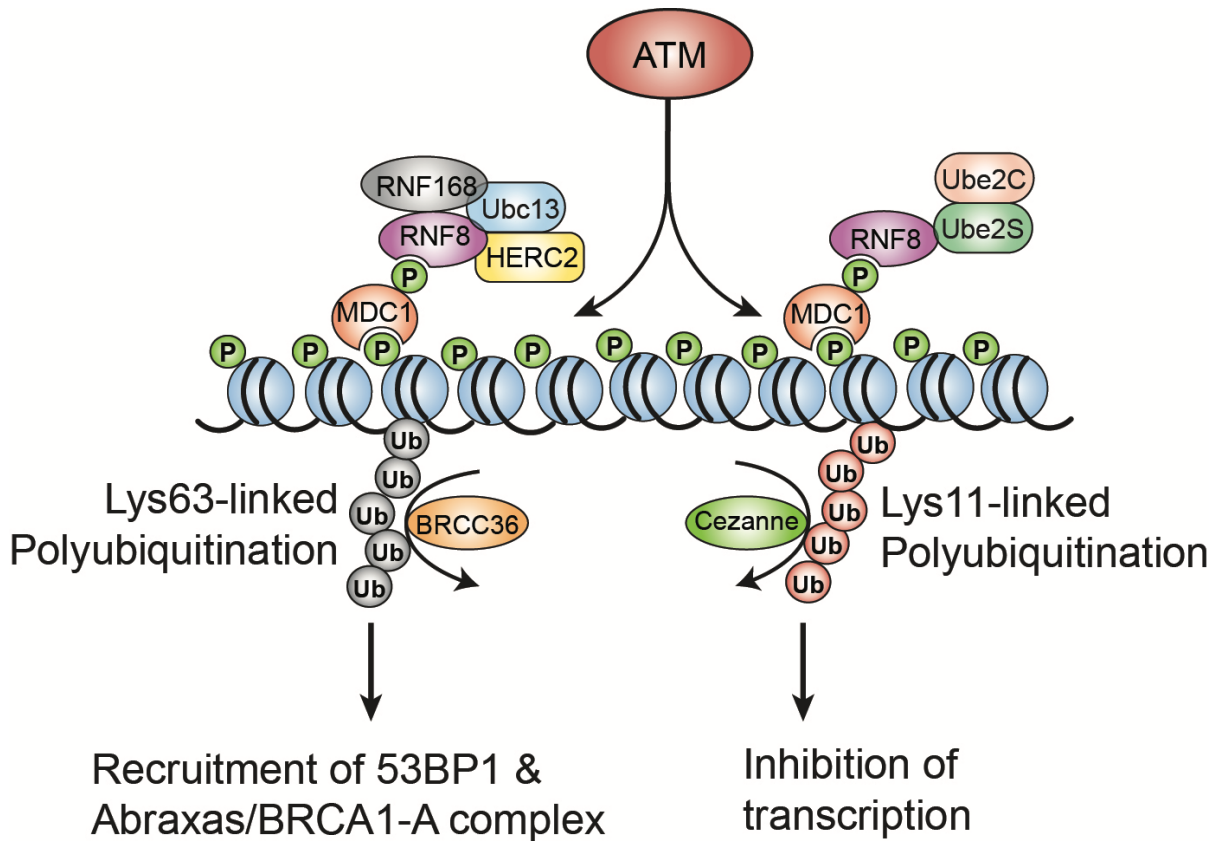
Figure 38: A proposed model for the Lys11-linkage ubiquitination at sites of DNA damage. DNA damage induces an ATM-MDC1-dependent Lys11-linked ubiquitination at damaged chromatin mediated by Ube2S conjugating enzyme and RNF8 ligase and is deubiquitinated by the DUB Cezanne. Lys11-linked chromatin ubiquitination modifies histone H2A and H2A.X at damaged chromatin along with other unidentified chromatin-bound proteins and while Lys11-linked chromatin ubiquitination does not regulate DDR factor recruitment to DSB sites, it plays an essential role in regulating transcription silencing.

aiming to examine the role of Lys11-linkage ubiquitin modification in various cellular processes is still limited, Lys11-linked ubiquitin chain conjugation also has been implicated in non-proteolytic pathways such as NF-κB activation (181-183). In our study, we didn't observe any changes in the steady-state level of chromatin-bound H2A/H2AX in cells depleted with Ube2S in presence or absence of DNA damage, indicating that Lys11-linked ubiquitination of histone H2A/H2AX is less likely to represent a proteolytic signal for protein degradation. However, we could not exclude the possibility that other yet unknown substrates of Lys11-linkage modification on damaged chromatin undergo proteasome-dependent degradation due to this modification. Recent crystallographic and NMR analysis showed that Lys11-linked di-ubiquitin adopts a compact structure distinct from the Lys48- and Lys63-linked ubiquitin chains (157, 184, 185), suggesting that Lys11-linked chains are capable of representing an independent signaling entity within cells.

In summary, this study demonstrates that Lys11-linkage ubiquitin modification is an important aspect of the complex ubiquitin landscape that exists in the vicinity of DNA damage regulating DNA damage-induced transcriptional silencing. My findings emphasize the complexity of ubiquitin signaling at the sites of damage involving different E2-E3 pair to assemble different ubiquitin linkages. It highlights the importance of linkage-specific ubiquitination in the DDR and supports the notion that polyubiquitin chains with different linkages should be regarded as independent posttranslational modification.

3.5 Future directions:

This study provides evidence for the first time that damaged chromatin is modified with Lys11-linked ubiquitin chain in an ATM-dependent manner by Ube2S and RNF8 enzymes and Lys11-linked chromatin ubiquitination is essential for inducing transcriptional silencing in the vicinity of the DNA damage. Although these findings expand our understanding of the linkage-specific ubiquitination at the DNA damage sites, this study also raises several important questions that require further investigation. First, I found that Ube2S/Ube2C depleted cells become sensitive to IR-induced DNA damage indicating these enzymes may involve in cellular resistance to IR and likely to play a role in DNA repair. However, the exact role of this enzymes and Lys11-linked ubiquitination in DNA repair still remains to be determined. Transcriptionally active regions have been shown to favor HR repair (186). Given I found that active transcription is not efficiently inhibited at the damage sites in Ube2S/Ube2C depleted cells, it will be interesting to examine whether depletion of Ube2S/Ube2C have any effects on HR repair. Second, my findings indicate that histone H2A/H2A.X are modified with Lys11-linked ubiquitin chain in DNA damage-dependent manner. However, the identity of the lysine residue(s) on histone H2A that is modified with Lys11 ubiquitin chain still requires further examination. H2A is known to be modified with Lys63-linked ubiquitin chain at Lys13 and Lys15 residue on H2A (143). A proteomic analysis of *in vivo* ubiquitination sites identified novel sites for ubiquitination on different histone proteins (142). Therefore, site-directed mutagenesis analysis should be performed to identify and characterize the H2A lysine residue(s) that is modified with Lys11 ubiquitin chain. Third, it is possible that

other non-histone proteins are also modified with Lys11-linked ubiquitin chain at the damage sites. Identification and characterization of these substrates will further our understanding of the role of Lys11-linked chromatin ubiquitination at the DNA damage sites. Fourth, does Lys11-linked ubiquitin chain trigger proteolytic signal at the damage sites? The chromatin fraction analysis showed that chromatin-bound protein modification with Lys11 ubiquitin chain is enhanced dramatically upon treating the cells with MG132. This raises the possibility that a fraction of the Lys11 ubiquitin-modified proteins is likely to be targeted by the proteasome. Although I could not detect any alteration in histone protein levels, it is possible that other non-histone proteins may undergo proteasomal degradation by Lys11-linked ubiquitination in DNA damage-dependent manner. Fifth, although my study uncovers a novel role of Lys11-linked chromatin ubiquitination in inducing transcriptional silencing at the DNA damage sites, the mechanism of this silencing event requires further investigation. There are several possibilities that can be tested to figure out the mechanism of transcription silencing at damaged chromatin. It is possible that histone H2A ubiquitination in the Lys11-linked manner directly recruits transcriptional repressor complex. Another possibility is, components of the RNAPII holoenzyme may be modified and degraded by Lys11 ubiquitin chain and thereby inducing transcription stalling until the damage is repaired. These possibilities should be tested in future studies. And lastly, given recognition of different ubiquitin chain by specific ubiquitin binding domain (UBD) containing proteins contributes to a diverse set of functional outcome, it will be interesting to examine specific UBDs that can bind to Lys11 ubiquitin chain. Identification of UBDs that recognize Lys11 ubiquitin

chain will, therefore, likely to reveal novel function this modification at the DNA

damage sites as well as other signaling events in the cell.

CHAPTER 4

DISCUSSION AND FINAL WORDS

4.1 Discussion

Since the discovery of DNA structure, a remarkable amount of effort has been dedicated to understanding how cells preserve its genetic material to maintain genetic integrity. It is the largest molecule that is subject for numerous lesions. It is estimated that cells experience around 10^4 to 10^6 DNA lesions per cell per day. Nevertheless, the cells must keep the DNA intact by deploying a repertoire of repair mechanisms in proliferating cells as well as in germ cells to ensure faithful transmission across generations (3, 4). Given injury to DNA interferes with DNA replication and transcription, resulting in genome instability, the DNA damage response signaling has evolved as the "sentinel of the genome" to repair DNA injury in a timely manner. Of note, DNA is wrapped in around histones forming the nucleosome, the fundamental unit of chromatin (187, 188). The nucleosome is further compacted into higher order chromatin structure with linker histone protein as well as non-histone proteins (189, 190). Although this higher order chromatin structure appears to be functioning as a barrier to DNA-associated processes such as replication, transcription as well as DNA repair; the highly dynamic chromatin structure is modulated by various ways such as DNA methylation (191), post-translational modifications of histones and non-histone proteins (10, 192), nucleosome/chromatin remodeling complexes (193). Among these different factors, post-translational modification of chromatin that can be dynamically added or removed by enzymatic reactions has emerged as a key regulatory player in modulating nucleosome in response to DNA damage. While phosphorylation, ubiquitination, acetylation, methylation, ubiquitination, SUMOylation and ADP-

ribosylation are among the best-studied modifications, recent studies indicate the existence of additional PTMS such as crotonylation, succinylation, and malonylation of histone and non-histone proteins (194). In addition to altering nucleosome dynamics, these above-mentioned PTMs recruit reader proteins that further modulate chromatin remodeling during events such as DNA repair and transcription. Although each of this modification entails a distinct set of enzymes that catalyze and disassemble chromatin PTMs, recent studies from different groups indicate that potential cross talks exist among different post-translational modifications that function in a coordinated fashion at the damaged chromatin to execute efficient DDR signaling. One classic example of this potential cross talk is γH2A.X and MDC1 phosphorylation-dependent H2A/H2A.X ubiquitination by the RNF8/RNF168-Ubc13 enzymatic machinery at the DNA double-strand break sites that function synergistically to activate the DDR signal and facilitates downstream DDR factors recruitment such as 53BP1 and components of the BRCA1-A complex (37-39, 41, 43-45). While this represents only a small fraction of crosstalk at the damaged chromatin, emerging evidence support a more complex picture of the crosstalk among different PTMs to induce efficient DSB response. This potential crosstalk not only transduce the damage signal, but also regulates recruitment of effector proteins at damage sites, transcriptional silencing as well as coordination with DNA replication (16, 195, 196), emphasizing the functional significance of different post-translational modifications at damaged chromatin.

In this study, I investigated the role of phosphorylation and ubiquitination, two of the most well studied post-translational modifications at damaged chromatin. The

novel findings obtained from this study highlight the significance of cross talk among phosphorylation and ubiquitination at DSB sites. In addition to γH2A.X and MDC1 phosphorylation and Lys63-linked ubiquitination-dependent BRCA1 localization at DBSs, I showed that DNA damage-induced Abraxas phosphorylation at the S404 site is crucial for efficient BRCA1 dimerization and efficient accumulation to damage sites to initiate DNA repair (87). Also, I showed that along with Lys63-linked ubiquitination, damage chromatin is modified with Lys11-linked ubiquitination in phosphorylation-dependent manner to induce transcriptional silencing at the vicinity of the DSB sites. These findings not only deepen our understanding of spatiotemporal regulation of DDR factors at the damage sites but also provide mechanistic insights into how damaged chromatin is orchestrated in response to DNA damage to inhibit transcription. While these studies reveal a regulatory role of post-translational modifications at the damage sites, they also open up new areas of research to understand the role PTMs in regulating the DDR pathway. Future studies aiming to understand PTMs in the DDR will likely identify novel molecules in the DNA damage response pathway and will provide potential therapeutic opportunities to diseases associated with defective DDR signaling.

4.2 Final words

The DNA damage response is absolutely essential for maintaining the genomic stability and defective DDR signaling has been characterized as one of the hallmarks of cancer (7) and has been attributed to many different types of cancer (197). While defects in the DDR signaling has been the major factor in tumorigenesis as well as other diseases, this provides a unique opportunity to exploit the DDR

system as a potential therapy of cancer with radiotherapy and chemotherapy regimens. This is best exemplified by the synthetic lethality approach with the PARP1 inhibitor to induce cell death in tumor cells defective in *BRCA1* or *BRCA2* genes. Olaparib, the PARP1 inhibitor, has recently been approved by the FDA for treatment of women with ovarian cancer. Recent analysis indicate that there are at least 450 genes integral to the DDR and choice of drug target depends on the type of DNA damage repair to be inhibited given multiple repair mechanisms exist in cells to repair damaged DNA. While many of the compounds for DDR targets are already approved or under clinical trials, a large number are still in the discovery phase, potentially representing next generation DDR targets (198). Interestingly, among different PTMs involved in the DDR pathway, phosphorylation and ubiquitin-modified proteome and corresponding enzymatic machinery have emerged as a highly druggable class of proteins that include protein kinases such as ATM, ATR, DNA-PK, Chk1, as well as many of the E3 ubiquitin ligases (24 total) involved in various DDR pathways (198). The promising results from these studies emphasize how post-translational modifications such as phosphorylation and ubiquitination and crosstalk among these PTMs in the DDR signaling can potentially be harnessed as a viable therapeutic approach in cancer cells. Therefore, detail understanding of PTMs in the DDR pathway will likely to identify new molecules in the near future that can be targeted for cancer therapy. In this light, my study provides crucial mechanistic insights into the DDR pathway. Although there remain questions that require further investigation, findings from this study will broaden our understanding of the

complexity of the DDR signaling as well as expand the list of DDR factors in DSB repair pathway.

Bibliography:

1. Blanpain, C., M. Mohrin, P. A. Sotiropoulou, and E. Passegue. 2011. DNA-damage response in tissue-specific and cancer stem cells. *Cell Stem Cell* 8: 16-29.

2. Lindahl, T., and D. E. Barnes. 2000. Repair of endogenous DNA damage. *Cold Spring Harbor symposia on quantitative biology* 65: 127-133.

3. Hoeijmakers, J. H. 2009. DNA damage, aging, and cancer. *The New England journal of medicine* 361: 1475-1485.

4. Ciccia, A., and S. J. Elledge. 2010. The DNA damage response: making it safe to play with knives. *Mol Cell* 40: 179-204.

5. Jackson, S. P., and J. Bartek. 2009. The DNA-damage response in human biology and disease. *Nature* 461: 1071-1078.

6. Bartek, J., J. Bartkova, and J. Lukas. 2007. DNA damage signalling guards against activated oncogenes and tumour progression. *Oncogene* 26: 7773-7779.

7. Hanahan, D., and R. A. Weinberg. 2011. Hallmarks of cancer: the next generation. *Cell* 144: 646-674.

8. Hoeijmakers, J. H. 2001. Genome maintenance mechanisms for preventing cancer. *Nature* 411: 366-374.

9. Harper, J. W., and S. J. Elledge. 2007. The DNA damage response: ten years after. *Mol Cell* 28: 739-745.

10. Polo, S. E., and S. P. Jackson. 2011. Dynamics of DNA damage response proteins at DNA breaks: a focus on protein modifications. *Genes Dev* 25: 409-433.

11. Huen, M. S., and J. Chen. 2008. The DNA damage response pathways: at the crossroad of protein modifications. *Cell Res* 18: 8-16.

12.   Dantuma, N. P., and H. van Attikum. 2016. Spatiotemporal regulation of posttranslational modifications in the DNA damage response. *EMBO J* 35: 6-23.

13.   Lukas, J., C. Lukas, and J. Bartek. 2011. More than just a focus: The chromatin response to DNA damage and its role in genome integrity maintenance. *Nat Cell Biol* 13: 1161-1169.

14.   Sancar, A., L. A. Lindsey-Boltz, K. Unsal-Kacmaz, and S. Linn. 2004. Molecular mechanisms of mammalian DNA repair and the DNA damage checkpoints. *Annual review of biochemistry* 73: 39-85.

15.   Kim, J. S., T. B. Krasieva, H. Kurumizaka, D. J. Chen, A. M. Taylor, and K. Yokomori. 2005. Independent and sequential recruitment of NHEJ and HR factors to DNA damage sites in mammalian cells. *J Cell Biol* 170: 341-347.

16.   Kuo, C. Y., C. Shieh, F. Cai, and D. K. Ann. 2011. Coordinate to guard: crosstalk of phosphorylation, sumoylation, and ubiquitylation in DNA damage response. *Front Oncol* 1: 61.

17.   Pellegrino, S., and M. Altmeyer. 2016. Interplay between Ubiquitin, SUMO, and Poly(ADP-Ribose) in the Cellular Response to Genotoxic Stress. *Front Genet* 7: 63.

18.   Matsuoka, S., B. A. Ballif, A. Smogorzewska, E. R. McDonald, 3rd, K. E. Hurov, J. Luo, C. E. Bakalarski, Z. Zhao, N. Solimini, Y. Lerenthal, Y. Shiloh, S. P. Gygi, and S. J. Elledge. 2007. ATM and ATR substrate analysis reveals extensive protein networks responsive to DNA damage. *Science* 316: 1160-1166.

19.   Cimprich, K. A., and D. Cortez. 2008. ATR: an essential regulator of genome integrity. *Nat Rev Mol Cell Biol* 9: 616-627.

20. Bakkenist, C. J., and M. B. Kastan. 2004. Initiating cellular stress responses. *Cell* 118: 9-17.

21. Lee, J. H., and T. T. Paull. 2004. Direct activation of the ATM protein kinase by the Mre11/Rad50/Nbs1 complex. *Science* 304: 93-96.

22. Lee, J. H., and T. T. Paull. 2005. ATM activation by DNA double-strand breaks through the Mre11-Rad50-Nbs1 complex. *Science* 308: 551-554.

23. Shiloh, Y., and Y. Ziv. 2013. The ATM protein kinase: regulating the cellular response to genotoxic stress, and more. *Nat Rev Mol Cell Biol* 14: 197-210.

24. Falck, J., J. Coates, and S. P. Jackson. 2005. Conserved modes of recruitment of ATM, ATR and DNA-PKcs to sites of DNA damage. *Nature* 434: 605-611.

25. Stracker, T. H., M. Morales, S. S. Couto, H. Hussein, and J. H. Petrini. 2007. The carboxy terminus of NBS1 is required for induction of apoptosis by the MRE11 complex. *Nature* 447: 218-221.

26. Paull, T. T. 2015. Mechanisms of ATM Activation. *Annual review of biochemistry* 84: 711-738.

27. Uziel, T., Y. Lerenthal, L. Moyal, Y. Andegeko, L. Mittelman, and Y. Shiloh. 2003. Requirement of the MRN complex for ATM activation by DNA damage. *EMBO J* 22: 5612-5621.

28. Bensimon, A., A. Schmidt, Y. Ziv, R. Elkon, S. Y. Wang, D. J. Chen, R. Aebersold, and Y. Shiloh. 2010. ATM-dependent and -independent dynamics of the nuclear phosphoproteome after DNA damage. *Sci Signal* 3: rs3.

29. Meier, A., H. Fiegler, P. Munoz, P. Ellis, D. Rigler, C. Langford, M. A. Blasco, N. Carter, and S. P. Jackson. 2007. Spreading of mammalian DNA-damage response factors studied by ChIP-chip at damaged telomeres. *EMBO J* 26: 2707-2718.

30. Savic, V., B. Yin, N. L. Maas, A. L. Bredemeyer, A. C. Carpenter, B. A. Helmink, K. S. Yang-Iott, B. P. Sleckman, and C. H. Bassing. 2009. Formation of dynamic gamma-H2AX domains along broken DNA strands is distinctly regulated by ATM and MDC1 and dependent upon H2AX densities in chromatin. *Mol Cell* 34: 298-310.

31. Fernandez-Capetillo, O., A. Lee, M. Nussenzweig, and A. Nussenzweig. 2004. H2AX: the histone guardian of the genome. *DNA Repair (Amst)* 3: 959-967.

32. Lee, M. S., R. A. Edwards, G. L. Thede, and J. N. Glover. 2005. Structure of the BRCT repeat domain of MDC1 and its specificity for the free COOH-terminal end of the gamma-H2AX histone tail. *J Biol Chem* 280: 32053-32056.

33. Stucki, M., J. A. Clapperton, D. Mohammad, M. B. Yaffe, S. J. Smerdon, and S. P. Jackson. 2005. MDC1 directly binds phosphorylated histone H2AX to regulate cellular responses to DNA double-strand breaks. *Cell* 123: 1213-1226.

34. Stucki, M., and S. P. Jackson. 2006. gammaH2AX and MDC1: anchoring the DNA-damage-response machinery to broken chromosomes. *DNA Repair (Amst)* 5: 534-543.

35. Lou, Z., K. Minter-Dykhouse, S. Franco, M. Gostissa, M. A. Rivera, A. Celeste, J. P. Manis, J. van Deursen, A. Nussenzweig, T. T. Paull, F. W. Alt, and J. Chen. 2006. MDC1 maintains genomic stability by participating in the amplification of ATM-dependent DNA damage signals. *Mol Cell* 21: 187-200.

36. Stewart, G. S., B. Wang, C. R. Bignell, A. M. Taylor, and S. J. Elledge. 2003. MDC1 is a mediator of the mammalian DNA damage checkpoint. *Nature* 421: 961-966.

37. Huen, M. S., R. Grant, I. Manke, K. Minn, X. Yu, M. B. Yaffe, and J. Chen. 2007. RNF8 transduces the DNA-damage signal via histone ubiquitylation and checkpoint protein assembly. *Cell* 131: 901-914.

38. Kolas, N. K., J. R. Chapman, S. Nakada, J. Ylanko, R. Chahwan, F. D. Sweeney, S. Panier, M. Mendez, J. Wildenhain, T. M. Thomson, L. Pelletier, S. P. Jackson, and D. Durocher. 2007. Orchestration of the DNA-damage response by the RNF8 ubiquitin ligase. *Science* 318: 1637-1640.

39. Mailand, N., S. Bekker-Jensen, H. Faustrup, F. Melander, J. Bartek, C. Lukas, and J. Lukas. 2007. RNF8 ubiquitylates histones at DNA double-strand breaks and promotes assembly of repair proteins. *Cell* 131: 887-900.

40. Bekker-Jensen, S., J. Rendtlew Danielsen, K. Fugger, I. Gromova, A. Nerstedt, C. Lukas, J. Bartek, J. Lukas, and N. Mailand. 2010. HERC2 coordinates ubiquitin-dependent assembly of DNA repair factors on damaged chromosomes. *Nat Cell Biol* 12: 80-86; sup pp 81-12.

41. Wang, B., and S. J. Elledge. 2007. Ubc13/Rnf8 ubiquitin ligases control foci formation of the Rap80/Abraxas/Brca1/Brcc36 complex in response to DNA damage. *Proc Natl Acad Sci U S A* 104: 20759-20763.

42. Christensen, D. E., P. S. Brzovic, and R. E. Klevit. 2007. E2-BRCA1 RING interactions dictate synthesis of mono- or specific polyubiquitin chain linkages. *Nat Struct Mol Biol* 14: 941-948.

43. Doil, C., N. Mailand, S. Bekker-Jensen, P. Menard, D. H. Larsen, R. Pepperkok, J. Ellenberg, S. Panier, D. Durocher, J. Bartek, J. Lukas, and C. Lukas. 2009. RNF168 binds and amplifies ubiquitin conjugates on damaged chromosomes to allow accumulation of repair proteins. *Cell* 136: 435-446.

44. Pinato, S., C. Scandiuzzi, N. Arnaudo, E. Citterio, G. Gaudino, and L. Penengo. 2009. RNF168, a new RING finger, MIU-containing protein that modifies chromatin by ubiquitination of histones H2A and H2AX. *BMC Mol Biol* 10: 55.

45. Stewart, G. S., S. Panier, K. Townsend, A. K. Al-Hakim, N. K. Kolas, E. S. Miller, S. Nakada, J. Ylanko, S. Olivarius, M. Mendez, C. Oldreive, J. Wildenhain, A. Tagliaferro, L. Pelletier, N. Taubenheim, A. Durandy, P. J. Byrd, T. Stankovic, A. M. Taylor, and D. Durocher. 2009. The RIDDLE syndrome protein mediates a ubiquitin-dependent signaling cascade at sites of DNA damage. *Cell* 136: 420-434.

46. Thorslund, T., A. Ripplinger, S. Hoffmann, T. Wild, M. Uckelmann, B. Villumsen, T. Narita, T. K. Sixma, C. Choudhary, S. Bekker-Jensen, and N. Mailand. 2015. Histone H1 couples initiation and amplification of ubiquitin signalling after DNA damage. *Nature* 527: 389-393.

47. Wang, B., S. Matsuoka, B. A. Ballif, D. Zhang, A. Smogorzewska, S. P. Gygi, and S. J. Elledge. 2007. Abraxas and RAP80 form a BRCA1 protein complex required for the DNA damage response. *Science* 316: 1194-1198.

48. Kim, H., J. Chen, and X. Yu. 2007. Ubiquitin-binding protein RAP80 mediates BRCA1-dependent DNA damage response. *Science* 316: 1202-1205.

49. Kim, H., J. Huang, and J. Chen. 2007. CCDC98 is a BRCA1-BRCT domain-binding protein involved in the DNA damage response. *Nat Struct Mol Biol* 14: 710-715.

50. Liu, Z., J. Wu, and X. Yu. 2007. CCDC98 targets BRCA1 to DNA damage sites. *Nat Struct Mol Biol* 14: 716-720.

51. Sobhian, B., G. Shao, D. R. Lilli, A. C. Culhane, L. A. Moreau, B. Xia, D. M. Livingston, and R. A. Greenberg. 2007. RAP80 targets BRCA1 to specific ubiquitin structures at DNA damage sites. *Science* 316: 1198-1202.

52. Feng, L., J. Huang, and J. Chen. 2009. MERIT40 facilitates BRCA1 localization and DNA damage repair. *Genes Dev* 23: 719-728.

53. Wang, B., K. Hurov, K. Hofmann, and S. J. Elledge. 2009. NBA1, a new player in the Brca1 A complex, is required for DNA damage resistance and checkpoint control. *Genes Dev* 23: 729-739.

54. Patterson-Fortin, J., G. Shao, H. Bretscher, T. E. Messick, and R. A. Greenberg. 2010. Differential regulation of JAMM domain deubiquitinating enzyme activity within the RAP80 complex. *J Biol Chem* 285: 30971-30981.

55. llo, A., A. Paul, B. Sun, T. H. Huang, Y. Wang, S. A. Yazinski, J. Tyler, L. Li, M. J. You, L. Zou, J. Yao, and B. Wang. 2014. The BRCA1-interacting protein Abraxas is required for genomic stability and tumor suppression. *Cell reports* 8: 807-817.

56. Gatti, M., S. Pinato, A. Maiolica, F. Rocchio, M. G. Prato, R. Aebersold, and L. Penengo. 2015. RNF168 promotes noncanonical K27 ubiquitination to signal DNA damage. *Cell reports* 10: 226-238.

57. Feng, L., and J. Chen. 2012. The E3 ligase RNF8 regulates KU80 removal and NHEJ repair. *Nat Struct Mol Biol* 19: 201-206.

58.   Lok, G. T., S. M. Sy, S. S. Dong, Y. P. Ching, S. W. Tsao, T. M. Thomson, and M. S. Huen. 2012. Differential regulation of RNF8-mediated Lys48- and Lys63-based poly-ubiquitylation. *Nucleic acids research* 40: 196-205.

59.   Adam, S., and S. E. Polo. 2014. Blurring the line between the DNA damage response and transcription: the importance of chromatin dynamics. *Exp Cell Res* 329: 148-153.

60.   Mayne, L. V., and A. R. Lehmann. 1982. Failure of RNA synthesis to recover after UV irradiation: an early defect in cells from individuals with Cockayne's syndrome and xeroderma pigmentosum. *Cancer research* 42: 1473-1478.

61.   Mone, M. J., M. Volker, O. Nikaido, L. H. Mullenders, A. A. van Zeeland, P. J. Verschure, E. M. Manders, and R. van Driel. 2001. Local UV-induced DNA damage in cell nuclei results in local transcription inhibition. *EMBO Rep* 2: 1013-1017.

62.   Solovjeva, L. V., M. P. Svetlova, V. O. Chagin, and N. V. Tomilin. 2007. Inhibition of transcription at radiation-induced nuclear foci of phosphorylated histone H2AX in mammalian cells. *Chromosome Res* 15: 787-797.

63.   Seiler, D. M., J. Rouquette, V. J. Schmid, H. Strickfaden, C. Ottmann, G. A. Drexler, B. Mazurek, C. Greubel, V. Hable, G. Dollinger, T. Cremer, and A. A. Friedl. 2011. Double-strand break-induced transcriptional silencing is associated with loss of tri-methylation at H3K4. *Chromosome Res* 19: 883-899.

64.   Vissers, J. H., M. van Lohuizen, and E. Citterio. 2012. The emerging role of Polycomb repressors in the response to DNA damage. *J Cell Sci* 125: 3939-3948.

65.   Ayrapetov, M. K., O. Gursoy-Yuzugullu, C. Xu, Y. Xu, and B. D. Price. 2014. DNA double-strand breaks promote methylation of histone H3 on lysine 9 and

transient formation of repressive chromatin. *Proc Natl Acad Sci U S A* 111: 9169-9174.

66. Chou, D. M., B. Adamson, N. E. Dephoure, X. Tan, A. C. Nottke, K. E. Hurov, S. P. Gygi, M. P. Colaiacovo, and S. J. Elledge. 2010. A chromatin localization screen reveals poly (ADP ribose)-regulated recruitment of the repressive polycomb and NuRD complexes to sites of DNA damage. *Proc Natl Acad Sci U S A* 107: 18475-18480.

67. Shanbhag, N. M., I. U. Rafalska-Metcalf, C. Balane-Bolivar, S. M. Janicki, and R. A. Greenberg. 2010. ATM-dependent chromatin changes silence transcription in cis to DNA double-strand breaks. *Cell* 141: 970-981.

68. Wang, B. 2012. BRCA1 tumor suppressor network: focusing on its tail. *Cell Biosci* 2: 6.

69. Huen, M. S., S. M. Sy, and J. Chen. 2010. BRCA1 and its toolbox for the maintenance of genome integrity. *Nat Rev Mol Cell Biol* 11: 138-148.

70. Venkitaraman, A. R. 2002. Cancer susceptibility and the functions of BRCA1 and BRCA2. *Cell* 108: 171-182.

71. Kobayashi, H., S. Ohno, Y. Sasaki, and M. Matsuura. 2013. Hereditary breast and ovarian cancer susceptibility genes (review). *Oncology reports* 30: 1019-1029.

72. Savage, K. I., and D. P. Harkin. 2015. BRCA1, a 'complex' protein involved in the maintenance of genomic stability. *FEBS J* 282: 630-646.

73. Futreal, P. A., Q. Liu, D. Shattuck-Eidens, C. Cochran, K. Harshman, S. Tavtigian, L. M. Bennett, A. Haugen-Strano, J. Swensen, Y. Miki, and et al. 1994. BRCA1 mutations in primary breast and ovarian carcinomas. *Science* 266: 120-122.

74. Miki, Y., J. Swensen, D. Shattuck-Eidens, P. A. Futreal, K. Harshman, S. Tavtigian, Q. Liu, C. Cochran, L. M. Bennett, W. Ding, and et al. 1994. A strong candidate for the breast and ovarian cancer susceptibility gene BRCA1. *Science* 266: 66-71.

75. Jiang, Q., and R. A. Greenberg. 2015. Deciphering the BRCA1 Tumor Suppressor Network. *J Biol Chem* 290: 17724-17732.

76. Huen, M. S. Y., S. M. H. Sy, and J. Chen. 2009. BRCA1 and its toolbox for the maintenance of genome integrity. *Nature Reviews Molecular Cell Biology* 11: 138-148.

77. Deng, C. X. 2006. BRCA1: cell cycle checkpoint, genetic instability, DNA damage response and cancer evolution. *Nucleic acids research* 34: 1416-1426.

78. Tirkkonen, M., O. Johannsson, B. A. Agnarsson, H. Olsson, S. Ingvarsson, R. Karhu, M. Tanner, J. Isola, R. B. Barkardottir, A. Borg, and O. P. Kallioniemi. 1997. Distinct somatic genetic changes associated with tumor progression in carriers of BRCA1 and BRCA2 germ-line mutations. *Cancer research* 57: 1222-1227.

79. Weaver, Z., C. Montagna, X. Xu, T. Howard, M. Gadina, S. G. Brodie, C. X. Deng, and T. Ried. 2002. Mammary tumors in mice conditionally mutant for Brca1 exhibit gross genomic instability and centrosome amplification yet display a recurring distribution of genomic imbalances that is similar to human breast cancer. *Oncogene* 21: 5097-5107.

80. Meza, J. E., P. S. Brzovic, M. C. King, and R. E. Klevit. 1999. Mapping the functional domains of BRCA1. Interaction of the ring finger domains of BRCA1 and BARD1. *J Biol Chem* 274: 5659-5665.

81. Mallery, D. L., C. J. Vandenberg, and K. Hiom. 2002. Activation of the E3 ligase function of the BRCA1/BARD1 complex by polyubiquitin chains. *EMBO J* 21: 6755-6762.

82. Wu-Baer, F., K. Lagrazon, W. Yuan, and R. Baer. 2003. The BRCA1/BARD1 heterodimer assembles polyubiquitin chains through an unconventional linkage involving lysine residue K6 of ubiquitin. *J Biol Chem* 278: 34743-34746.

83. Morris, J. R., and E. Solomon. 2004. BRCA1 : BARD1 induces the formation of conjugated ubiquitin structures, dependent on K6 of ubiquitin, in cells during DNA replication and repair. *Human molecular genetics* 13: 807-817.

84. Nishikawa, H., S. Ooka, K. Sato, K. Arima, J. Okamoto, R. E. Klevit, M. Fukuda, and T. Ohta. 2004. Mass spectrometric and mutational analyses reveal Lys-6-linked polyubiquitin chains catalyzed by BRCA1-BARD1 ubiquitin ligase. *J Biol Chem* 279: 3916-3924.

85. Shakya, R., L. J. Reid, C. R. Reczek, F. Cole, D. Egli, C. S. Lin, D. G. deRooij, S. Hirsch, K. Ravi, J. B. Hicks, M. Szabolcs, M. Jasin, R. Baer, and T. Ludwig. 2011. BRCA1 tumor suppression depends on BRCT phosphoprotein binding, but not its E3 ligase activity. *Science* 334: 525-528.

86. Williams, R. S., R. Green, and J. N. Glover. 2001. Crystal structure of the BRCT repeat region from the breast cancer-associated protein BRCA1. *Nat Struct Biol* 8: 838-842.

87. Wu, Q., A. Paul, D. Su, S. Mehmood, T. K. Foo, T. Ochi, E. L. Bunting, B. Xia, C. V. Robinson, B. Wang, and T. L. Blundell. 2016. Structure of BRCA1-BRCT/Abraxas

Complex Reveals Phosphorylation-Dependent BRCT Dimerization at DNA Damage Sites. *Mol Cell* 61: 434-448.

88. Hu, X., J. A. Kim, A. Castillo, M. Huang, J. Liu, and B. Wang. 2011. NBA1/MERIT40 and BRE interaction is required for the integrity of two distinct deubiquitinating enzyme BRCC36-containing complexes. *J Biol Chem* 286: 11734-11745.

89. Komander, D., M. J. Clague, and S. Urbe. 2009. Breaking the chains: structure and function of the deubiquitinases. *Nat Rev Mol Cell Biol* 10: 550-563.

90. Cooper, E. M., C. Cutcliffe, T. Z. Kristiansen, A. Pandey, C. M. Pickart, and R. E. Cohen. 2009. K63-specific deubiquitination by two JAMM/MPN+ complexes: BRISC-associated Brcc36 and proteasomal Poh1. *EMBO J* 28: 621-631.

91. Feng, L., J. Wang, and J. Chen. 2010. The Lys63-specific deubiquitinating enzyme BRCC36 is regulated by two scaffold proteins localizing in different subcellular compartments. *J Biol Chem* 285: 30982-30988.

92. Szabo, C., A. Masiello, J. F. Ryan, and L. C. Brody. 2000. The breast cancer information core: database design, structure, and scope. *Human mutation* 16: 123-131.

93. Wang, B. 2012. BRCA1 tumor suppressor network: focusing on its tail. *Cell Biosci* 2: 6.

94. Clapperton, J. A., I. A. Manke, D. M. Lowery, T. Ho, L. F. Haire, M. B. Yaffe, and S. J. Smerdon. 2004. Structure and mechanism of BRCA1 BRCT domain recognition of phosphorylated BACH1 with implications for cancer. *Nat Struct Mol Biol* 11: 512-518.

95. Williams, R. S., M. S. Lee, D. D. Hau, and J. N. Glover. 2004. Structural basis of phosphopeptide recognition by the BRCT domain of BRCA1. *Nat Struct Mol Biol* 11: 519-525.

96. Shiozaki, E. N., L. Gu, N. Yan, and Y. Shi. 2004. Structure of the BRCT repeats of BRCA1 bound to a BACH1 phosphopeptide: implications for signaling. *Mol Cell* 14: 405-412.

97. Varma, A. K., R. S. Brown, G. Birrane, and J. A. Ladias. 2005. Structural basis for cell cycle checkpoint control by the BRCA1-CtIP complex. *Biochemistry* 44: 10941-10946.

98. Neeley, W. L., and J. M. Essigmann. 2006. Mechanisms of formation, genotoxicity, and mutation of guanine oxidation products. *Chem Res Toxicol* 19: 491-505.

99. Stock, J. K., S. Giadrossi, M. Casanova, E. Brookes, M. Vidal, H. Koseki, N. Brockdorff, A. G. Fisher, and A. Pombo. 2007. Ring1-mediated ubiquitination of H2A restrains poised RNA polymerase II at bivalent genes in mouse ES cells. *Nat Cell Biol* 9: 1428-1435.

100. Ciehanover, A., Y. Hod, and A. Hershko. 1978. A heat-stable polypeptide component of an ATP-dependent proteolytic system from reticulocytes. *Biochemical and biophysical research communications* 81: 1100-1105.

101. Hershko, A., A. Ciechanover, H. Heller, A. L. Haas, and I. A. Rose. 1980. Proposed role of ATP in protein breakdown: conjugation of protein with multiple chains of the polypeptide of ATP-dependent proteolysis. *Proc Natl Acad Sci U S A* 77: 1783-1786.

102. Wilkinson, K. D., M. K. Urban, and A. L. Haas. 1980. Ubiquitin is the ATP-dependent proteolysis factor I of rabbit reticulocytes. *J Biol Chem* 255: 7529-7532.

103. Chen, Z. J., and L. J. Sun. 2009. Nonproteolytic functions of ubiquitin in cell signaling. *Mol Cell* 33: 275-286.

104. Pickart, C. M. 2001. Mechanisms underlying ubiquitination. *Annual review of biochemistry* 70: 503-533.

105. Schulman, B. A., and J. W. Harper. 2009. Ubiquitin-like protein activation by E1 enzymes: the apex for downstream signalling pathways. *Nat Rev Mol Cell Biol* 10: 319-331.

106. Ye, Y., and M. Rape. 2009. Building ubiquitin chains: E2 enzymes at work. *Nat Rev Mol Cell Biol* 10: 755-764.

107. Welchman, R. L., C. Gordon, and R. J. Mayer. 2005. Ubiquitin and ubiquitin-like proteins as multifunctional signals. *Nat Rev Mol Cell Biol* 6: 599-609.

108. Kaiser, S. E., B. E. Riley, T. A. Shaler, R. S. Trevino, C. H. Becker, H. Schulman, and R. R. Kopito. 2011. Protein standard absolute quantification (PSAQ) method for the measurement of cellular ubiquitin pools. *Nature methods* 8: 691-696.

109. Haglund, K., S. Sigismund, S. Polo, I. Szymkiewicz, P. P. Di Fiore, and I. Dikic. 2003. Multiple monoubiquitination of RTKs is sufficient for their endocytosis and degradation. *Nat Cell Biol* 5: 461-466.

110. Swatek, K. N., and D. Komander. 2016. Ubiquitin modifications. *Cell Res* 26: 399-422.

111. Akutsu, M., I. Dikic, and A. Bremm. 2016. Ubiquitin chain diversity at a glance. *J Cell Sci* 129: 875-880.

112. Iwai, K., H. Fujita, and Y. Sasaki. 2014. Linear ubiquitin chains: NF-kappaB signalling, cell death and beyond. *Nat Rev Mol Cell Biol* 15: 503-508.

113. Meierhofer, D., X. Wang, L. Huang, and P. Kaiser. 2008. Quantitative analysis of global ubiquitination in HeLa cells by mass spectrometry. *Journal of proteome research* 7: 4566-4576.

114. Xu, P., D. M. Duong, N. T. Seyfried, D. Cheng, Y. Xie, J. Robert, J. Rush, M. Hochstrasser, D. Finley, and J. Peng. 2009. Quantitative proteomics reveals the function of unconventional ubiquitin chains in proteasomal degradation. *Cell* 137: 133-145.

115. Peng, J., D. Schwartz, J. E. Elias, C. C. Thoreen, D. Cheng, G. Marsischky, J. Roelofs, D. Finley, and S. P. Gygi. 2003. A proteomics approach to understanding protein ubiquitination. *Nat Biotechnol* 21: 921-926.

116. Hurley, J. H., S. Lee, and G. Prag. 2006. Ubiquitin-binding domains. *Biochem J* 399: 361-372.

117. Dikic, I., S. Wakatsuki, and K. J. Walters. 2009. Ubiquitin-binding domains - from structures to functions. *Nat Rev Mol Cell Biol* 10: 659-671.

118. Stewart, M. D., T. Ritterhoff, R. E. Klevit, and P. S. Brzovic. 2016. E2 enzymes: more than just middle men. *Cell Res* 26: 423-440.

119. Chau, V., J. W. Tobias, A. Bachmair, D. Marriott, D. J. Ecker, D. K. Gonda, and A. Varshavsky. 1989. A multiubiquitin chain is confined to specific lysine in a targeted short-lived protein. *Science* 243: 1576-1583.

120. Hochstrasser, M. 1996. Ubiquitin-dependent protein degradation. *Annual review of genetics* 30: 405-439.

121. Spence, J., S. Sadis, A. L. Haas, and D. Finley. 1995. A ubiquitin mutant with specific defects in DNA repair and multiubiquitination. *Mol Cell Biol* 15: 1265-1273.

122. Hofmann, R. M., and C. M. Pickart. 1999. Noncanonical MMS2-encoded ubiquitin-conjugating enzyme functions in assembly of novel polyubiquitin chains for DNA repair. *Cell* 96: 645-653.

123. Deng, L., C. Wang, E. Spencer, L. Yang, A. Braun, J. You, C. Slaughter, C. Pickart, and Z. J. Chen. 2000. Activation of the IkappaB kinase complex by TRAF6 requires a dimeric ubiquitin-conjugating enzyme complex and a unique polyubiquitin chain. *Cell* 103: 351-361.

124. Zhou, H., I. Wertz, K. O'Rourke, M. Ultsch, S. Seshagiri, M. Eby, W. Xiao, and V. M. Dixit. 2004. Bcl10 activates the NF-kappaB pathway through ubiquitination of NEMO. *Nature* 427: 167-171.

125. Galan, J. M., and R. Haguenauer-Tsapis. 1997. Ubiquitin lys63 is involved in ubiquitination of a yeast plasma membrane protein. *EMBO J* 16: 5847-5854.

126. Jung, J. W., S. J. Bae, G. Y. Kang, K. H. Kim, W. S. Yeo, S. H. Park, J. H. Seol, E. C. Yi, and K. P. Kim. 2013. Analysis of the biochemical role of Lys-11 in polyubiquitin chain formation using quantitative mass spectrometry. *Rapid Commun Mass Spectrom* 27: 339-346.

127. Ordureau, A., C. Munch, and J. W. Harper. 2015. Quantifying ubiquitin signaling. *Mol Cell* 58: 660-676.

128. Phu, L., A. Izrael-Tomasevic, M. L. Matsumoto, D. Bustos, J. N. Dynek, A. V. Fedorova, C. E. Bakalarski, D. Arnott, K. Deshayes, V. M. Dixit, R. F. Kelley, D. Vucic, and D. S. Kirkpatrick. 2011. Improved quantitative mass spectrometry methods for characterizing complex ubiquitin signals. *Molecular & cellular proteomics : MCP* 10: M110 003756.

129. Kirkpatrick, D. S., N. A. Hathaway, J. Hanna, S. Elsasser, J. Rush, D. Finley, R. W. King, and S. P. Gygi. 2006. Quantitative analysis of in vitro ubiquitinated cyclin B1 reveals complex chain topology. *Nat Cell Biol* 8: 700-710.

130. Hofmann, R. M., and C. M. Pickart. 2001. In vitro assembly and recognition of Lys-63 polyubiquitin chains. *J Biol Chem* 276: 27936-27943.

131. Plans, V., J. Scheper, M. Soler, N. Loukili, Y. Okano, and T. M. Thomson. 2006. The RING finger protein RNF8 recruits UBC13 for lysine 63-based self polyubiquitylation. *J Cell Biochem* 97: 572-582.

132. Sims, J. J., and R. E. Cohen. 2009. Linkage-specific avidity defines the lysine 63-linked polyubiquitin-binding preference of rap80. *Mol Cell* 33: 775-783.

133. Hu, Y., R. Scully, B. Sobhian, A. Xie, E. Shestakova, and D. M. Livingston. 2011. RAP80-directed tuning of BRCA1 homologous recombination function at ionizing radiation-induced nuclear foci. *Genes Dev* 25: 685-700.

134. Botuyan, M. V., J. Lee, I. M. Ward, J. E. Kim, J. R. Thompson, J. Chen, and G. Mer. 2006. Structural basis for the methylation state-specific recognition of histone H4-K20 by 53BP1 and Crb2 in DNA repair. *Cell* 127: 1361-1373.

135. Fradet-Turcotte, A., M. D. Canny, C. Escribano-Diaz, A. Orthwein, C. C. Leung, H. Huang, M. C. Landry, J. Kitevski-LeBlanc, S. M. Noordermeer, F. Sicheri, and D.

Durocher. 2013. 53BP1 is a reader of the DNA-damage-induced H2A Lys 15 ubiquitin mark. *Nature* 499: 50-54.

136.   Thorslund, T., A. Ripplinger, S. Hoffmann, T. Wild, M. Uckelmann, B. Villumsen, T. Narita, T. K. Sixma, C. Choudhary, S. Bekker-Jensen, and N. Mailand. 2015. Histone H1 couples initiation and amplification of ubiquitin signalling after DNA damage. *Nature*.

137.   Wu, W., H. Nishikawa, R. Hayami, K. Sato, A. Honda, S. Aratani, T. Nakajima, M. Fukuda, and T. Ohta. 2007. BRCA1 ubiquitinates RPB8 in response to DNA damage. *Cancer research* 67: 951-958.

138.   Elia, A. E., A. P. Boardman, D. C. Wang, E. L. Huttlin, R. A. Everley, N. Dephoure, C. Zhou, I. Koren, S. P. Gygi, and S. J. Elledge. 2015. Quantitative Proteomic Atlas of Ubiquitination and Acetylation in the DNA Damage Response. *Mol Cell* 59: 867-881.

139.   Pathania, S., J. Nguyen, S. J. Hill, R. Scully, G. O. Adelmant, J. A. Marto, J. Feunteun, and D. M. Livingston. 2011. BRCA1 is required for postreplication repair after UV-induced DNA damage. *Mol Cell* 44: 235-251.

140.   Lu, C. S., L. N. Truong, A. Aslanian, L. Z. Shi, Y. Li, P. Y. Hwang, K. H. Koh, T. Hunter, J. R. Yates, 3rd, M. W. Berns, and X. Wu. 2012. The RING finger protein RNF8 ubiquitinates Nbs1 to promote DNA double-strand break repair by homologous recombination. *J Biol Chem* 287: 43984-43994.

141.   Kim, W., E. J. Bennett, E. L. Huttlin, A. Guo, J. Li, A. Possemato, M. E. Sowa, R. Rad, J. Rush, M. J. Comb, J. W. Harper, and S. P. Gygi. 2011. Systematic and quantitative assessment of the ubiquitin-modified proteome. *Mol Cell* 44: 325-340.

142. Wagner, S. A., P. Beli, B. T. Weinert, M. L. Nielsen, J. Cox, M. Mann, and C. Choudhary. 2011. A proteome-wide, quantitative survey of in vivo ubiquitylation sites reveals widespread regulatory roles. *Molecular & cellular proteomics : MCP* 10: M111 013284.

143. Mattiroli, F., J. H. Vissers, W. J. van Dijk, P. Ikpa, E. Citterio, W. Vermeulen, J. A. Marteijn, and T. K. Sixma. 2012. RNF168 ubiquitinates K13-15 on H2A/H2AX to drive DNA damage signaling. *Cell* 150: 1182-1195.

144. Postow, L., C. Ghenoiu, E. M. Woo, A. N. Krutchinsky, B. T. Chait, and H. Funabiki. 2008. Ku80 removal from DNA through double strand break-induced ubiquitylation. *J Cell Biol* 182: 467-479.

145. Postow, L., and H. Funabiki. 2013. An SCF complex containing Fbxl12 mediates DNA damage-induced Ku80 ubiquitylation. *Cell Cycle* 12: 587-595.

146. Shi, W., Z. Ma, H. Willers, K. Akhtar, S. P. Scott, J. Zhang, S. Powell, and J. Zhang. 2008. Disassembly of MDC1 foci is controlled by ubiquitin-proteasome-dependent degradation. *J Biol Chem* 283: 31608-31616.

147. Liu, W., W. Zong, G. Wu, T. Fujita, W. Li, J. Wu, and Y. Wan. 2010. Turnover of BRCA1 involves in radiation-induced apoptosis. *PloS one* 5: e14484.

148. Ramadan, K., and M. Meerang. 2011. Degradation-linked ubiquitin signal and proteasome are integral components of DNA double strand break repair: New perspectives for anti-cancer therapy. *FEBS Lett* 585: 2868-2875.

149. Ramadan, K. 2012. p97/VCP- and Lys48-linked polyubiquitination form a new signaling pathway in DNA damage response. *Cell Cycle* 11: 1062-1069.

150. Baboshina, O. V., and A. L. Haas. 1996. Novel multiubiquitin chain linkages catalyzed by the conjugating enzymes E2EPF and RAD6 are recognized by 26 S proteasome subunit 5. *J Biol Chem* 271: 2823-2831.

151. Jin, L., A. Williamson, S. Banerjee, I. Philipp, and M. Rape. 2008. Mechanism of ubiquitin-chain formation by the human anaphase-promoting complex. *Cell* 133: 653-665.

152. Garnett, M. J., J. Mansfeld, C. Godwin, T. Matsusaka, J. Wu, P. Russell, J. Pines, and A. R. Venkitaraman. 2009. UBE2S elongates ubiquitin chains on APC/C substrates to promote mitotic exit. *Nat Cell Biol* 11: 1363-1369.

153. Williamson, A., K. E. Wickliffe, B. G. Mellone, L. Song, G. H. Karpen, and M. Rape. 2009. Identification of a physiological E2 module for the human anaphase-promoting complex. *Proc Natl Acad Sci U S A* 106: 18213-18218.

154. Wu, T., Y. Merbl, Y. Huo, J. L. Gallop, A. Tzur, and M. W. Kirschner. 2010. UBE2S drives elongation of K11-linked ubiquitin chains by the anaphase-promoting complex. *Proc Natl Acad Sci U S A* 107: 1355-1360.

155. Wickliffe, K. E., A. Williamson, H. J. Meyer, A. Kelly, and M. Rape. 2011. K11-linked ubiquitin chains as novel regulators of cell division. *Trends Cell Biol* 21: 656-663.

156. Pines, J. 2011. Cubism and the cell cycle: the many faces of the APC/C. *Nat Rev Mol Cell Biol* 12: 427-438.

157. Bremm, A., S. M. Freund, and D. Komander. 2010. Lys11-linked ubiquitin chains adopt compact conformations and are preferentially hydrolyzed by the deubiquitinase Cezanne. *Nat Struct Mol Biol* 17: 939-947.

158. Bremm, A., S. Moniz, J. Mader, S. Rocha, and D. Komander. 2014. Cezanne (OTUD7B) regulates HIF-1alpha homeostasis in a proteasome-independent manner. *EMBO Rep* 15: 1268-1277.

159. Bennett, E. J., T. A. Shaler, B. Woodman, K. Y. Ryu, T. S. Zaitseva, C. H. Becker, G. P. Bates, H. Schulman, and R. R. Kopito. 2007. Global changes to the ubiquitin system in Huntington's disease. *Nature* 448: 704-708.

160. Shiio, Y., and R. N. Eisenman. 2003. Histone sumoylation is associated with transcriptional repression. *Proc Natl Acad Sci U S A* 100: 13225-13230.

161. Lim, K. L., K. C. Chew, J. M. Tan, C. Wang, K. K. Chung, Y. Zhang, Y. Tanaka, W. Smith, S. Engelender, C. A. Ross, V. L. Dawson, and T. M. Dawson. 2005. Parkin mediates nonclassical, proteasomal-independent ubiquitination of synphilin-1: implications for Lewy body formation. *The Journal of neuroscience : the official journal of the Society for Neuroscience* 25: 2002-2009.

162. Jackson, S. P., and D. Durocher. 2013. Regulation of DNA damage responses by ubiquitin and SUMO. *Mol Cell* 49: 795-807.

163. Wickliffe, K. E., S. Lorenz, D. E. Wemmer, J. Kuriyan, and M. Rape. 2011. The mechanism of linkage-specific ubiquitin chain elongation by a single-subunit E2. *Cell* 144: 769-781.

164. Peters, J. M. 2006. The anaphase promoting complex/cyclosome: a machine designed to destroy. *Nat Rev Mol Cell Biol* 7: 644-656.

165. Rape, M. 2010. Assembly of k11-linked ubiquitin chains by the anaphase-promoting complex. *Sub-cellular biochemistry* 54: 107-115.

166. Zeng, X., F. Sigoillot, S. Gaur, S. Choi, K. L. Pfaff, D. C. Oh, N. Hathaway, N. Dimova, G. D. Cuny, and R. W. King. 2010. Pharmacologic inhibition of the anaphase-promoting complex induces a spindle checkpoint-dependent mitotic arrest in the absence of spindle damage. *Cancer Cell* 18: 382-395.

167. Lorick, K. L., J. P. Jensen, S. Fang, A. M. Ong, S. Hatakeyama, and A. M. Weissman. 1999. RING fingers mediate ubiquitin-conjugating enzyme (E2)-dependent ubiquitination. *Proc Natl Acad Sci U S A* 96: 11364-11369.

168. Deshaies, R. J., and C. A. Joazeiro. 2009. RING domain E3 ubiquitin ligases. *Annual review of biochemistry* 78: 399-434.

169. de Napoles, M., J. E. Mermoud, R. Wakao, Y. A. Tang, M. Endoh, R. Appanah, T. B. Nesterova, J. Silva, A. P. Otte, M. Vidal, H. Koseki, and N. Brockdorff. 2004. Polycomb group proteins Ring1A/B link ubiquitylation of histone H2A to heritable gene silencing and X inactivation. *Dev Cell* 7: 663-676.

170. Fang, J., T. Chen, B. Chadwick, E. Li, and Y. Zhang. 2004. Ring1b-mediated H2A ubiquitination associates with inactive X chromosomes and is involved in initiation of X inactivation. *The Journal of biological chemistry* 279: 52812-52815.

171. Wang, H., L. Wang, H. Erdjument-Bromage, M. Vidal, P. Tempst, R. S. Jones, and Y. Zhang. 2004. Role of histone H2A ubiquitination in Polycomb silencing. *Nature* 431: 873-878.

172. Zhou, W., P. Zhu, J. Wang, G. Pascual, K. A. Ohgi, J. Lozach, C. K. Glass, and M. G. Rosenfeld. 2008. Histone H2A monoubiquitination represses transcription by inhibiting RNA polymerase II transcriptional elongation. *Mol Cell* 29: 69-80.

173. Gong, F., L. Y. Chiu, B. Cox, F. Aymard, T. Clouaire, J. W. Leung, M. Cammarata, M. Perez, P. Agarwal, J. S. Brodbelt, G. Legube, and K. M. Miller. 2015. Screen identifies bromodomain protein ZMYND8 in chromatin recognition of transcription-associated DNA damage that promotes homologous recombination. *Genes Dev* 29: 197-211.

174. Palancade, B., and O. Bensaude. 2003. Investigating RNA polymerase II carboxyl-terminal domain (CTD) phosphorylation. *European journal of biochemistry / FEBS* 270: 3859-3870.

175. Phatnani, H. P., and A. L. Greenleaf. 2006. Phosphorylation and functions of the RNA polymerase II CTD. *Genes Dev* 20: 2922-2936.

176. Hsin, J. P., and J. L. Manley. 2012. The RNA polymerase II CTD coordinates transcription and RNA processing. *Genes Dev* 26: 2119-2137.

177. Komarnitsky, P., E. J. Cho, and S. Buratowski. 2000. Different phosphorylated forms of RNA polymerase II and associated mRNA processing factors during transcription. *Genes Dev* 14: 2452-2460.

178. Williamson, A., S. Banerjee, X. Zhu, I. Philipp, A. T. Iavarone, and M. Rape. 2011. Regulation of ubiquitin chain initiation to control the timing of substrate degradation. *Mol Cell* 42: 744-757.

179. Pankotai, T., C. Bonhomme, D. Chen, and E. Soutoglou. 2012. DNAPKcs-dependent arrest of RNA polymerase II transcription in the presence of DNA breaks. *Nat Struct Mol Biol* 19: 276-282.

180. Weake, V. M., and J. L. Workman. 2008. Histone ubiquitination: triggering gene activity. *Mol Cell* 29: 653-663.

181. Iwai, K. 2012. Diverse ubiquitin signaling in NF-kappaB activation. *Trends Cell Biol* 22: 355-364.

182. Dynek, J. N., T. Goncharov, E. C. Dueber, A. V. Fedorova, A. Izrael-Tomasevic, L. Phu, E. Helgason, W. J. Fairbrother, K. Deshayes, D. S. Kirkpatrick, and D. Vucic. 2010. c-IAP1 and UbcH5 promote K11-linked polyubiquitination of RIP1 in TNF signalling. *EMBO J* 29: 4198-4209.

183. Bremm, A., and D. Komander. 2011. Emerging roles for Lys11-linked polyubiquitin in cellular regulation. *Trends Biochem Sci* 36: 355-363.

184. Matsumoto, M. L., K. E. Wickliffe, K. C. Dong, C. Yu, I. Bosanac, D. Bustos, L. Phu, D. S. Kirkpatrick, S. G. Hymowitz, M. Rape, R. F. Kelley, and V. M. Dixit. 2010. K11-linked polyubiquitination in cell cycle control revealed by a K11 linkage-specific antibody. *Mol Cell* 39: 477-484.

185. Castaneda, C. A., T. R. Kashyap, M. A. Nakasone, S. Krueger, and D. Fushman. 2013. Unique structural, dynamical, and functional properties of k11-linked polyubiquitin chains. *Structure* 21: 1168-1181.

186. Aymard, F., B. Bugler, C. K. Schmidt, E. Guillou, P. Caron, S. Briois, J. S. Iacovoni, V. Daburon, K. M. Miller, S. P. Jackson, and G. Legube. 2014. Transcriptionally active chromatin recruits homologous recombination at DNA double-strand breaks. *Nat Struct Mol Biol* 21: 366-374.

187. Kornberg, R. D. 1977. Structure of chromatin. *Annual review of biochemistry* 46: 931-954.

188. Luger, K., A. W. Mader, R. K. Richmond, D. F. Sargent, and T. J. Richmond. 1997. Crystal structure of the nucleosome core particle at 2.8 A resolution. *Nature* 389: 251-260.

189. Tremethick, D. J. 2007. Higher-order structures of chromatin: the elusive 30 nm fiber. *Cell* 128: 651-654.

190. Luger, K., M. L. Dechassa, and D. J. Tremethick. 2012. New insights into nucleosome and chromatin structure: an ordered state or a disordered affair? *Nat Rev Mol Cell Biol* 13: 436-447.

191. Kulis, M., and M. Esteller. 2010. DNA methylation and cancer. *Adv Genet* 70: 27-56.

192. Kouzarides, T. 2007. Chromatin modifications and their function. *Cell* 128: 693-705.

193. Clapier, C. R., and B. R. Cairns. 2009. The biology of chromatin remodeling complexes. *Annual review of biochemistry* 78: 273-304.

194. Olsen, C. A. 2012. Expansion of the lysine acylation landscape. *Angewandte Chemie* 51: 3755-3756.

195. van Attikum, H., and S. M. Gasser. 2009. Crosstalk between histone modifications during the DNA damage response. *Trends Cell Biol* 19: 207-217.

196. Zhao, Y., J. R. Brickner, M. C. Majid, and N. Mosammaparast. 2014. Crosstalk between ubiquitin and other post-translational modifications on chromatin during double-strand break repair. *Trends Cell Biol* 24: 426-434.

197. Vogelstein, B., N. Papadopoulos, V. E. Velculescu, S. Zhou, L. A. Diaz, Jr., and K. W. Kinzler. 2013. Cancer genome landscapes. *Science* 339: 1546-1558.

198.	Pearl, L. H., A. C. Schierz, S. E. Ward, B. Al-Lazikani, and F. M. Pearl. 2015. Therapeutic opportunities within the DNA damage response. *Nat Rev Cancer* 15: 166-180.

VITA

Atanu Paul was born in Kanchrapara in the state of West Bengal, India. He was born on 23rd July 1983 to Mr. Bimal Kanti Paul and Mrs. Banani Paul. After completing high school at Kanchrapara Harnett High School in Kanchrapara, Atanu, continued his college education at West Bengal University of Animal & Fishery Sciences, Kolkata, India from 2002-2007. Following his undergraduate training, Atanu moved to the United States to pursue Master's of Science majoring in Biology at the University of Texas at El Paso (UTEP). At UTEP, Atanu completed his Master's dissertation project entitled " A specific regulatory role for SGTα on the maturation and activation of steroid hormone receptors" under the supervision of Dr. Marc B. Cox. Following his graduation from UTEP, Atanu joined the PhD program at the Graduate School of Biomedical Sciences, a joint venture of The University of Texas Health Science Center at Houston and The University of Texas MD Anderson Cancer Center, Houston in August 2010. Atanu joined the lab of Dr. Bin Wang in the Department of Genetics in the Genes & Development graduate program to pursue his PhD dissertation. Atanu's PhD project focuses on examining the role of post-translational modifications in the DNA damage response pathway.

Permanent Address:

9, Abdul Jabbar Road, Kanchrapara

North 24 Pgs, West Bengal, India, 743145